Evaluation of waste tyre-derived char and crumb as adsorbents for gold recovery from acidic solutions

by

Tshepisho Thabiso Praise Maapola

Thesis presented in partial fulfilment
of the requirements for the Degree

of

MASTER OF ENGINEERING
(CHEMICAL ENGINEERING)

in the Faculty of Engineering
at Stellenbosch University

The financial assistance of the National Research Foundation (NRF) towards this research is hereby acknowledged. Opinions expressed, and conclusions arrived at, are those of the author and are not necessarily to be attributed to the NRF.

Supervisor

(Dr. L.J. du Preez)

Co-Supervisor

(Dr. I. Iraola-Arregui)

April 2019

DECLARATION

By submitting this thesis electronically, I declare that the entirety of the work contained therein is my own, original work, that I am the sole author thereof (save to the extent explicitly otherwise stated), that reproduction and publication thereof by Stellenbosch University will not infringe any third party rights and that I have not previously in its entirety or in part submitted it for obtaining any qualification.

Date: April 2019

PLAGIARISM DECLARATION

1. Plagiarism is the use of ideas, material and other intellectual property of another's work and to present is as my own.
2. I agree that plagiarism is a punishable offence because it constitutes theft.
3. I also understand that direct translations are plagiarism.
4. Accordingly, all quotations and contributions from any source whatsoever (including the internet) have been cited fully. I understand that the reproduction of text without quotation marks (even when the source is cited) is plagiarism.
5. I declare that the work contained in this assignment, except where otherwise stated, is my original work and that I have not previously (in its entirety or in part) submitted it for grading in this module/assignment or another assignment/ module.

Initials and surname: T.T.P Maapola .....

Date: April 2019

ABSTRACT

Each year the number of vehicles is growing worldwide; therefore, the number of tyres is increasing at a faster rate daily. Tyres do not present a risk to the health on their own, the inappropriate disposal and mismanagement of large amounts can cause serious problems not only to the environment but also to human beings. Waste tyre management is therefore very important. Several ways of waste tyres management and valorisation have been attempted; of which pyrolysis is one of the most attractive technique. Pyrolysis of waste tyres produce potentially valuable products such as tyre derived pyrolytic oil, gas and char.

The main aim of this project is to study the adsorption capacity of tyre-derived char and crumb as alternative low-cost adsorbents for adsorption of gold in a form of gold chloride complex ion, $AuCl_4^-$, from acidic solutions. Pyrolytic tyre char (PT-char), which is a carbonaceous solid material that constitutes 30–40 wt.% of the entire pyrolysis product, and tyre crumb (T-crumb) will be of interest in this project as alternative low-cost adsorbents. However, there is a major drawback in applications of the crude form of these adsorbents due to their high level of impurities, which could pose a threat to their economic and market value. Hence, demineralisation as a purification approach is employed to remove or reduce the ash content. Untreated PT-char and T-crumb were demineralised first with 1M NaOH and subsequently with 1M HNO_3. The untreated and treated samples were characterised and used as adsorbents in adsorption of gold from acidic chloride solutions. The performance of the untreated samples was compared with that of treated PT-char and T-crumb based on adsorption capacity. Since there is no work reported yet on the application of tyre char and crumb as adsorbents for gold, then this initiative is the novelty of this project.

Demineralisation of PT-char and T-crumb under acid-base medium proved to enhance the BET surface area which increased from 63.96 to 78.89 m^2/g for PT-char and from 0.322 to 3.49 m^2/g for T-crumb. The impurities which are regarded as ash content in this case, were significantly reduced with 90% of ash removed from UPT-char and 50% ash removed from UT-crumb. The effective pH for the adsorption of Au(III) ions with all the adsorbents was 2.0 with maximum adsorption percentage as high as 90%. The maximum

capacity for untreated adsorbents was reached within 48h and for treated adsorbents was reached in 24h contact time. To study the adsorption isotherm, Langmuir and Freundlich isotherm models were used and for kinetic studies pseudo-first and second kinetic models where used. The adsorbents obeyed Langmuir isotherm model with calculated Q_e of 416.7, 19.2, 47.4 and 21.1 mg/g for UPT-char, TPT-char, UT-crumb and TT-crumb, respectively. And they obeyed pseudo-second order kinetic model with calculated Q_e of 434.8, 21.6, 61.7 and 21.7 mg/g for UPT-char, TPT-char, UT-crumb and TT-crumb respectively.

The SEM micrograph images of the treated and untreated adsorbents after adsorption revealed that the adsorbed gold was reduced from Au(III) to Au(0) nanoparticles on the adsorbent surface. A major part of UPT-char surface was occupied with gold nanoparticles randomly distributed on specific binding sites. On the surface of the treated adsorbents the gold nanoparticles were very few which proved that the treated adsorbents had few active binding sites for gold. The reduction of gold to gold nanoparticles was due to the presence of sulphur content on the adsorbent surface which served as a reductant reducing gold via electron transfer.

In conclusion, these results show that demineralisation of PT-char and T-crumb is not beneficial regarding adsorption of gold, but useful in leaching out contaminants and reducing ash content, consequently improving the surface area. The high adsorption capacity of the untreated adsorbents proved to have high affinity for gold and stand a good chance to be used as low-cost adsorbents. Sulphur content on the adsorbents surface behaved as the binding site for gold ions during adsorption. Using tyre-derived adsorbents before undergoing expensive processes such as activation and chemical treatments to manufacture expensive adsorbents such as activated carbon could be beneficial as part of valorisation of waste tyres. Recovery of gold from acidic solutions such as e-waste leachates with low-cost tyre-derived adsorbents would also be beneficial both on economic and environmental point of view.

Keywords: Demineralisation; Au(III) adsorption; Adsorption capacity; Kinetics; Isotherm

ABSTRAK

Elke jaar groei die hoeveelheid voertuie wêreldwyd. Daarom groei die hoeveelheid bande teen 'n vinniger koers daagliks. Bande bied nie 'n gesondheidsrisiko op hul eie nie, maar die onvanpaste wegmaking en wanbestuur van groot hoeveelhede kan ernstige probleme vir nie net die omgewing nie, maar ook vir mense, veroorsaak. Die bestuur van afvalbande is daarom baie belangrik. Verskeie maniere van bestuur van afvalbande en valorisasie is gepoog, waarvan pirolise een van die mees aantreklike tegnieke is. Pirolise van afvalbande lewer potensiële waardevolle produkte soos band-afkomstige pirolitiese olie, gas en verkoolsel.

Die hoofdoel van hierdie projek is om die adsorpsie kapasiteit van band-afkomstige verkoolsel en krummel as alternatiewe lae-koste adsorbeermiddels vir adsorpsie van goud in 'n vorm van goud chloried kompleks ioon, $AuCl_4^-$, vanuit suurvormende oplossings, te bestudeer. Pirolitiese bandverkoolsel (PT-char), wat 'n koolstofryke vastestof materiaal is wat 30–40 wt.% van die hele pirolise produk uitmaak, en bandkrummel (T-crumb) sal van belang wees in hierdie projek as alternatiewe lae-koste adsorbeermiddels. Daar is egter 'n groot nadeel in toepassings van die ru vorm van hierdie adsorbeermiddels as gevolg van hul hoë vlakke van onsuiwerhede, wat 'n bedreiging vir hul ekonomiese en markwaarde kan wees. Demineralisasie as 'n suiweringsbenadering is egter gebruik om die asinhoud te verwyder of verminder. Onbehandelde PT-char (UPT-char) en T-crumb (UT-crumb) was eers gedemineraliseer met 1 M NaOH en gevolglik met 1 M HNO_3. Die onbehandelde en behandelde monsters is gekarakteriseer en gebruik as adsorbeermiddels in adsorpsie van goud uit suur chloriedoplossings. Die werkverrigting van die onbehandelde monsters is vergelyk met dié van behandelde PT-char (TPT-char) en T-crumb (TT-crumb) gebaseer op adsorpsie kapasiteit. Aangesien daar nog geen werk gerapporteer is van die toepassing van bandverkoolsel en krummel as adsorbeermiddels vir goud nie, is hierdie inisiatief die nuutheid van hierdie projek.

Demineralisasie van PT-char en T-crumb onder suurbasismedium is bewys om die BET-oppervlakarea te vergroot, wat van 63.96 na 78.89 m^2/g toegeneem het vir PT-char en van 0.322 tot 3.49 m^2/g vir T-crumb. Die onsuiwerhede, wat beskou word as asinhoud in

hierdie geval, het beduidend verminder met 90% van die as verwyder uit UPT-char en 50% as verwyder uit UT-crumb. Die doeltreffende pH vir die adsorpsie van Au(III)-ione met al die adsorbeermiddels was 2.0 met maksimum adsorpsie persentasie so hoog soos 90%. Die maksimum kapasiteit vir onbehandelde adsorbeermiddels is binne 48 uur bereik, en binne 24 uur kontaktyd vir behandelde adsorbeermiddels. Om die adsorbsie isoterm te bestudeer is Langmuir en Freundlich isotermmodelle gebruik, en vir kinetiese studies pseudo-eerste en -tweede orde kinetiese modelle. Die adsorbeermiddels het die Langmuir isotermmodel gevolg met berekende Q_e van 416.7, 19.2, 47.4 en 21.1 mg/g vir UPT-char, TPT-char, UT-crumb en TT-crumb, onderskeidelik. En dit het die pseudo-tweede orde kinetiese model gevolg met berekende Q_e van 434.8, 21.6, 61.7 en 21.7 mg/g vir UPT-char, TPT-char, UT-crumb en TT-crumb, onderskeidelik.

Die SEM-mikrograafbeelde van die behandelde en onbehandelde adsorbeermiddels het bekendgemaak dat die geadsorbeerde goud gereduseer is van Au(III) na Au(0)-nanopartikels op die adsorbeermiddeloppervlak. ’n Groot deel van die UPT-char-oppervlak was betrek met goud nanopartikels wat lukraak versprei is op spesifieke verbindingsplekke. Op die oppervlak van die behandelde adsorbeermiddels was die goud nanopartikels baie min, wat bewys dat die behandelde adsorbeermiddels min aktiewe verbindingsplekke vir goud gehad het. Die reduksie van goud na goud nanopartikels is as gevolg van die teenwoordigheid van swaelinhoud op die adsorbeermiddeloppervlak wat as reduseermiddel gedien het deur elektronoordrag.

Ten slotte, hierdie resultate wys dat demineralisasie van PT-char en T-crumb nie voordelig is ten opsigte van adsorpsie van goud nie, maar handig is in uitloging van onsuiwerhede en die vermindering van asinhoud, wat die oppervlakarea gevolglik verbeter. Die hoë adsorpsie kapasiteit van die onbehandelde adsorbeermiddels is bewys om hoë affiniteit vir goud te hê en staan ’n goeie kans om as lae-koste adsorbeermiddel gebruik te word. Swaelinhoud op die adsorbeermiddeloppervlak het opgetree as die verbindingsplek vir goud-ione gedurende adsorpsie. Om band-afkomstige adsorbeermiddels te gebruik voordat duur prosesse, soos aktivering en chemiese behandeling, gebruik word om duur adsorbeermiddels, soos geaktiveerde koolstof, te vervaardig, kan voordelig wees as deel van valorisasie van afvalbande. Herwinning van goud uit suurvormende oplossings soos e-afval uitloogsels met lae-koste band-

afkomstige adsorbeermiddels kan ook voordelig wees van beide 'n ekonomiese en omgewingsstandpunt.

Sleutelwoorde: Demineralisasie, Au(III), Adsorpsie, Adorspie kapasiteit, Kinetika, Isoterm.

DEDICATION

I dedicate this work to a very special person in my life, Itumeleng Pearl Maapola.

ACKNOWLEDGEMENT

I would like to express my deepest gratitude to the following people and organisation for their selfless support and contribution in making this project a success:

- My loving heavenly Father God (Jesus) for strength and grace
- Dr L.J. du Preez and Dr I. Iraola-Arregui for guidance and supervising my project
- Mrs. L. Simmers, Mrs Hanlie Botha, and Mr. J. Van Rooyen for assistance with analytical instruments
- REDISA and National Research Foundation (NRF) for financial assistance
- My family and friends for motivating me during difficult times
- Process Engineering Department for the opportunity to study

TABLE OF CONTENT

LIST OF FIGURES

LIST OF TABLES

NOMENCLATURE

Q	Amount of Au(III) ions adsorbed per unit weight of adsorbent in mg/g
Q_e	Adsorption capacity at equilibrium
Q_t	Adsorption capacity at time t
Q_{max}	Maximum adsorption capacity
AAS	Atomic adsorption spectroscopy
FAAS	Flame Atomic adsorption spectroscopy
BET	Brunauer-Emmett-Teller
ICP-OES	Inductively coupled plasma optical emission spectrometry
SEM-EDS	Scanning electron microscopy energy dispersive X-ray spectroscopy
FTIR	Fourier Transform Infrared Spectroscopy
TPT-char	Treated pyrolytic tyre char
TT-crumb	Treated tyre crumb
T-crumb	Tyre crumb
UPT-char	Untreated pyrolytic tyre char
UT-crumb	Untreated tyre crumb
UV-Vis	Ultraviolet-visible spectroscopy
g/L	Gram per litre
mg/L	Milligram per litre
m_{ads}	Adsorbent mass
ppm	Parts per million
ρ	Density
R^2	Correlation coefficient
Ref	Reference
Con.	Concentration
wt.%	Weight percentage
T	Temperature
t_{con}	Contact time
h	Hour

1. INTRODUCTION

1.1 Background and motivation

A high demand and production of tyres due to a rapid growth in automobile industry for transportation purposes have led to accumulation of waste tyres on landfill which cause a global environmental concern. Nearly 1.5 billion waste tyres are generated annually [1] and currently there are about 4 billion waste tyres on landfill [2]. In 2017, the demand for tyres reached an estimate of 2.9 billion units [3]. Tyre rubbers are made to withstand harsh conditions which also make them difficult to bio-degrade and recycle [4]. The risks of having large amounts of waste tyres on landfills are derived from auto-ignition or accidental fires and incinerations which cause emission of harmful gases [2,3,5]. Stock piling of these waste tyres take up a large amount of available space, residing on landfill for longer periods and serving as breeding ground for disease-causing flies and mosquitoes which affects human health [4]. Moreover, the pyrolytic oil and ash content produced because of the incineration contains toxic heavy metals capable of causing water (especially groundwater) pollution that can last up to 100 years [3]. Therefore, inappropriate disposal of an increasing number of these non-biodegradable waste tyres on landfills is a serious environmental and economic problem which require an urgent management plan [2,3,5,6].

The current management routes for waste tyres can be divided into four main categories including pyrolysis, energy recovery, landfill and recycling [7]. Among them pyrolysis has gained special attention recently as an efficient route for valorisation of waste tyres. This is due to production of three main commercially feasible products, namely tyre derived oil (TDO), gases and pyrolytic tyre char (PT-char) [2,3,5,8]. Additionally, pyrolysis of waste tyres is environmentally friendly [2,3] since less emissions are generated during the process [3,8]. In this thesis the focus will be on PT-char out of the three waste tyre pyrolysis products and on the waste tyre rubber in a form of tyre crumb. The PT-char produced from pyrolysis of waste tyres have low market value due to its high level of contaminants which needs to be carefully removed. The contaminants are such as heavy metals, trace oil and volatile matters [9] with silica and zinc being the main contaminants [10]. The basic lifecycle of a tyre is depicted in *Figure 1-1* [3,7].

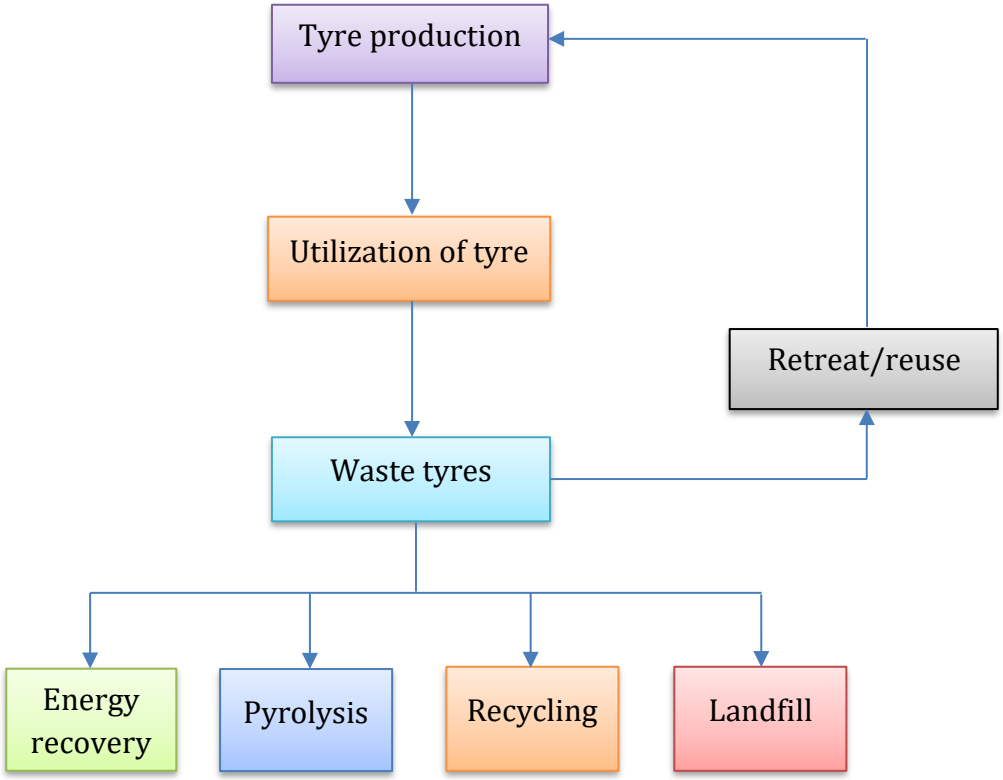

Figure 1-1: The basic lifecycle of a tyre [3,7]

Electronic wastes (e-waste) are another environmental concern and considered the fastest growing waste stream in the world [11,12]. The advancement in modern technology has tremendously contributed to the production of more technological devices with a very short lifespan and the old ones being abandoned in abundance [11,13]. This accelerates the number of e-waste produced annually which was reported to be 41.8 million tonnes per year globally [13]. To mention a few, some technological devices that are widely used daily are mainly electronic and electrical devices such as desktop computer, television, printers, mobile phones, laptop etc., [14]. When these devices have reached the end of their lifespan they get disposed to the environment. An inappropriate disposal of e-wastes via landfilling has contributed to several environmental and health problems by causing environmental pollution. One of these health hazards is water pollution caused by heavy metals leached from the e-waste to underground water and eventually to water streams [15]. However, e-wastes contain valuable metals including gold and can serve as a secondary source of precious and base metals [16]. Therefore, the recovery of these valuable metals is both environmentally and economically beneficial [17,18].

Gold is one of the most valuable precious metals in the e-wastes and its concentration is significantly higher in the e-waste than its ore [19,20]. It is more abundant in printed circuit boards (PCB) with its concentration almost 10 times higher than that in natural ore [19]. Each ton of waste PCB contains about 0.35 kg of Au and the economic value contribution of Au together with Pd in each ton of waste PCB is over 80% on average [18]. Due to its high demand [20-22] and market price [22,23], the recovery of gold from e-waste leachates and aqueous solutions has gained a serious attention in an economic point of view.

Currently activated carbon is a mainly used adsorbent for recovery of gold [23-25] but its high preparation and regeneration costs limit the application of this operation and make adsorption very costly [24]. Therefore, a need for more economical and cost-effective adsorbents is of utmost importance. The utilisation of waste material as precursors for generation of low-cost adsorbents is a good approach and more research is currently being done in this regard [6]. Carbonaceous adsorbents are in high demand and waste tyre rubber contains high carbon content hence they can serve as perfect raw material to produce carbonaceous adsorbents such as carbon black [6,26] and PT-char via pyrolysis and eventually to activated carbon [6,9]. The use of waste tyre rubbers as low-cost adsorbents for the removal of inorganics [26-30] and organics [26,27,31] from water and wastewater has also been reviewed by other authors. PT-char is not only used as a precursor for activated carbon [5,6,9] it is also being used as a catalyst for various catalytic reactions [32] and as carbon black in tyre production [33].

Using adsorbents derived from waste tyres (which are readily available and accessible in huge amounts on landfill) for recovery of gold could have a great contribution to valorisation of waste tyres for economic and environmental benefits. At the present moment, there is no work reported yet in literature for recovery of gold using waste tyre-derived char and crumb.

The scope of this project is summarized in *Figure 1-2*.

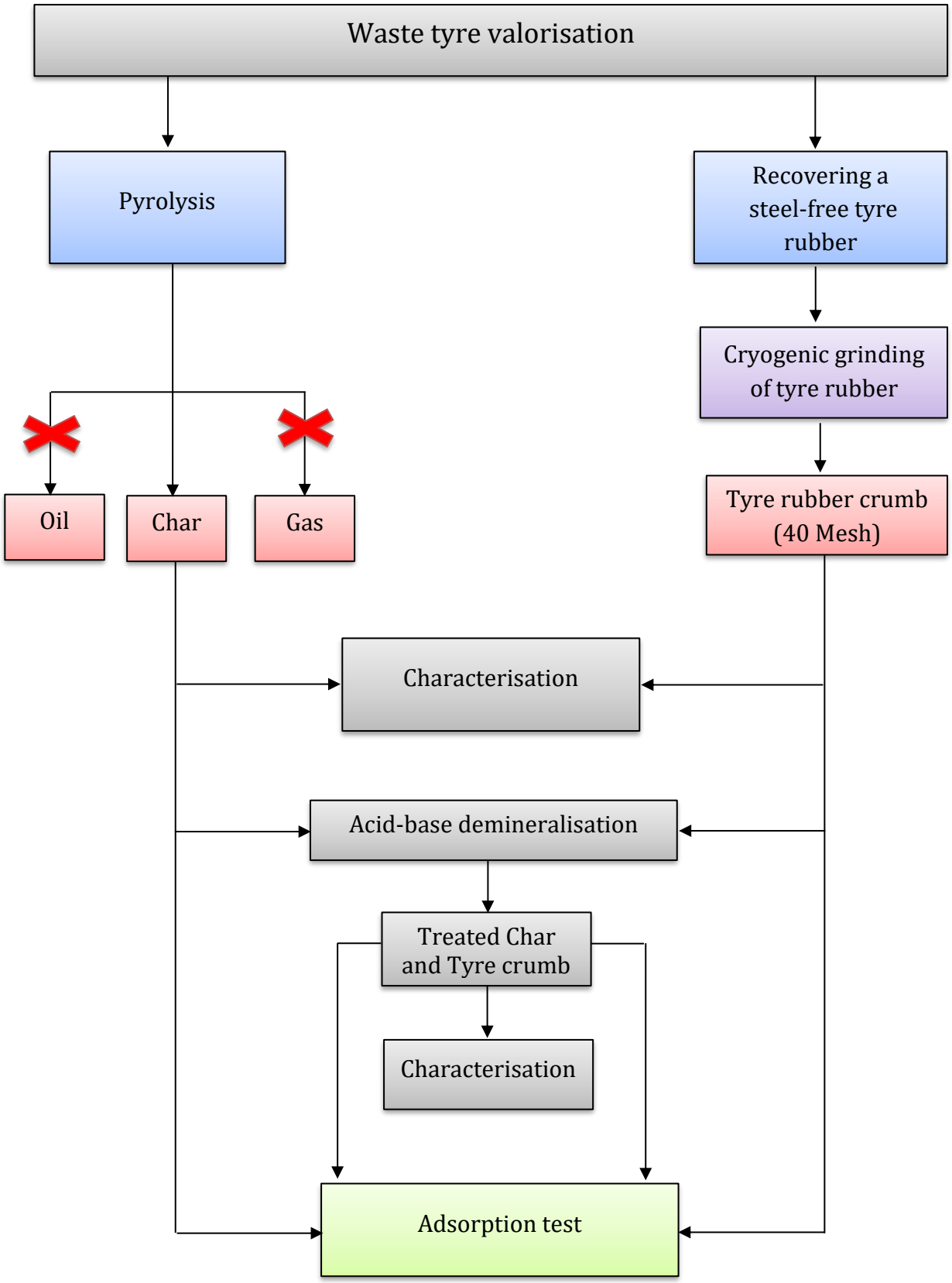

Figure 1-2: Overview of the project scope

2. LITERATURE REVIEW

There is a gap in literature concerning the use of low-cost waste tyre-derived adsorbents (PT-char and crumb) for adsorption of precious metals. In this thesis we aim to provide an in-depth state of the art of recovery of gold from acidic solutions using PT-char and tyre crumb adsorbents. PT-char and tyre crumb have high sulphur content which is considered to have desirable properties as an efficient chelating agent for metals and precious metals. The bonding mechanism of sulphur as a chelating agent with metals, particularly with gold, is well explained by Pearson using hard–soft acid–base (HSAB) theory in complex formation reactions. The HSAB theory suggest that sulphur forms strong and highly stable bonds with gold in water, organic solvents and air at room temperatures. Additionally, sulphur has a very high affinity for gold: therefore, adsorbents with high and accessible sulphur on their surface can enhance adsorption capacity and selectivity for gold ions [22,34].

2.1 Tyre overview

This section provides the necessary background of tyre structure and composition that may directly or indirectly affect the properties of waste tyre crumb (WT-crumb) and resultant PT-char as adsorbents for adsorption of gold. It is of utmost importance to understand the composition of waste tyres before any kind of treatment to understand the composition and characteristics of the resultant products after treatments such as demineralisation and pyrolysis.

2.1.1 Tyre structure

Tyres are composed of three basic materials: rubber, textile fibres and metal wire, as well as additional inorganic and organic components [3,35]. The typical cross section structure of a modern tyre is depicted in *Figure 2-1* [36] and all the components that are used to manufacture a modern tyre can add up to more than 200 components [37]. Some of the components of a tyre in *Figure 2-1* can be described briefly according to their functions and location in the following sentences. The *tread* is the part of the tyre that come directly in contact with the ground and is made of natural and synthetic rubber. It is purposely made to be resistant to traction and abrasion. *Liner* represents the interior walls/surface of the tyre made of synthetic rubber. *Ply or plies* are layers stacked together

to stabilise the tyre and can be classified according to their composition; belt plies are those composed of metal and rubber and casing piles are composed of nylon and rubber. The region of the tyre between the tread and the portion that is to be enclose by rim flange is called *sidewall*; it is composed of natural and synthetic rubber, additives and carbon black in small quantities [36,38]. The *tread grooves* are the spaces between the adjacent treads. *Bead* refers to ring-shaped steel wires covered with a hard rubber layer designed to fit and hold the tyre onto the rim. *Carcass* is the internal cord layer designed to support the load and *Chafer* is used to avoid damages of the carcass by protecting it from chafing by the rim [36].

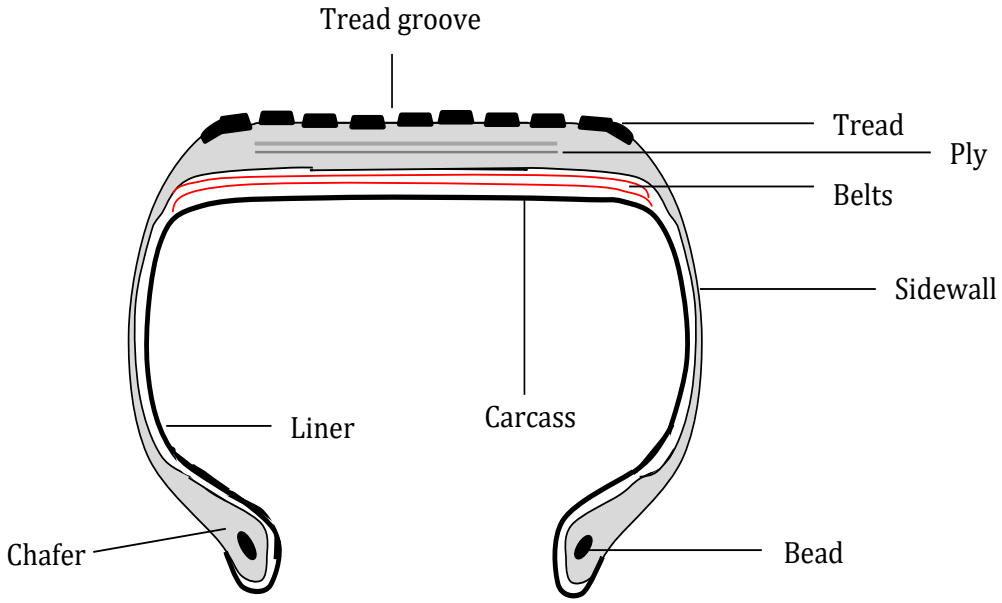

Figure 2-1: Typical structure of a modern tyre [36]

2.1.2 Tyre composition

The main components of the tyre are a rubber which constituents 60-65 wt.% and carbon black which constituents 25-35 wt.% of the total weight of the waste tire [39]. The total carbon content in carbon black is at least 70-75 wt.% [40,41]. The rubbery material is derived from the hardening of a mixture of elastomers together with other additives such as sulphur, carbon black and zinc oxide [40]. Tyre rubbers are hydrophobic, durable and resistant to degradation even during harsh weather conditions. The durability of tyre rubbers is due to its constituents such as amorphous silica and carbon black which is used as filler [36]. The elastomers which form part of tyre rubber constituents includes;

natural rubber (NR) and synthetic rubber (SR), the SR's are such as styrene-butadiene rubber (SBR) and butadiene rubber (BR). The natural rubber has special elastic properties and is a crucial element of a tyre [3,39]. The basic structures of the organic natural and synthetic rubber polymers used in tyre production are shown in *Figure 2-2*.

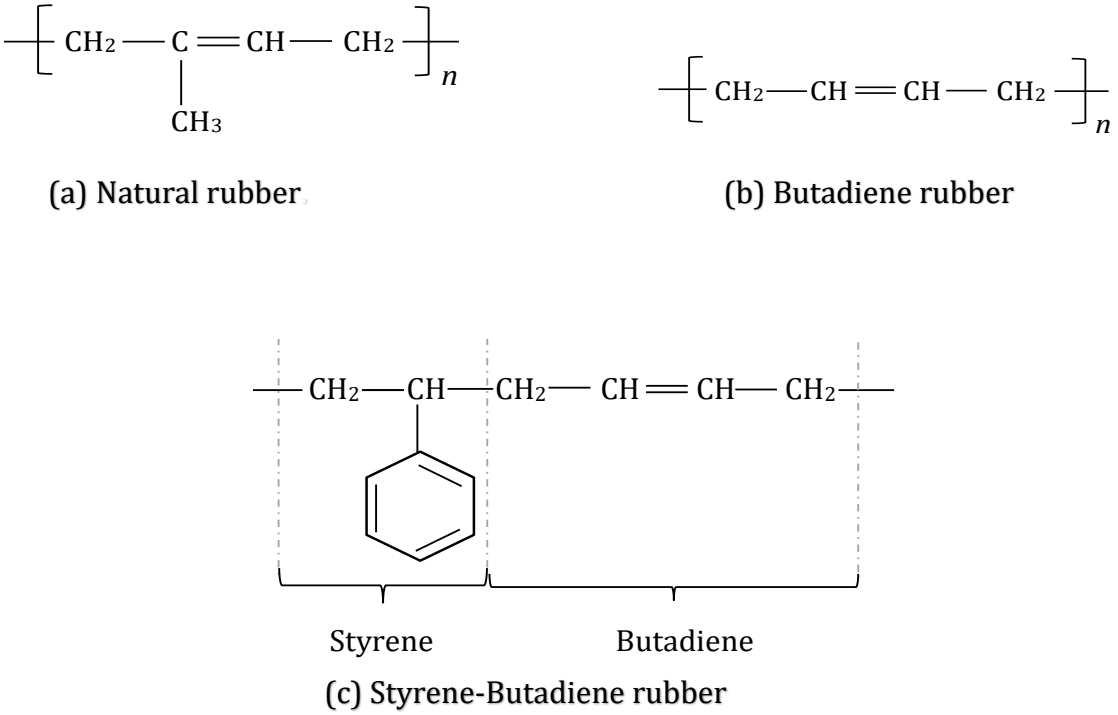

Figure 2-2: Rubber polymers used in tyre production (a) natural rubber, (b) butadiene rubber, and (c) styrene-butadiene rubber [42,43]

Sulphur content in tyre rubber plays a significant role of improving its performance and greatly affects its structure and properties. It is used to cross-link individual polymer strands through vulcanisation process *Figure 2-3* [45,46]. Vulcanisation can be defined as a chemical process that use vulcanising agents, activators and accelerators to form bridges (crosslinks) between organic polymer chains at high temperatures. In tyre production the vulcanising activators/agents are sulphur and zinc oxide that forms a three-dimensional network structures of rubber with great mechanical stability and durability [36,46]. The sulphur content in waste tyres is very high due to vulcanisation and evenly distributed both on the external carbon surfaces and throughout the whole material [47,48]. After pyrolysis of waste tyres, most of the sulphur in the tyres proceeds to and form part of the resultant pyrolytic tyre char with low surface area and poor pore

properties [47]. On the pyrolytic tyre char the sulphur may exist in different forms which may include sulphide, sulphate and organic sulphur (such as alkyl sulphide and thiophene groups), however ZnS is reported to be the most dominant [47].

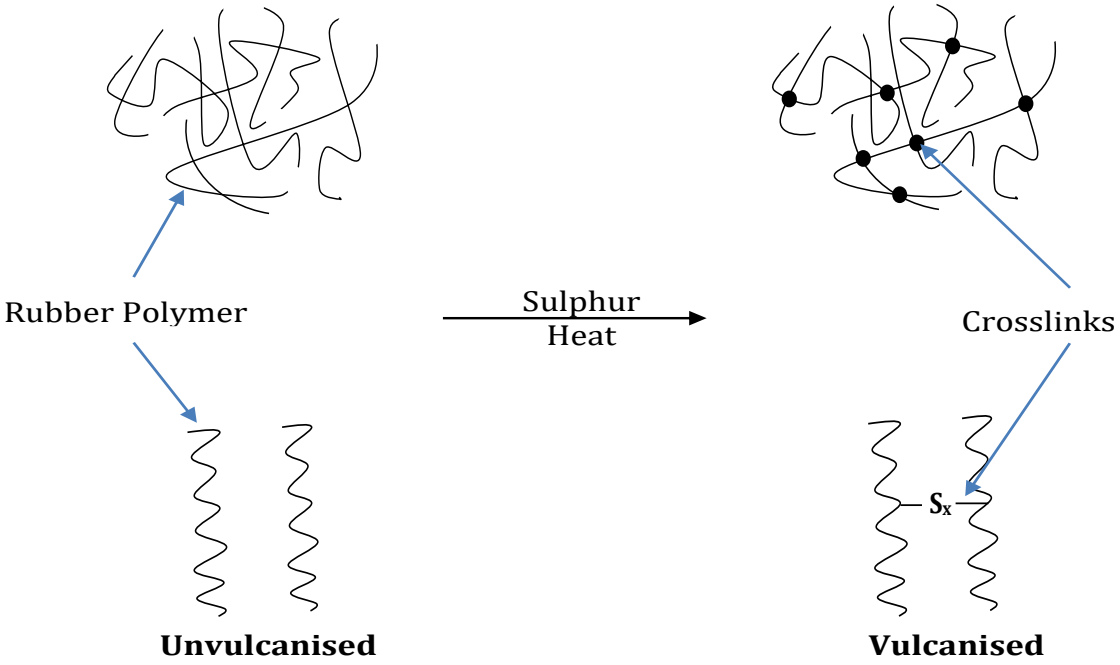

Figure 2-3: Sulphur vulcanisation of tyre rubber [46]

Tyres differ in properties and chemical composition based on the type of automobiles they are made for and the type of work they will be used for [35]. Additionally, the difference in tyre composition may be due to age and the tyre brand which cause variety in physicochemical properties of the resultant pyrolysis products [41]. The tyres in heavy vehicles are stronger than those in light vehicles and can be categorised as passenger car, truck, bus and agro tyres [35]. *Table 2-1* shows the comparison in composition between passenger car and truck tyres. *Table 2-2* shows the difference in natural and synthetic rubber content between passenger car tyre (PCT) and truck tyre (TT). The natural rubber is much higher in truck tyres than passenger car tyres [41]. In this study truck tyres were used for pyrolysis and as source of the rubber crumb.

Table 2-1: The comparison in composition between passenger car tyre and truck tyre [7,49]

Material	***Passenger car tyre (wt.%)***	***Trucks tyre (wt.%)***
Rubber	47	45
Carbon black	21.5	22
Metal	16.5	21.5
Textile	5.5	0–10
Zinc oxide	1	2
Sulphur	1	1
Additives	7.5	5

Table 2-2: The chemical composition of passenger car tyre and truck tyre [39]

Material	***Passenger car tyre (wt.%)***	***Trucks tyre (wt.%)***
Natural rubber	14	27
Synthetic rubber	27	14
Carbon black	28	28
Steel	14–15	14–15
Fabric, fillers, accelerators, antiozonants, etc.	16–17	16–17

2.2 Waste tyre management

Tyres are designed to be resistant to harsh weather and mechanical conditions such as light, bacteria and ozone (considered the most damaging feature on rubbers). The three-dimensional network structure of the tyre formed by crosslinked elastomers, cannot be damaged easily and it offers high strength and resistance to abrasion. These features make it difficult to degrade tyres and therefore, making it nearly impossible to manage waste tyres through recycling or other treatments [39].

The management of waste tyres is crucial to minimise environmental pollution and the landfill problem. Several approaches for waste tyre management have being suggested including; recycling, energy or chemical recovery, landfilling and reuse [39,50]. The search for techniques which will provide environmental and economic benefits to solve

the problem of waste tyre disposal is therefore in high demand and a priority according to constitution that governs waste management systems [39].

Disposal of waste tyre in landfills is surely not the best method and hence the European Union banned it. Recycling is insufficient to completely reduce the problem of waste tyre disposal single-handedly. The method of reuse can be used but its application is limited. However, energy recovery appears to be the best method for valorisation of waste tyres through thermochemical processes such as combustion, pyrolysis and gasification [39]. The most attractive and commonly used recycling process for waste tyres valorisation is pyrolysis.

2.2.1 Pyrolysis

Pyrolysis is an endothermic thermal degradation process carried out in the absence of air or oxygen (inert environment). It is currently an alternative and attractive method (both environmentally and economically) for recycling waste tyres due to its simplicity, environmental friendliness and production of potentially valuable products [51-55]. The temperature range to which thermal degradation usually occurs in pyrolysis is 400-800°C [54] and a typical temperature for pyrolysis is 500°C [39,49].

Pyrolysis conditions such as operating temperature, pyrolysis time, speed, feed size, pressure, rate of heat transfer, etc., have a great impact on product distribution and yield [52,54]. The physicochemical properties of the resultant pyrolysis products are also affected by these conditions [39]. Variations in temperature lead to changes in the state/phase of the products. High pyrolysis temperatures favour the yield of gases, whereas low temperatures favour the yield of liquid products. The rate at which heat is transferred and the pyrolytic decomposition speed also affect product distribution and yield. Slow pyrolytic decomposition (at low temperatures) favours the production of pyrolytic char [54].

In the pyrolysis of waste tyres, potentially valuable end products are formed which are in three distinctive states (i.e., liquid, solid and gas). The liquid product is usually organic oil (a mixture of olefins, paraffin and aromatics) which is normally used directly as fuel. And can give a calorific value of 28-44 MJ/kg more than that of wood charcoal, bituminous

coal and waste tyres. But there are other valuable liquid products that are produced from pyrolysis oil such as limonene. Then the combustible and non-condensable organic gases such as methane, ethene, propene, H_2, H_2S, CO, CO_2, etc. which can also be used as fuels in energy/heat-generating processes. Therefore, one of the advantages and huge contribution of waste tyre pyrolysis is recovery of energy. Lastly, the solid product is a highly carbonaceous solid material called char which constitute 30-40 wt.% of the original tyre weight [51-55].

2.3 Pyrolytic tyre char

Pyrolytic tyre char (PT-char) is a highly carbonaceous, amorphous, mesoporous [56], solid black and carbon-rich material produced from pyrolysis of waste tyres [51,52]. The PT-char is sometimes referred to as pyrolytic carbon black (pCB) and it is one of the three potentially valuable products of waste tyre pyrolysis [39]. The main contributor of the resultant char is the carbon black which was used as a filler in the tyre manufacturing and the rubbers only contribute a little to the char yield [49]. Williams [49] reported that only about 4 wt.% of char is produced from NR (polyisoprene), SBR, and polybutadiene rubber. It consists mainly of fixed carbon together with ash content which include the inorganic rubber additives (e.g., silica, zinc, and calcium) [39]. The organic matter of the feedstock is converted to char and some of the non-volatile hydrocarbons referred to as tyre derived oil (TDO) may be trapped within its porous quasi-graphitic structure [39,52]. It is expedient that the char produced is of great quality and yield to legitimise pyrolysis as one of the best ways for waste tyre valorisation [39].

Additional carbon deposits are usually formed on the char from organic vapours produced by pyrolysis which get adsorbed on the surface of the char. These carbon deposits result in particle sizes that are much coarser in PT-char as compared to its precursor carbon black. Consequently, the possibility is that during pyrolysis the carbon black particles may function as nuclei whereby subsequent carbon structures grow from it in an ordered manner through crosslinking and cyclisation [39].

2.3.1 Properties and composition

The pyrolysis conditions and the composition of the waste tyre feedstock mentioned earlier have a major contribution in the physicochemical properties of the resultant char

[39,49,57]. However, it is expected that the yield of the PT-char be equal to the initial carbon black plus the ash content after pyrolysis. Secondary reactions are also likely to occur during pyrolysis whereby the inorganic compounds previously present in the waste tyre feedstock react and affects the properties of the resultant char. The secondary reactions can be reduced by working under vacuum pyrolysis pressure which results in an increment in quantity of active sites of the resultant char and improvement of its surface area. It was mentioned by Martínez et al. [39] that Zhang et al. observed an improvement in the resultant char's surface area that was equivalent to the commercial carbon black, however, the ash content was much higher in the char. Another advantage of vacuum pressure in pyrolysis, it does not allow the volatiles to spend too much time within the porous structure by forcing them to diffuse quickly to the outside before they further react and form carbon deposits that may block the pores and occupy the active sites of the resultant char [39,49]. This observation suggest that the PT-char produced by vacuum pyrolysis could have equivalent carbon quantity as the original CB since at low pyrolysis pressure, the carbon deposits are not likely to form and adsorb onto the char's surface [39,58].

Cunliffe and Williams [59] and Conesa et al. [60] investigated the influence of pyrolysis temperature on the characteristics of the resultant char in a range of 450-1000°C and they discovered that the pyrolysis temperature have less effect on the sulphur and metal content. However, at higher temperatures the mesopore volume and surface area increased while the hydrogen and volatile content decreased. This is due to the widening of the micropores caused by loss of bulky hydrocarbons as temperature increased. As a result, the formation of mesopores led to an increase in surface area [59]. Conesa et al. [60] also reported that although the metal content remained the same as temperature increased from 450 to 750°C, but at 1000°C the Zn content of the char decreased by evaporation forming part of emissions.

PT-char is known to have high carbon, ash and sulphur content. The high carbon content is due to the CB filler and the high ash content is due to the inorganic metal additives used during tyre manufacturing with zinc being the highest in concentration. The high sulphur content is derived from vulcanisation of the rubber polymers during tyre rubber formation [33]. The carbon content in PT-char is reported to be as high as 90 wt.% while

the ash content ranges from 8.27 to 15.33 wt.% and sulphur content in a range of 1.9-2.7 wt.% [49]. Cunliffe and Williams [59] reported that a typical PT-char have a low surface area that is within 20-80 m^2/g range and contains ash content and sulphur content within a range of 7-16 wt.% and 2-3 wt.% respectively. Since the surface area of PT-char may be affected by the quality and type of waste tyre feedstock, Kyari et al. [61] investigated the effect of tyre brand and type on the surface area of the resultant char and they observed that indeed the surface area of the resultant char can be dependent on the tyre brand and type. The chars produced had variety of surface area within a range of 64.5-83.8 m^2/g [49]. The surface area of different PT-char reported in literature are presented in *Table 2-3*.

Carbon black has similar properties to activated carbon except for a notably lower internal surface area [39,65]. Carbon black in the waste tyre is about 32 wt.% with 70-75 wt.% carbon content [65]. The additional carbon deposits formed on PT-char during pyrolysis changes its surface morphology and chemical nature. Due to this type of modifications, the PT-char differs greatly in chemical composition, structure and morphology with its precursor carbon black [32,58]. However, some authors reported that the structure of PT-char is similar to that of graphite with an exception to the manner the graphene sheets are bonded to each other. The PT-char had deformities in its graphene sheets covalent bonding [9]. The surface area of different types of carbon black that are used in manufacturing of tyres are presented in *Table 2-4*.

Table 2-3: Surface areas of PT-char reported in literature

Pyrolysis temperature (°C)	***Surface Area (m^2/g)***	***Reference***
450	61.0	[59]
475	65.0	
500	64.0	
525	68.0	
560	67.0	
600	65.0	
500	73.5	[10]
600	77.6	
700	71.6	
550	56.5	[62]
650	63.5	
800	63.5	
650	47.5	[63]
500	64.0	[64]
500	67.9	[65]
500	69.5	[61]
450	93.0	[66]
425	46.5	[67]
600	116.3	[67]
500	83.0	[68]
500	63.0	[69]
500	65.2	[70]
550	72.0	[71]
550	68.0	[72]
900	61.0	[72]
550	32.0	[73]
800	100.0	[73]
550	64.0	[74]

Table 2-4: Surface areas of carbon black used in tyres reported in literature [75]

Name [a]	**Carbon black**	***Surface Area (m^2/g)***
Super abrasion furnace	N110	143
Intermediate SAF	N220	117
-	N234	120
-	N326	96
High abrasion furnace	N330	80
-	N339	96
-	N351	75
-	N375	105
Fast extruding furnace	N550	41
-	N660	34
-	N774	30
Medium thermal	N990	9

"[a]" *Reported by* [39]

2.3.1.1 PT-char metal content

The ash content "impurities" present in PT-char is derived from some of the inorganic components of the waste tyre which were retained during pyrolysis. The most abundant inorganic compound in PT-char is zinc oxides (ZnO) [33,49,56,59] which further reacts with sulphur to form ZnS during pyrolysis [4,57,58]. Darmstadt et al. [58] concluded that as the pyrolysis temperature is elevated, the more ZnO is converted to ZnS which eventually remains the only form of zinc on the surface of PT-char. In support of Darmstadt et al. [58] statement, Hu et al. [76] also reported that ZnS was the only sulphide detected in the PT-char samples produced below 800°C pyrolysis temperatures. ZnO, ZnS and Fe_3C are reported to be the only existing crystalline compounds in PT-char with ZnS in a form of discrete particles that can be easily removed from the PT-char organic matrix [58].

About 78 wt.% of sulphur in waste tyre feedstock is retained during pyrolysis which also form part of the ash content in PT-char [57]. Cunliffe and Williams [59] reported that upon the analysis of the ash content in the resultant char with X-ray fluorescence and atomic adsorption spectrometry (AAS), the main inorganic constituents were zinc, silica

and calcium. Other elements present were iron, titanium, potassium, aluminium, magnesium and phosphorus [59,77]. These elements may exist in a form of oxides, carbonates, salts, sulphates, or in their elemental form depending on their stability [77]. *Table 2-5* show some of the reported from chemical composition that are present in tyre char and crumb.

In PT-char, sulphur may react further on the char surface to form metal compounds with iron and zinc such as ZnS and FeS_2 respectively [77]. The metal content of PT-char reported in literature is presented in *Table 2-6*.

Table 2-5: Chemical composition of minerals found in carbonaceous materials [77]

Elements	***Possible chemical composition***
Zn	ZnS, ZnO, $ZnCO_3$
Si	SiO_2
Fe	Fe_2O_3, FeS_2, $FeCO_3$
Al	Al_2O_3
S	SO_3
Ca	$CaCO_3$, CaO, $CaSO_4$
Mg	MgO
Ti	TiO_2
Na	Na_2O, NaCl
K	K_2O, KCl
Cu	CuO

Table 2-6: Metal content of PT-char reported in literature

Ref.	**[78][a]**	**[59]**					**[60]**			**[38]**			**[79]**		**[32]**	**[4]**	**[80]**	**[63]**
PT (°C)	**-**	***450***	***500***	***525***	***560***	***600***	***450***	***750***	***1000***	***450***	***500***	***550***	***550***		***500***	***500***	***800***	***550***
Units	***wt.%***	***wt.%***	***wt.%***	***wt.%***	***wt.%***	***wt.%***	***wt.%***	***wt.%***	***wt.%***	***wt.%***	***wt.%***	***wt.%***	***wt.%***	***ppm***	***wt.%***	***ppm***	***wt.%***	***ppm***
Zn	40.8	3.6	4.1	3.7	4.0	3.5	6.68	6.33	0.935	6.68	4.1	4.06	22.0	2848.2	29.6	58539	6.5	20260
Si	27.9	1.0	0.9	1.1	0.5	1.4	1.69	1.64	3.66	1.69	0.42	-	52.0	3347.2	27.0	-	-	-
Ca	8.4	0.6	1.2	1.0	1.8	0.8	0.127	0.146	0.29	0.13	1.2	-	5.8	452.7	10.2	5894	0.95	3000
Fe	0.14	0.3	0.3	0.3	0.2	0.3	0.0393	0.057	0.108	0.04	0.2	0.54	1.3	76.9	2.1	1329	0.69	3820
K	0.05	0.1	0.1	0.1	0.1	0.1	0.0969	0.0958	0.225	-	-	-	0.7	80.0	0.1	937	0.05	800
Ti	-	0.02	0.02	0.04	0.02	0.04	0.0171	0.0201	0.0384	-	-	-	<2	33.0	-	-	-	-
Al	3.1	0.3	0.3	0.4	0.2	0.3	-	-	-	-	0.15	1.09	4.8	204.0	11.5	-	-	1380
Na	1.4	-	-	-	-	2.4	-	-	-	-	-	-	0.8	878.6	2.4	-	-	550
Cu	-	-	-	-	-	-	-	-	-	-	-	-	0.08	4.4	-	-	-	340
Mg	1.3	-	-	-	-	0.6	0.147	0.147	0.248	-	-	-	1.1	74.7	1.0	-	-	740
Pb	-	-	-	-	-	-	0.0109	0.0019	0.0019	0.01	-	-	-	30.0	-	-	-	110

"[a]" *Chemical analysis of ash in tyre rubber* [78]

"*PT*" *is the pyrolysis temperature*

2.3.1.2 Proximate and ultimate analysis

The knowledge in physicochemical properties of waste tyre-derived solid materials is very important and thorough qualitative and quantitative characterisation is required to understand their interaction with other substances when used. The composition of waste tyre crumb and the resultant pyrolytic tyre char can be determined through chemical, ultimate and proximate analysis [49,78]:

- **Ultimate analysis** can be used for qualitative analysis to determine the elemental composition of the solid samples, particularly carbon, hydrogen, sulphur, nitrogen and oxygen.

- **Proximate analysis** can be used to predict the ash content, fixed carbon, moisture content and volatile matter [81,82].

In ultimate analysis the carbon, hydrogen, sulphur and nitrogen can be determined experimentally, and the results obtained then be used to calculate oxygen content based on the weight difference according to the following equation.

$$\boldsymbol{Oxygen} = 100 - (Carbon + Hydrogen + Sulphur + Nitrogen) \quad (2.1)$$

And in the proximate analysis the ash content, volatile matter and moisture content can be determined experimentally, and the results obtained then be used to calculate fixed carbon content based on the weight difference according to the following equation [81].

$$\boldsymbol{Fixed\ carbon} = 100 - (Ash + Moisture + Volatile\ matter) \quad (2.2)$$

Chemical analysis provides information regarding the chemical composition of the material and coal is used as a reference carbonaceous solid material in this context. Khandelwal and Singh [18] stated that chemical composition of solid samples such as coal can either be determined by proximate or ultimate analysis; but, in their case both techniques were used in determining the chemical composition. The advantage of proximate analysis is that it is a simple technique that is operated with simple equipment at lower costs; however, ultimate analysis method is a sophisticated technique [83].

The ultimate and proximate analysis of tyre-derived rubber and the resultant pyrolytic tyre char are presented in (*Table 2-7* and *Table 2-8*, respectively) from literature.

Table 2-7: The ultimate analysis of tyre rubber and char from various authors

Material	***Carbon***	***Hydrogen***	***Nitrogen***	***Sulphur***	***Oxygen*** [a]	***Ref***
Tyre rubber	83.8	7.13	0.37	2.00	6.80	[78]
Tyre rubber	86.5	8.10	0.60	1.10	3.70	[84]
Tyre char	83.5	0.90	5.10	1.60	8.90	[63]
Tyre char	86.1	7.20	0.20	1.50	0.10	[85]
Tyre rubber	81.6	8.41	0.37	1.95	0.81	[4]
Tyre char (673)	80.3	2.12	0.27	2.44	7.66	
Tyre char (873)	81.3	1.76	0.24	2.33	4.15	
Tyre char (973)	83.5	1.57	0.25	2.51	1.80	
Tyre char (1073)	83.3	0.99	0.20	2.51	0.07	
Tyre char (1) [b]	82.4	1.16	0.24	1.67	5.68	
Tyre char (2) [b]	81.2	1.58	0.24	1.67	6.34	
Tyre char (3) [b]	78.6	1.16	0.20	2.26	8.88	
Tyre char (4) [b]	76.5	1.38	0.23	2.29	10.36	
Tyre char (1000-2000) [c]	81.2	1.58	0.24	1.67	6.34	
Tyre char (500-710) [c]	88.9	0.20	0.49	1.40	1.19	
Tyre char (550)	85.3	1.77	0.34	2.13	10.46	[86]
Tyre char (600)	85.6	1.33	0.28	2.32	10.47	
Tyre char (680)	85.2	0.93	0.22	2.57	11.08	

Tyre rubber	85.2	7.27	0.38	2.30	0.54	
Tyre char	80.3	1.30	0.30	2.70	15.4	[68]
Tyre char (500)	90.6	0.90	0.70	2.30	5.5	[59]
Tyre char (600)	95.9	0.80	1.10	2.30	-	
Tyre rubber	86.4	8.00	0.50	1.70	3.40	
Tyre rubber	89.4	7.00	0.20	2.00	1.40	[60]
Tyre char (450)	88.2	0.60	0.10	1.90	9.20	
Tyre char (1000)	92.1	0.17	0.00	1.23	6.50	
Tyre char (500)	82.2	2.28	0.61	2.32	12.68	[87]
Tyre rubber	84.1	6.71	0.49	1.51	1.73	[87]

"[a]" Calculated by weight difference
(Parentless) Pyrolysis temperature
(Parentless) [b] Pyrolysis time in hours
(Parentless) [c] Particle size in µm

Table 2-8: The proximate analysis of tyre rubber and char from various authors.

Material	***Volatile***	***Fixed carbon***	***Moisture***	***Ash***	***Ref***
Units	*wt.%*	*wt.%*	*wt.%*	*wt.%*	*wt.%*
Tyre rubber	63.2	30.2	0.9	5.7	[78]
Tyre rubber	63.8	27.0	2.0	7.2	[84]
Tyre char	61.6	33.5 [a]	2.0	2.9	[85]
Tyre rubber	61.3	33.5	1.2	5.2	[86]
Tyre char (550)	12.8	71.9	3.6	15.3	
Tyre char (600)	10.8	76.1	3.0	13.2	
Tyre char (680)	5.2	82.9	1.4	11.8	
Tyre char (500)	2.8	85.2 [a]	0.4	11.6	[59]
Tyre char (600)	2.3	85.2 [a]	0.4	12.1	
Tyre rubber	62.2	29.4	1.3	7.1	
Tyre rubber	65.5	29.4	0.9	3.7	[60]
Tyre char (450)	7.8	83.5 [a]	0.4	8.3	
Tyre char (1000)	1.1	93.0 [a]	0.3	5.6	
Tyre rubber	62.2	32.3	1.1	4.4	[87]

"[a]" *Calculated by weight difference*
(Parentless) Pyrolysis temperature

2.3.2 Possible applications of PT-char

The char produced from pyrolysis of waste tyres (WTs) has physicochemical properties that make it a potential material for many different applications. One of the most desirable properties of the resultant char is the high carbon content that it contains, however the high ash content of the resultant char lowers its market value. With proper post-pyrolysis treatments, the resultant char can be upgraded to a useful commercial material [88].

Pyrolytic tyre char is currently being investigated and processed to be used as a solid fuel due to its high calorific values within 25-34 MJ/kg range, carbonaceous adsorbent in wastewater treatment, low-cost activated carbon precursor, printing ink pigment or potential carbon black of low-grade as a rubber reinforcing filler [49,59,87]. Additionally, PT-char may be used as a filler in construction of road pavements and manufacturing tyres after being upgraded to carbon black [39,88]. Application of PT-char as carbon black is not widely practiced due to its undesirable properties that affects its reinforcing properties such as low surface area, organic impurities, large particle size, high ash content and lack of a suitable particle structure for rubber blending [39,57]. In tyre manufacturing, a carbon black with less than 0.5 wt.% ash content is a requirement [49].

Due to high sulphur content in PT-char and the ability of sulphur to act as a chelating agent for metals, PT-char materials are potential candidates for manufacturing of porous sulphur-impregnated carbonaceous materials with a variety of applications such as adsorbents and catalyst supporters [56].

A widely studied application of PT-char is its conversion to a powerful adsorbent such as activated carbon (AC) which have a variety of applications including waste water purification [59,63,88]. Activated carbons derived from waste tyres through activation processes with CO_2 and steam are reported to have high BET surface area of up to 1000 m^2/g [39,63,88]. The characteristics of the WT-derived activated carbon depend on the operating temperature of activation, type of activating agent (CO_2 or steam) used and the extend of activation. Activated carbons produced with steam activating agent have higher BET surface area than those activated with CO_2 which is attributed to the fact that the steam water molecules diffuse faster into the porous structure of char due to their smaller

size as compared to CO_2 molecules [88]. Surface area, pore size and volume are some of the key parameters that can predict how porous materials are likely to perform as adsorbents. The high surface area in activated carbons (within a range of 164-1260 m^2/g) and pore volume (as high as 1.62 cm^3/g) are desirable features that make them powerful adsorbents. The hierarchy of pores in the structure of AC with micro- and mesopores facilitate it in adsorbing large molecules such as dyes [88]. *Table 2-9* represent WT-derived activated carbons with different surface area.

Table 2-9: WT-derived activated carbon with different surface area [88]

Activation conditions (°C, h)	***Chemical treatment***	***Surface Area (m^2/g)***
925, 10.7	steam	1070
800, 24		346
850, 1.3		553
850, 0.5		164
900, 0.5		600
850, 3		1177
850, 4		1119
900, 3		272
877, –		528
935, –		640
850, 3		1000
850, 3		978
900, 1		1031
850, 3		888
850, –		1031
920, 1		607
900, 3		1260
875, 7	CO_2	270
900, 2		832
1000, 5		431
1000, 7		284
850, 1.5	KOH/N_2	820
700, 0		474

2.4 PT-char and tyre rubber crumb as adsorbents

Although PT-char is usually used as a precursor for AC, studies has also been conducted in the application of PT-char as a carbonaceous adsorbent for removal of pollutants such as heavy metals and organic dyes [26,88]. However, in many cases the PT-char is processed first before they are utilised either through gasification, oxidation or demineralisation to reduce the ash content and improve its surface chemistry, porosity and surface area. The improvements of these properties will enhance their adsorption performance [26].

Additionally, besides the use of WTs as precursor of char, CB and AC they are also used as carbonaceous adsorbent especially in removal of organic dyes and heavy metals in contaminated water [26]. This is due to the presence of considerable amount of carbon black and disulphide bond in WT rubber [39,78]. However, the surface area of tyre rubber crumb is quite small and ranges from 0.059 to 3.5 m^2/g. The accessibility of tyre rubber crumb is very limited and hence it would be nearly impossible for molecules to penetrate the internal surface area which can be a major drawback in adsorption [77].

Troca-Torrado et al. [26] studied the adsorption of phenolic compounds (phenol, p-chlorophenol, p-nitrophenol and p-aminophenol) and metallic ions (cadmium, lead, chromium and mercury) with used tyre rubber and carbonaceous adsorbents derived from it. The carbonaceous adsorbents were chemically treated with HNO_3, NaOH and HCl solutions and one sample labelled H900 was pyrolysed at 900°C under N_2 atmosphere environment for 2 h. Upon characterisation of these adsorbents, Troca-Torrado et al. [26] reported that their porosity was poorly developed with an exception of H900 sample. In their conclusion, they commented that the pyrolysed sample (H900) with well-developed porosity performed better for both the phenolic compounds and metallic ions.

Edward et al. [4] used PT-char in adsorption of Acid Yellow 117, Acid Blue 25 and Methylene Blue organic dyes and its performance was compared to a commercial microporous carbon (F400) adsorbent. They found out that even though commercial microporous carbon performed better, PT-char still had high adsorption capacity despite its very low surface area compared to the surface area of commercial microporous carbon which was 5.3% higher. Consequently, they concluded that surface area is not the only

parameter that determine the capacity of an adsorbent. Adsorption of some adsorbates may be influenced differently by specific properties of an adsorbent.

In an article published by Knocke and Hemphill [28] for adsorption of mercury (Hg) by waste tyre rubber, they reported that based on previous studies the high adsorption capacity of the rubber to mercury was attributed to the presence of disulphide bonds in the vulcanised tyre rubber. Additionally, based on previous studies the process of precipitating Hg with sulphur is efficient and rapid which form HgS of low solubility. However, in their own conclusion they reported that sulphur may be linked to adsorption of mercury, but it is not the only factor that facilitate mercury adsorption on vulcanised tyre rubber since mercury was also adsorbed on a sulphur-free rubber.

Lastly, a clear mechanism of mercury removal by sulphur containing PT-char pyrolysed at 600°C was investigated by Li et al. [47]. Other samples of the resultant char were acid treated with HNO_3 or H_2SO_4 which resulted in the improvement of the pore structure. They reported that sulphur on the surface of the resultant char predominately existed in a form of ZnS and the reaction of this compound with oxygen increased the active sites for the adsorption of Hg. Their major findings were that the adsorption of Hg was mainly due to the sulphur on the char surface. The mechanism behind involves the reaction of ZnS and oxygen first on the char surface which resulted in the formation of elemental sulphur. The elemental sulphur functioned as an adsorption site and reacted with Hg^o forming HgS. The adsorption of Hg on acid treated char decreased and the reason behind is that HNO_3 or H_2SO_4 acid reacts with sulphur during the acid treatment and reduce its concentration on the surface of the char consequently reducing the adsorption active sites for Hg [47]. The mechanism of Hg adsorption on the sulphur-rich PT-char surface is depicted in *Figure 2-4* redrawn from literature.

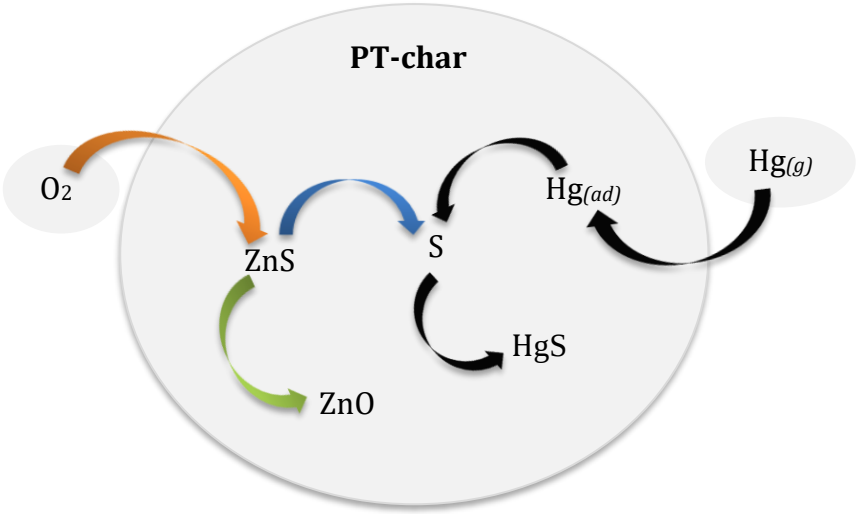

Figure 2-4: Mechanism of Hg adsorption on the sulphur-rich PT-char surface [47]

2.4.1 Benefits of high sulphur content in PT-char and tyre crumb adsorbent

Sulphur is used in type manufacturing to strengthen and improve the quality of tyre rubber. In WTs, sulphur is existing mainly in the form of inorganic sulphides and organic compounds characterised by C-S bonds such as thiophene [76]. As mentioned before that during pyrolysis of waste tyres, most of the sulphur is retained in the resultant char [47,76] while some may be released in a gaseous form (mainly H_2S) as part of pyrolysis gasses or it may be transferred into pyrolysis tar [76]. The sulphur that remained in the resultant char is predominantly existing in a form of inorganic sulphides [76]. Hu et al. [76] explained that according to their X-ray diffraction (XRD) results, the only sulphide detected on the char surface was ZnS and according to their X-ray photoelectron spectroscopy (XPS) results sulphates were also present on the char surface of samples produced at pyrolysis temperatures below 800°C. Additionally, another forms of sulphur compounds such as sulfones and thiophene were found in char.

In the application of carbonaceous materials, the surface chemistry plays a significant role and it must be suitable for the intended application. The surface chemistry and pore structures of porous carbon materials can be altered for a specific application. This may include grafting new functional groups on the surface and into the carbon matrix. An example of this is the incorporation of sulphur onto the carbon surface with H_2S chemical agent at elevated temperatures. However, the precursor of PT-char is WTs which already contain heteroatoms such as sulphur in its organic structure; therefore, the need for post-

treatment may not be necessary since the resultant char will already be functionalized which is an advantage on economic point of view [89].

Carbon materials can bind sulphur on their surface and those that bind covalently are very stable and resistant to breaking away from the carbon surface by solvents. The presence of sulphur on the carbon surface increase its polarity which facilitate the adsorption of heavy metals by ion exchange through chemisorption. Carbonaceous adsorbents rich in sulphur on their surface are reported to have high affinity for recovery of precious metals such as gold (Au). Pearson's theory suggests that the strong interaction between sulphur and heavy metals can be well explained by soft base–soft acid interaction concept. Normally, soft base prefers to coordinate with soft acid and hard base with hard acid during acid-base reactions. Sulphur is considered a soft base which would prefer to coordinate with soft acids such as heavy metals hence the strong affinity. It is worth noting that the chemical nature of the carbon surface greatly influences the rate and capacity of adsorption [89].

In some cases when sulphur is not covalently bound to the carbon matrix of the adsorbent may call for concern since the sulphur will be leached into the solution during adsorption and results in low adsorption capacity [89].

In conclusion, despite the poor pore structure and low surface area of PT-char and tyre rubber crumb, the high sulphur content is advantageous for these carbonaceous solids as adsorbents for the adsorption of heavy metals and precious metals. It creates binding sites for metals which increase adsorption capacity and rate.

Highlights: Since zinc is in abundance in WTs as ZnO, it reacts with sulphur to form ZnS which form discrete crystalline particles that are easily removable [4,58,76]. This reaction is the reason there is high ash and sulphur content in the resultant char [4]. During pyrolysis, the high zinc content trap and immobilise sulphur from escaping into pyrolysis tar and gas by forming thermally stable sulphides which then results in high sulphur content in char than pyrolysis tar and gas [4,76].

2.5 Upgrading PT-char and tyre crumb

A major drawback in application of PT-char is its high ash content [57,77] and to reduce the ash content and possibly improve its market value, demineralisation as a purification approach is employed [6,9,27,32]. It is expedient that the char produced is of great quality to legitimise pyrolysis as one of the best ways for waste tyre valorisation [39]. The application of PT-char as a carbonaceous adsorbent might be affected by the inorganic ash content and the condensed tyre derived oils which block its pore structure and reduce its surface area [32,77,88]. With proper and effective demineralisation, PT-char can be upgraded to a commercial carbon black or to a carbonaceous adsorbent with improved surface area and well-developed pore structure (i.e., increased micro- and mesopore volumes) [77,88].

The chemical treatment of tyre rubber crumb is usually difficult to conduct since the sulphur cross-linked organic polymers offers properties that make tyre rubber resistant to chemicals, heat and degradation [77].

2.5.1 Demineralisation

Demineralisation can be defined as a process of removing minerals and mineral salts from a solid material using acidic, neutral and basic aqueous solutions. The contact between the permeable and insoluble solid material with a liquid lixiviant results in complete or partial removal of the undesired soluble substances. The fundamental mechanism involved in demineralisation is; first, the physical contact between the solvent (liquid lixiviant) and the solid material. The solvent then permeates within the porous solid matrix through its pores by diffusion and chemically interacts with the undesired soluble substances on the solid surface. The liquid lixiviant dissolve the soluble substances which then diffuse into the solution from the solid [77]. The pregnant solution and the solid material can easily be separated by filtration. The schematic diagram representing the demineralisation mechanism is presented in *Figure 2-5*.

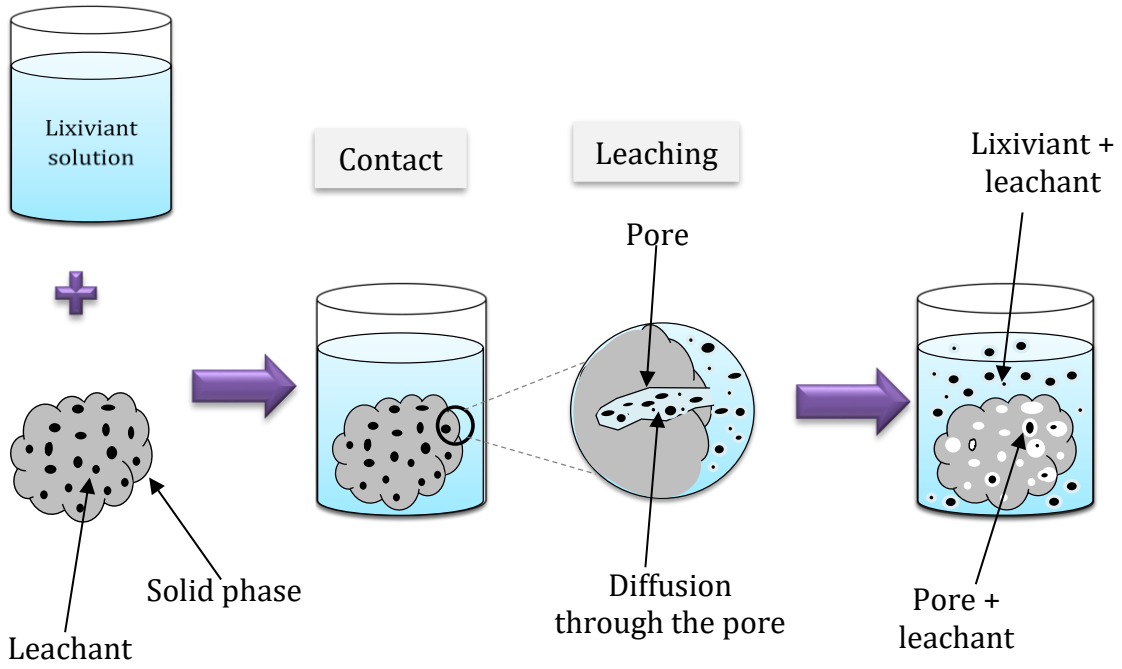

Figure 2-5: Basic demineralisation mechanism [77]

Demineralisation can be affected by various parameters such as operating temperature, solvent type, solution pH, leaching rate, contact time, solid surface area and particle size [32,77]. The solvent chemical nature is important, and the best solvent is picked based on its strength and ability to dissolve as many soluble as possible. The solvents used in demineralisation are categorised into three classes based on pH. The solvent of pH lower than seven, equal to seven and higher than seven are classified as acidic, neutral and alkaline respectively [77]. In this work the focus is on acidic and alkaline solvents.

2.5.2 Solvents

2.5.1.1 Alkaline

Based on literature survey, sodium hydroxide (NaOH) is reported to be the best alkaline solvent for demineralisation among other well-known alkaline solvents such as KOH, NH_4^+, $Ca(OH)_2$ and Na_2CO_3. Sodium hydroxide is likely to dissolve some elements present in tyre rubber crumb and PT-char, most especially alumina and silica with the possibility on some sulphur-containing compounds. These interactions can be explained according to the following reaction equations [77]:

$$SiO_2 + 2NaOH \longrightarrow Na_2SiO_3 + H_2O \quad (2.3)$$

$$Al_2O_3 + 2NaOH \longrightarrow NaAlO_2 + H_2O \quad (2.4)$$

2.5.1.2 Acidic

Acids are the most used and efficient solvents in demineralisation due to their corrosive nature and ability to dissolve many metals. This is because majority of these metals react only with acids since they are basic in nature. Various acids are reported in literature from weak (e.g., HNO_3 and HF) to strong acids (e.g., H_2SO_4 and HCl) [77].

According to Seng-eiad and Jitkarnka [9] the use of nitric acid in acid treatment of PT-char was successful and able to demineralise the char from Zn, Ca, K, P, Si, Mg, Fe, Al, Na, elements and improved its surface area. They also reported that after the treatment with HNO_3 the char's pore size and surface acidity increased and unlike with other acids its pore structure was preserved. The increment in HNO_3 treated char's total surface acidity was due to the introduction of more carboxyl (-COOH) groups upon the char surface. Since nitric acid can act as an oxidizing agent [77] thus the introduction of more carboxyl (-COOH) groups is caused by oxidation of the carbon surface of the char by nitric acid. Moreover, nitric acid greatly reduced the Zn and S elements which are derived from ZnS compound from the char surface [9].

Li et al. [47] studied the effect of H_2SO_4 and HNO_3 acid treatment on the properties of PT-char. The acid treatments increased the surface area and micropore volume of the char which is significant in adsorption. An increase in fixed carbon and decrease in ash content was also observed which are likely to improve PT-char quality and market value as either a carbonaceous adsorbent or carbon black. Ash and sulphur content were greatly reduced with HNO_3 acid treatment than H_2SO_4 [47]. As mentioned before that nitric acid is an oxidizing agent, there is a possibility that it can change sulphide to sulphate. Both acids resulted in an increase in oxygen-containing function groups on the char carbon surface, particularly with HNO_3 acid treatment [47].

2.5.1.3 Alkali-acid demineralisation

Since some elements in PT-char and tyre crumb can only be dissolved by either acids or alkaline only; therefore, it would be beneficial to treat the materials with both acid and alkaline solvents for efficient demineralisation [90]. Aslam et al. [91] studied the acid-base demineralisation of PT-char using NaOH and a variety of acids and acid mixtures such as sulphuric acid (H_2SO_4), Hydrochloric acid (HCl), Nitric acid (HNO_3) and aqua regia. They concluded that acid-base demineralisation of PT-char was efficient in reducing the ash content, consequently increasing its surface area. Lastly, they reported that the maximum activation of PT-char through alkali-acid demineralisation was achieved when using HNO_3 and NaOH in 1:1.

2.6 Adsorption

Adsorption is basically a mass transfer process whereby an adsorbent (usually solid substances) interact with an adsorbate on the surface of the adsorbent. This involves the accumulation of adsorbate into the porous solid adsorbent. The solid material that carries out adsorption is called adsorbent and the one that is being adsorbed is called adsorbate. Adsorbent and adsorbate interaction may be; liquid-solid, gas-solid, liquid-liquid or gas-liquid interfaces [90].

Adsorption can be classified as chemical adsorption (chemisorption) or physical adsorption (physisorption) depending on the value of adsorption enthalpy. The adsorption enthalpy for physisorption is usually less than 50 kJ/mol and greater than 50 kJ/mol for chemisorption. Physisorption occur due to weak van der Waal forces such as dispersion forces, induction forces and dipole-dipole interactions. Whereas chemisorption occurs due to chemical reactions between the adsorbate and the adsorbent surface-active sites [91].

The reverse process of adsorption is referred to as desorption and it can be attained by changing the properties (such as pH, concentration and temperature) of the aqueous solution used as the medium of adsorption. The basics of adsorption and desorption processes are depicted on *Figure 2-6* [91].

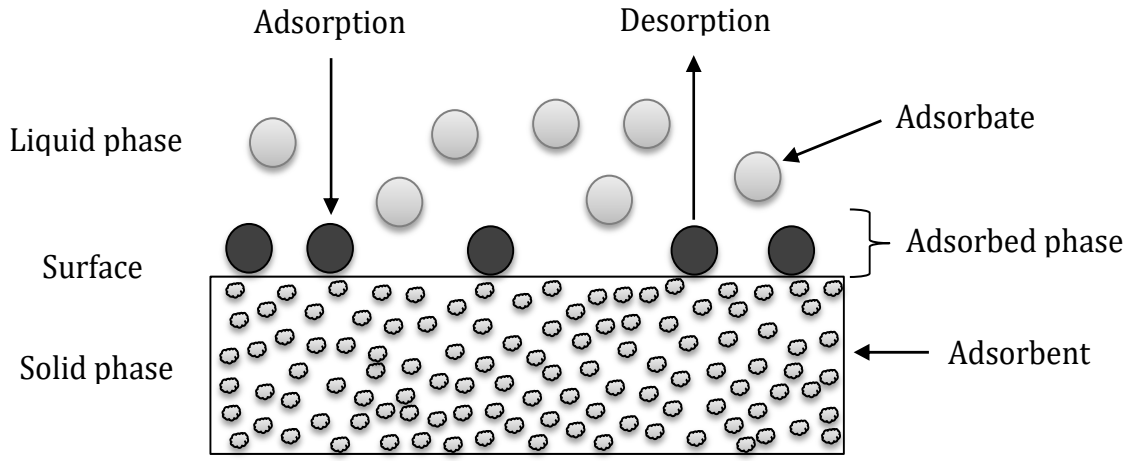

Figure 2-6: Basic terms of adsorption [91]

2.6.1 Adsorption of gold

There are several techniques in literature that have been investigated and applied for recovery of gold such as adsorption [21,22], cementation [22], membrane filtration [21], ion exchange [21,22], and precipitation [20] from various aqueous solutions. Most of these techniques have shortcomings such as production of toxic sludge, environmentally unfriendliness, high maintenance and high operational costs. However, among them adsorption was proven to be the most suitable technique due to high efficiency (even in very low concentrations of ppm) [21,24], simplicity in operation and implementation [24] and low operational costs [21,22,24].

Gold exist in different forms in leachates and aqueous solutions depending on the method used for the chemical leaching. *Table 2-10* shows different leaching methods of gold from e-wastes and the resultant stable gold form in the solution. As seen from table 1, most of the leaching methods results in the formation of an anionic gold complex in the leachate solutions. An alkaline cyanide leaching commonly referred to as cyanidation is a commonly used leaching method for precious metals including gold from their ores [92]. Recently, aqua regia method is usually preferred over other leaching methods due to its environmental friendliness, efficiency and low costs. Using this method results in the formation of chloroauric acid ($HAuCl_4$), which is present and adsorbed in leachate solutions as an anionic chloride complex ($AuCl_4^-$) [93].

The step by step chemical reactions that occur during gold leaching or dissolution with aqua regia are presented in *Equations (2.5)-(2.7)*.

$$2HNO_3 + 6HCl \rightarrow 2NO + 4H_2O + 3Cl_2 \quad (2.5)$$

$$2Au + 3HNO_3 + 9HCl \rightarrow 2AuCl_3 + 3NOCl + 6H_2O \quad (2.6)$$

$$HNO_3 + 3HCl \rightarrow NOCl + 2H_2O + Cl_2 \quad (2.7)$$

Table 2-10: Different leaching reagents and the resultant gold form in the solution

Leaching reagents	***Gold ionic complex formed***	***Ref***
Bromine leaching	$AuBr_4^-$	[94]
Aqua regia	$AuCl_4^-$	[95]
Ammonium thiosulfate	$Au(NH_3)_2^+$ or $Au(S_2O_3)_2^{3-}$	
Thiourea	$Au(CS(NH_2)_2)_2^+$	
Iodine–iodide	AuI_2^-	[96]
Cyanidation	$Au(CN)_2^-$	[97]
Glycine	$Au(NH_2CH_2COO)_2^-$	[98]

The major problem with the selective adsorption of gold in the leachates is the interference of other metals that are also leached during the process [18,93,99]. Therefore, adsorbents with high selectivity are required to selectively adsorb gold ions in the midst of all the co-existing metals. On many occasions the co-existing base metals such as Ni(II), Fe(III) and Cu(II) are present as neutral or cationic species unlike the precious metals which exist as anionic chloride complexes after aqua regia leaching [18,99].

Since base metals and precious metals in the leachate solutions coexist in different ionic states, then the selective adsorption of precious metals from base metals can easily be attained by the manipulation of the solution pH. Highly acidic solutions would favour the adsorption of precious metals over base metals. This is due to the protonation of the adsorbent's surface in very low pH conditions making it positively charged and strongly

attracting negatively charged species by electrostatic interactions. The positively charged base metals suffer the electrostatic repulsion from the adsorbent's positively charged surface. Many publications demonstrated that adsorption of gold is highly favoured in very low pH acidic chloride solutions [99-101].

The concentration of hydrochloric acid in Au(III) solution is very important as it is a source of chloride ions which inhibit the precipitation of gold and favour the formation and adsorption of $AuCl_4^-$ [102]. Chand et al. [99] reported that the adsorption of coexisting Pt(IV) and Pd(II) decreased as the concentration of HCl was increased from 0.1 M to 6.0 M, due to their competition with chloride ions during adsorption. However, Au(III) remained constant throughout. Yang et al. [102] also reported that Au(III) adsorption increased as the HCl concentration increased.

The surface functional groups of carbonaceous adsorbents play a vital role in facilitating the adsorption of an adsorbate. A hydrophilic surface and the presence of polar oxygen-containing functional groups on the adsorbent surface are advantageous since they enhance the hydrogen bonding and ion-exchange between an adsorbate and adsorbent during adsorption [100].

It was reported by Gao et al. [101] that carboxyl (-COOH), hydroxyl (-OH), grafted -C=S and amino functional groups are the main binding sites for gold ions with oxygen, nitrogen and sulphur being the active elements. They also reported that the hydroxyl functional group of the bio-sorbent used was responsible for the reduction of gold from Au(III) to Au(0) and lastly precipitated the reduced form to nanoparticle colloids.

2.6.2 Mechanisms for adsorption of gold

The interaction between the metal ions and the adsorbent's functional groups can happen in different mechanisms and the possible adsorption mechanisms for gold could be ion-exchange, complexation, reduction, electrostatic interaction and chelation [101]. The bonding mechanism of gold is well described by according to hard-soft acid-base (HSAB) theory. This theory suggest that soft acid prefers to bond with soft base and hard acid with hard base. Gold is a soft acid which preferably tend to bond with soft Lewis base such as sulphur [22].

The strong affinity between gold and sulphur has opened doors for applications of sulphur-containing adsorbents such as sulphur-impregnated activated carbon [92], molybdenum disulfide nanoflakes [103], sulfur-grafted chitosan [34], thiol-ene hydrogel [104], thioctic acid functionalized silica coated magnetite nanoparticles [22], which displayed high selectivity and high adsorption capacity for gold. However, the drawback of these adsorbents is their complicated and expensive preparation, as well as low accessible sulphur content.

The mechanism of electrostatic interaction, chelation and reduction were briefly explained by Gao et al. [101] from the results they obtained. They indicated that the nitrogen and oxygen containing groups such as $-NH_2$, C–O–H and C–O–C facilitated the adsorption through the electrostatic interaction mechanism. This mechanism is dependent on the solution pH in which under highly acidic conditions the above-mentioned groups become positive centres due to protonation. The metal ion species are then attracted or repelled (depending on their ionic state) by the electrostatic force [101].

They also indicated that for the chelation mechanism; nitrogen, oxygen, and sulfur were the active elements for chelation between anionic metal chloride complexes (e.g. $AuCl_4^-$) and the adsorbent. The nitrogen-bearing group was the amino group, for oxygen was carboxyl and hydroxyl groups and for sulfur was the –C=S group [101]. Lastly, for the reduction mechanism the active group was hydroxyl functional group which reduced aqueous gold from Au(III) to metallic gold Au(0) through the oxidation of hydroxyl to aldehyde group following the reaction scheme below [101,105]:

$$2AuCl_4^- + 3RCH_2OH \rightarrow 2Au(0) + 3RHCO + 6H^+ + 8Cl^-$$

2.7 Gold desorption

Desorption or elution of the adsorbed gold is a very crucial step in recovery of gold. The elution process ought to be efficient and not damage the structure of the adsorbent for a successful application. Among other chemicals used for elution of gold, the mostly used are hydrochloric acid and thiourea and sometimes the mixture of the two. The ability of thiourea to form complexes with Au(III) due to the presence of sulphur and nitrogen makes it an efficient and widely used chemical in elution of precious metals [22].

Other elution methods used include incineration which is burning off the gold-adsorbed adsorbent and the reduced gold remains. Yang et al. [102] applied incineration on cellulose acetate adsorbent and the adsorbed gold was recovered in a metallic form.

The widely used gold elution process on activated carbons is Zadra process which uses hot solutions of 0.2% w/v NaCN and 1% w/v NaOH for duration of 72 h at temperature range 95-100 °C [106]. Alternatively, the Anglo elution procedure can be used which use deionised water at temperature range 100-120 °C with 1% w/v NaOH and 5% w/v NaCN. Feng et al. [106] investigated the ultrasonic radiation method on gold-adsorbed activated carbon and found that it enhanced the gold recovery and the kinetics of elution.

Yi et al. [18] also used acidic thiourea to desorb the adsorbed precious metals, Au(III) and Pd(II), from the adsorbent surface and found it to be efficient. However, in this study the elution process of gold is excluded but strongly recommended for future study.

Conclusion

In conclusion, the combination of HNO_3 and NaOH might be the best chemical agents for demineralisation of tyre-derived carbonaceous solids material. The advantages offered by using HNO_3 is the improvement of PT-char surface area, surface acidity, pore size and preservation of the pore structure. Nitric acid is also a good oxidizing agent and nitrogen source which can also act as a binding site for Au(III) ions. However, a disadvantage of using HNO_3 acid in this case would be the removal of sulphur which is a key binding site for Au(III) ions.

Treating PT-char first with NaOH will dissolve some elements, reduce ash and form hydroxides which can be dissolved with HNO_3 used on the second stage of demineralisation. HNO_3 also oxidise the char carbon surface which introduce functional groups that might increase its adsorption capacity. Therefore, it is beneficial to use acid-base demineralisation method.

3. RESEARCH QUESTIONS, AIM AND OBJECTIVES

3.1 Research question and aim

In this research project, the answers for the following questions, which are obtained based on a comprehensive literature survey, are critically investigated and provided through research. The research questions are mainly based on novelty, economic and environmental benefits. Therefore, the aim of this study is to investigate the application of waste tyre-derived pyrolytic char and waste tyre rubber crumb as possible alternative low-cost adsorbents for adsorption of gold in a form of gold chloride complex ion, $AuCl_4^-$, from acidic solutions.

1. What is the maximum adsorption capacity of pyrolytic tyre char and tyre rubber crumb for adsorption of gold from acidic solutions?

2. Can the high sulphur content in pyrolytic tyre char and tyre rubber crumb be beneficial for adsorption of gold as predicted in literature?

3. What are the best operating parameters for adsorption of gold from acidic solutions with pyrolytic tyre char and tyre rubber crumb as adsorbent?

4. Which isotherm and kinetic model best describe the adsorption of gold by pyrolytic tyre char and tyre rubber crumb?

5. Would the demineralisation of pyrolytic tyre char and tyre rubber crumb improve their adsorptive capacity for gold?

3.2 Objectives

1. Investigate the effect of the minerals present on the surface (of crumb and char) on the adsorption capacity

2. To evaluate and identify the best pH, adsorbent dosage and contact time for adsorption of gold with PT-char and tyre rubber crumb

3. Analyse the effect of sulphur content of crumb and char on the adsorption capacity

4. Evaluate the effect of acid-base demineralisation on the adsorption of gold with PT-char and tyre rubber crumb

5. Investigate the possible applications in which crumb and char can be used before undergoing expensive treatments

6. Evaluate the effect of acid-base demineralisation on the physiochemical properties of PT-char and tyre rubber crumb.

7. Compare the performance of PT-char and tyre rubber crumb with adsorbents reported in literature based on adsorption capacity.

4. RESEARCH METHODOLOGY

Introduction

This section provides all necessary details of methodology and materials used to achieve the main goal of this project through the objectives listed in section 3.3 as guideline.

4.1 Adsorbent preparation

In this work four different adsorbents were used all derived from the same source which is waste truck tyres but subjected to different conditions and applied as different materials. The adsorbents that were used are; UT-crumb, TT-crumb, UPT-char and TPT-char. The T-crumb which was used in this work is obtained from (EnviroServ, Western Cape) in South Africa. The same T-crumb was used as a precursor to acquire a pyrolysed tyre derivative carbonaceous solid material (PT-char) through pyrolysis. Additionally, the PT-char and T-crumb were also used as precursors to obtain TPT-char and UT-crumb through alkali-acid demineralisation process. The pyrolysis of the tyre crumb was carried out in temperature range of (500–550 °C) with fast pyrolysis method. The pyrolysis reactor used was fluidising bed reactor which used nitrogen gas as a fluidising gas and sand as fluidising agent. Before the crumb can be used for pyrolysis, a stainless-steel sieve was used to attain uniform particle size of the crumb to be 10 Mesh (2 mm) for pyrolysis. A 40 Mesh T-crumb was used for adsorption tests.

4.2 Alkali-acid demineralisation

This section includes the demineralisation of PT-char and T-crumb to obtain treated PT-char (TPT-char) and treated T-crumb (TT-crumb). The leaching of metal content in tyre char and crumb was carried out with 1M NaOH and 1M HNO_3 at 90 °C for 24 h at mass to volume ratio of 1g/12ml. The choice of each parameter and solvents were carefully studied in literature and chosen based on the main goal we intended to achieve. The main goal of the acid-base demineralisation is to improve the tyre-derived char and crumb in application as carbonaceous adsorbents for gold ions in acidic solutions. The objective of this treatment is to evaluate the effect of the metals present on the surface of tyre char and crumb. Our research team also worked in the optimisation of parameters such as operating temperature, contact time, solvent concentration, solvent type and mass to volume ratio.

In the chemical treatments, 15 g of PT-char or T-crumb was placed in a 250 mL Schott bottle and 180 mL of 1M NaOH solution was added. The system was allowed to react at 90 °C for 24 h under continuous agitation with a magnetic stirrer bar throughout the reaction time on a heating plate. After 24 h the solid and solvent mixture was separated through vacuum filtration as illustrated in *Figure 4-1*. After that, the resulting solid products were thoroughly washed with distilled water until neutral pH is attained in the residual liquid. The char adsorbents were oven-dried at 120 °C and crumb at 60 °C for 24 h. The 1M NaOH treated char and crumb were then treated again with 1M HNO_3 following the same procedure and the adsorbents were stored in a plastic container. For comparison purpose, other experiments were conducted at a lower scale using 1 g of PT-char and T-crumb with 1M NaOH and HNO_3 solvents following the same procedure. All experiments were repeated twice and carried out in a fume hood.

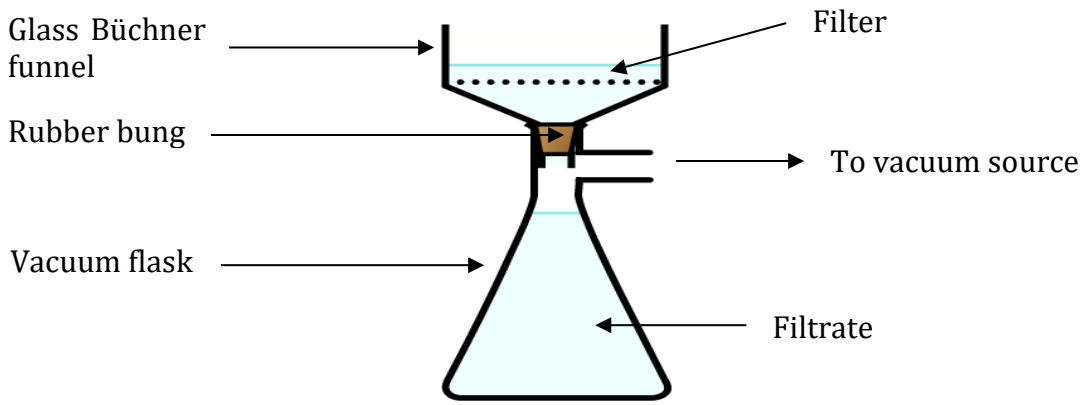

Figure 4-1: Vacuum filtration diagram

4.3 Aqua regia

Aqua regia is a mixture of concentrated nitric acid (HNO_3) and concentrated hydrochloric acid (HCl) in a molar ratio of 1:3. The mixture forms an extremely corrosive yellowish solution according to the following chemical reaction [107];

$$1\ HNO_{3\,(aq)} + 3\ HCl_{\,(aq)} \rightarrow NOCl_{\,(g)} + Cl_{2\,(g)} + 2\ H_2O_{\,(l)}. \quad (4.1)$$

Chlorine (Cl_2) and nitrosyl chloride (NOCl) are volatile gases and nitrosyl chloride can decompose further into nitric oxide gas (NO_2) and chlorine;

$$2\ NOCl_{(g)} \rightarrow 2\ NO_{(g)} + Cl_{2\ (g)}. \quad (4.2)$$

Aqua regia digestion is usually used to determine the total extractable metal content in different samples such as soil and for this reason it is oftentimes referred to as pseudo-total digestion [108,109].

4.3.1 Aqua regia preparation

The aqua regia solution was prepared with concentrated HNO_3 and concentrated HCl acid in a molar ratio of 1:3. The properties of the acids used are presented in *Table 4-1* below.

Table 4-1: Properties of nitric acid and hydrochloric acid

Acids	***Assay (%)***	***Molar Con. (M)***	***Density (g/mL)***	***Molar mass (g/mol)***	***Supplier***
HNO_3	55	11.69	1.34	63.01	Merck chemicals
HCl	32	10.18	1.16	36.46	SCIENCEWORLD

About 23.5 mL of concentrated HCl was measured with a 1-10 mL pipette and placed into a 100 mL beaker. The same pipette was also used to measure about 6.8 mL of concentrated HNO_3 which was added dropwise into the beaker containing concentrated HCl in a fumed hood. The mixture was agitated slowly until the solution colour changed to yellow.

NB: Do not add concentrated hydrochloric acid into concentrated nitric acid!

4.3.2 Aqua regia digestion methodology

The methodology for waste tyre crumb and pyrolytic tyre char aqua regia chemical treatment was adopted from literature [110]. The conventional aqua regia digestion was carried out in 100mL Schott bottles at mass to volume ratio of 1:15 (g/mL) for both samples. The 1g sample was mixed with 15mL aqua regia solution and heated at 110 ^{0}C on a hotplate with stirring using magnetic stirrer bar for 3 hrs. The pregnant solution was

allowed to cool down before slowly opening the bottle. The solution was then filtered through Double Rings no. 103 (12.5cm) filter paper and stored in 100mL Schott bottles. The aqua regia digestion procedure is represented in *Figure 4-2*

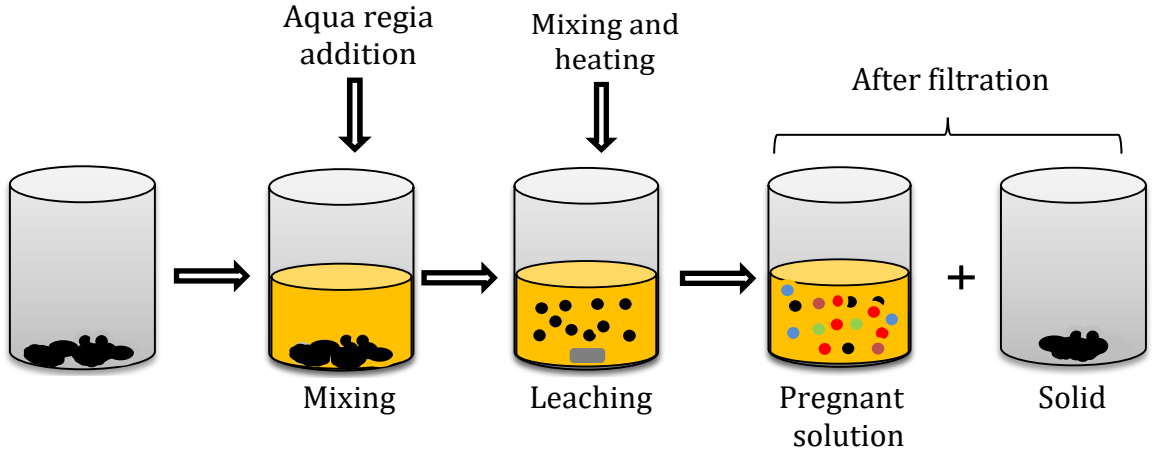

Figure 4-2: Aqua regia digestion procedure

4.4 Analytical methods

This section includes detailed methodology of the analytical instruments used and their summarised principle of operation.

4.4.1 ICP-OES sample preparation

After filtration the pregnant leachate solution was prepared for ICP-OES elemental analysis by doing 50x dilution. Two millilitres (2mL) of the leachate solution from acid-base demineralisation and aqua regia was transferred into a 100mL volumetric flask and distilled water was added to the mark.

After ICP analysis of the leachate solution, the concentration obtained from each element is converted to initial concentration of that element using dilution factor according to calculations in section 8.4.1 of the Appendix.

4.4.2 FAAS analysis

The flame atomic absorption spectrometer (FAAS) was used to determine the concentration of the prepared gold stock solutions, initial gold concentration and the final gold concentration that remains in the solution after adsorption. The FAAS used have a

detection limit of 0.1ppm for gold, the instrument model is (novAA® 400 P) and the software used is (ASpect® LS). The carrier gases for the flame were: compressed air (oxidising agent) and acetylene gas (fuel) usually operated at maximum pressure of 600 and 1000kPa, respectively. The calibration curves are presented in Appendix 8.6.

4.4.3 SEM-EDS analysis

The scanning electron microscope (SEM) of (Zeiss EVO® MA15) model with (Oxford INCA software) was used to analyse the surface morphology of the treated, untreated and gold-adsorbed tyre-derived adsorbents. SEM coupled with Energy Dispersive X-Ray Spectroscopy (EDX or EDS) detector of (Oxford Instruments® X-Max 20 mm) was also used for identification and quantification of the elements on the surface of each sample. The surface of the samples was first coated with a thin layer of gold for conductivity purposes. For analysis of gold-adsorbed adsorbents after adsorption, the coating was done with fine particles of carbon which are both transparent to SEM electron beam and conductive. The 20kV SEM electron beam had a working distance, current, and counting time of 9.5 mm, (150pA for gold-free adsorbents and 9.0nA for gold-adsorbed adsorbents samples) and 10 seconds, respectively. Identification of the samples was achieved with secondary electron images.

A basic principle involved is first the release of electron beam from SEM to the sample's surface. Electrons of each atom on the sample surface are ejected by this beam of electrons which results in x-rays emitted. The energy of the emitted x-ray is a representative of an element from which the x-ray was emitted. The x-rays emitted are detected by EDS which measures the relative quantity of x-ray emitted against their energy.

4.4.4 Ultimate and proximate analysis

The ultimate analysis of all the samples was conducted with Vario EL Cube elemental analyser for carbon, hydrogen, nitrogen and sulphur. Approximately 5 mg of each sample was sealed in a tin boat and combusted at 1800 °C in a combustion tube. A mixture of gaseous products produced from combustion was carried by an inert carrier gas and passed through a copper tube which trap and remove additional oxygen that did not react during combustion and further convert nitrogen oxides to nitrogen gas. The combustion

products contain gases such as carbon dioxide (CO_2) from carbon, water from hydrogen, sulphur dioxide (SO_2) from sulphur and nitrogen gas/oxides from nitrogen which get separated in a separation system. These gases are then detected by thermal conductivity detector (TCD). In ultimate analysis the carbon, hydrogen, sulphur and nitrogen can be determined experimentally, and the results obtained then be used to calculate oxygen content based on the weight difference according to *Equation (2.1)*.

Proximate analysis of all the samples was analysed using Mettler Toledo TGA/DCC1 following the ASTM E1131-08 method which was slightly adjusted to suit the properties of the samples. And in the proximate analysis the ash content, volatile matter and moisture content can be determined experimentally, and the results obtained then be used to calculate fixed carbon content based on the weight difference according to the *Equation (2.2)*.

4.4.5 FTIR

To study the functional groups present in the tyre char adsorbents, the Fourier Transform Infrared spectroscopy (FTIR) was used. The FTIR instrument used is Nexus-Thermo Nicolet FTIR spectrometer and the experiments were conducted according to ASTM D2734-94. About 5mg of the sample was mixed with 95mg of finely ground KBr and the mixture was compressed into thin pellets with a hydraulic press using 400 p.s.i of pressure and held for 5min. The pellets were inserted into the spectrophotometer and 64 scans were recorded at wavenumber scan range of 500-4000 cm^{-1} with a resolution of 4 cm^{-1}. The instrument operates by passing infrared radiation through the sample and some of the infrared radiation is absorbed by the sample resulting in absorption signals at different wavelength. The detector collects the signals and the computer will convert the detector output to an interpretable spectrum.

4.4.6 BET analysis

Brunauer Emmett Teller (BET) surface area measurements were made using Micromeritics 3Flex nitrogen adsorption at 77 K.

4.5 Adsorption

In this section the batch adsorption experiments were conducted to determine maximum adsorption capacity, isotherm and kinetics of the tyre-derived adsorbents. The parameters that were investigated during the batch study are adsorbate concentration in (mg/L), pH, contact time in (hours) and adsorbent concentration in (g/L). Each parameter was carefully investigated and selected based on literature study and preliminary results. The range for each parameter is tabulated in *Table 4-2* and the chemicals and materials used are listed in *Table 4-3*. Adsorption raw data is presented in Appendix 8.7.

Table 4-2: Investigated parameters and their range

Parameter	***Range***			
	UPT-char	*TPT-char*	*UT-crumb*	*TT-crumb*
pH	1-8	1-8	1-8	1-8
Adsorbent con. (g/L)	0.12-1	0.6-1	0.6-10	0.6-10
Adsorbate con. (mg/L)	45-188	20-100	10-190	0-100
Contact time (h)	0-72	0-72	0-72	0-72

4.5.1 Chemicals and materials

All the chemicals were supplied by Sigma-Aldrich (Merck chemicals) except for HCl which was supplied by Scienceworld.

Table 4-3: Properties of chemicals used

Chemicals	***Molar mass (g/mol)***	***Density (kg/L)***	***Concentration (ppm)***	***Assay***
$HAuCl_4$	-	1.033	1000	-
CH_3COOH	60.05	1.050	-	97%
CH_3COONa	82.03	-	-	99%
HCl	36.46	1.160	-	32%
KCl	74.55	1.980	-	99.8%
K_2HPO_4	174.18	-	-	99.5%
$NaOH$	40.00	-	-	98.5%

To get a constant agitation of the solution adsorbent mixture, a DRAGONLAB MS-M-S10 magnetic stirrer was used. Stirring was constant during all experimental runs at about 350 rpm. The scale used to weigh out the required masses was a RADWAG AS220.R2 with a readability of 0,1 mg. Different types of laboratory glassware such as volumetric flasks, Erlenmeyer flasks, beakers, etc. were used to prepare and store the synthetic solutions. The pH of the solutions was checked with a HANNA INSTRUMENTS HI2211 pH/ORP Meter. It was calibrated with buffer solutions of pH 4, 7 and 10. For the filtration of the solution adsorbent mixture after the adsorption process, Double Rings 102-Qualitative-12,5 cm filter paper was used. The samples of each experiment were put into plastic sample cups with screw-tops.

4.5.2 Experimental plan

After preliminary experiments, a simplified experimental plan was designed according to *Table 4-4*. In this design, each parameter was studied individually when other parameters were kept constant except for adsorbent concentration which was studied with varied contact time as a function of equilibrium time at (24 and 48 h). For each experimental run, the studied parameter is varied within its optimum range until a maximum point is reached and it is then used and kept constant in the consequent experiments. This setup goes on until a collective data of optimum points are collected and utilized for additional experiments. Temperature was kept constant at 25 °C throughout.

Table 4-4: Simplified experimental plan

Studied effect:	***Parameters***			
	pH	t_{con}	m_{ads}	$[Au^{3+}]_0$
Influence of pH	**varied**	constant	constant	constant
Influence of Adsorbent con.	constant	**varied**	**varied**	constant
Influence of Contact time	constant	**varied**	constant	constant
Influence of Adsorbate con.	constant	constant	constant	**varied**

For all experiments, 250ml Schott bottles were used in which 25ml of Au(III) solution was added together with an appropriate adsorbent dosage for a specific adsorbent. A

measured amount of adsorbent was first added into a Schott bottle followed by a magnetic stirrer and a measured volume of gold solution was added last. The Schott bottles containing different types of adsorbents are then put in a water bath which is set at a desired temperature. A DRAGONLAB MS-M-S10 magnetic stirrer plate set at the speed of about 550 rpm was then switched on. The magnetic stirrer plate had 10 stirrer points and was placed beneath the water bath. The water bath setup that was used for all adsorption experiments is illustrated in *Figure 4-3* below.

(a) Exterior

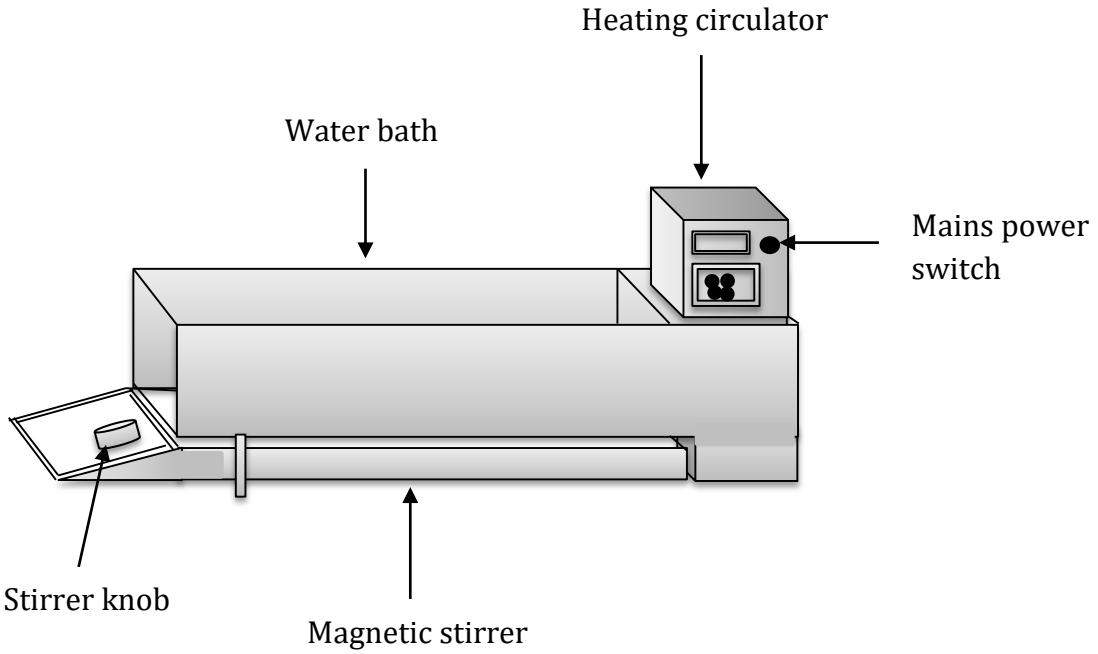

(b) Interior

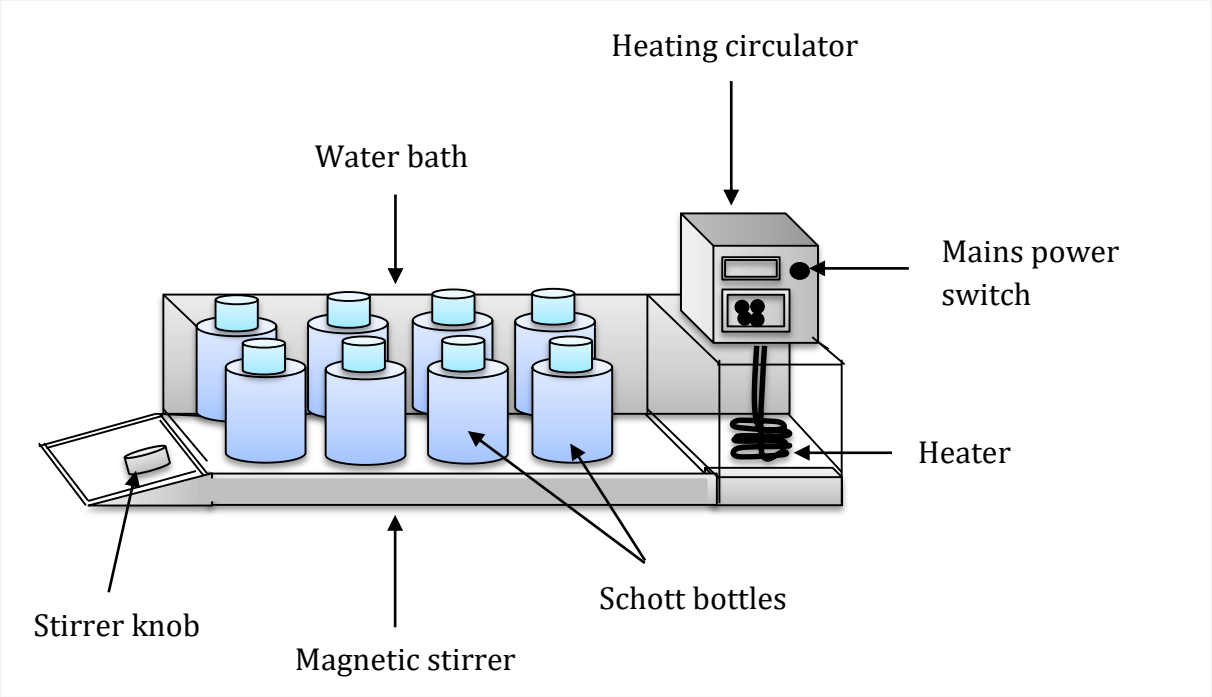

Figure 4-3: The (a) exterior and (b) interior setup of the water bath equipment

The solid phase was separated from the liquid phase immediately after adsorption experiments via filtration to investigate the influence of the selected parameters. The final concentration of the metal ion adsorbates in the filtrates was analysed with AAS. The adsorption capacity at any given time *t*, Q_t (mg/g), was determined using *Equation (4.3)* and the equilibrium adsorption capacity, Q_e (mg/g), was determined using *Equation (4.4)* as:

$$Q_t = \left(\frac{C_0 - C_t}{m}\right) * V \tag{4.3}$$

$$Q_e = \left(\frac{C_0 - C_e}{m}\right) * V \tag{4.4}$$

where C_0 (mg/L) is the initial adsorbate concentration, C_t (mg/L) is the adsorbate concentration at time *t*, C_e (mg/L) is the equilibrium adsorbate concentration, V (L) is the volume of the solution and m (g) is the mass of the adsorbent.

The adsorption percentage ($\%A$) was determined using *Equation (4.5)* as:

$$\%A = \left(\frac{C_0 - C_e}{C_0}\right) * 100\% \quad (4.5)$$

where C_0 (mg/L) is the initial adsorbate concentration and C_e (mg/L) the equilibrium adsorbate concentration.

4.5.3 Influence of the parameters

To study the effect of solution pH, a series of different buffer solutions with different pH values ranging from 1 to 8 were prepared according to measurements in *Table 4-5*. Refer to (section 8.5) of Appendix for all step by step buffer preparation and calculations.

Table 4-5: Buffer solutions and measurements for a specific pH

Buffer solution	***Volume measurements***	***pH***
HCl/KCl	250 mL KCl + 670 mL HCl + 7 mL water	1
	250 mL KCl + 65 mL HCl + 685 mL water	2
Acetate buffer (CH_3COONa/ CH_3COOH)	982.3 mL CH_3COOH + 17.7 mL CH_3COONa	3
	847 mL CH_3COOH + 153 mL CH_3COONa	4
	357mL CH_3COOH + 643mL CH_3COONa	5
	52.2 mL CH_3COOH + 947.8mL CH_3COONa	6
Phosphate buffer (K_2HPO_4/HCl)	756.0 mL K_2HPO_4 + 244 mL HCl	7
	955.1 mL K_2HPO_4 + 44.9 mL HCl	8

The standard solutions with a targeted initial gold concentration was prepared and adjusted with each buffer at a specific pH of interest. It is worth noting that the initial pH of the buffer solution dropped in some cases when mixed with the gold stock solution, $HAuCl_4$, during the preparing of gold standard solutions because the gold stock solution is highly acidic with very pH. In this case, the volume measurements should be changed slightly to a volume ratio that is suitable for the targeted pH. Alternatively, a buffer solution of higher pH value than the targeted pH value might be used. For example, in this project a gold standard solution of a final pH 2 was attained when acetate buffer of pH 3

was used. To study the effect of adsorbent concentration, the adsorption contact time was varied from 24 and 48h in order to obtain optimum amount of adsorbent mass (m_{ads}) at equilibrium contact time.

For the equilibrium, a series of standard solutions with different initial gold concentration ranging according to the values in *Table 4-2* were prepared. The optimal pH attained in the previous experiments was used and the rest of other parameters were kept constant. The initial gold concentration at which an equilibrium was reached for each adsorbent was used to study the effect of contact time. All the experiments were repeated three times and the average values were reported.

4.5.4 Batch adsorption isotherm

In this work two adsorption isotherm models were used including Langmuir and Freundlich isotherm models to fit the experimental data for adsorption of Au(III). The Langmuir isotherm assumes that adsorption occurs on the homogeneously distributed binding sites of an adsorbent's surface resulting in a monolayer formation of adsorbed species. Additionally, it suggests that the energy of adsorption is uniform, and the adsorbed species do not interact with each other on the surface. To study the Langmuir isotherm model, a linear and non-linear *Equation (4.6)* and *(4.7)* respectively, can be used.

$$\frac{C_e}{Q_e} = \left(\frac{1}{\mathrm{Q_{max}}}\right) C_e + \left(\frac{1}{\mathrm{K_L Q_{max}}}\right) \tag{4.6}$$

$$Q_e = \left(\frac{Q_{max} K_L C_e}{1 + K_L C_e}\right) \tag{4.7}$$

where C_e is the equilibrium Au(III) concentration in the solution (mg/L), Q_e and Q_{max} are the equilibrium and maximum adsorption capacity of Au(III) adsorbed (mg/g) and K_L is the Langmuir equilibrium constant (L/mg), which is related to energy of adsorption and represents the affinity between adsorbent and adsorbate.

An essential characteristic of the Langmuir isotherm is a dimensionless separation factor R_L, a constant which is expressed by the given *Equation (4.8)* below:

$$R_L = \left(\frac{1}{1 + K_L C_o}\right) \tag{4.8}$$

where C_o is the initial Au(III) concentration (mg/L). The R_L parameter indicates the shape of the isotherm and it is used to describe the nature of the adsorption according to the following boundaries:

Table 4-6: Description of a constant of Langmuir isotherm separation factor

$R_L = 0$	Irreversible adsorption
$R_L = 1$	Linear adsorption
$0 < R_L < 1$	Favourable adsorption
$R_L > 1$	Unfavourable adsorption

Contrary to Langmuir isotherm model, the Freundlich isotherm model do not conform to monolayer coverage and uniform adsorption energies. It suggests that adsorption occurs on a heterogeneous surface of the adsorbent in which more than one layers of adsorbates are formed. The Freundlich model can be best expressed by the linear and non-linear form of Freundlich *Equations (4.9)* and *(4.10)* below:

$$Log\mathrm{Q_e} = \left(\frac{1}{\eta}\right) Log\mathrm{C_e} + Log\mathrm{K_F} \tag{4.9}$$

$$Q_e = \mathrm{K_F} C_e^{\frac{1}{\eta}} \tag{4.10}$$

Where C_e is the equilibrium Au(III) concentration in the solution (mg/L), Q_e is the adsorption capacity of Au(III) adsorbed at equilibrium (mg/g), K_F and η are Freundlich constants that are related to adsorption capacity and adsorption intensity, respectively. The Freundlich constant K_F, can also be described as a binding energy reflecting the affinity of the adsorbent towards metal ions (mg/g).

4.5.5 Batch adsorption kinetics

The batch adsorption kinetics were studied by determining the amount of Au(III) adsorbed per unit weight of adsorbent at any given contact time (Q_t) and at equilibrium

(Q_e) through different time intervals. *Equation (4.11)* and *(4.12)* of pseudo-first order and pseudo-second order kinetic models, respectively, were used to model the adsorption kinetics.

$$Log(Q_e - Q_t) = LogQ_e - \left(\frac{K_1}{2.303}\right)t \quad (4.11)$$

where Q_e (mg/g) is the amount of Au(III) adsorbed per unit weight of adsorbent at equilibrium, Q_t (mg/g) is the amount of Au(III) adsorbed per unit weight of adsorbent at contact time *t*, K_1 (h^{-1}) is the pseudo-first order rate constant and *t* (h) is the contact time. The kinetic parameters can be obtained from a kinetic plot of *Log* (Q_e – Q_t) vs *t* which gives a straight-line plot with a slope that is equal to $K_1/2.303$ and an intercept equal to $LogQ_e$.

Pseudo-second order kinetic model can be expressed by *Equation (4.12)*;

$$\frac{t}{Q_t} = \left(\frac{1}{Q_e}\right)t + \left(\frac{1}{K_2 Q_e^2}\right) \quad (4.12)$$

where K_2 (g/mg/h) is the pseudo-second order rate constant which can be calculated from the intercept of a straight-line kinetic plot of t/Q_t against *t*. The same plot can be used to calculate adsorption capacity, Q_e, of Au(III).

5. RESULTS AND DISCUSSION

5.1 Characterisation of tyre char and crumb

Physicochemical properties of waste tyre-derived solid materials are very important and thorough qualitative and quantitative characterisation is required to understand their interaction with other substances when used. The untreated PT-char and Tyre crumb are denoted as UPT-char and UT-crumb respectively.

This section provides detailed characterisation of PT-char and Tyre crumb which includes; proximate and ultimate analysis, BET surface area measurements, surface morphology, FT-IR and SEM-EDS metal content. Additionally, the particle size distribution profile of each adsorbent is included in Appendix 8.1.

5.1.1 Proximate and ultimate

The proximate analysis results of UPT-char and UT-crumb are given in *Table 5-1* and ultimate analysis are given in *Table 5-2*.

Table 5-1: Proximate analysis results of UPT-char and UT-crumb

	Volatile	***Fixed carbon***	***Moisture***	***Ash***	***Total***
Units	*wt.%*	*wt.%*	*wt.%*	*wt.%*	*wt.%*
UPT-char	7.80	75.25	0.45	16.5	100
UT-crumb	61.6	30.0	0.6	7.8	100

According to the results in *Table 5-1*, UPT-char have high ash content than its precursor UT-crumb. The high ash content in the untreated PT-char is due to the presence of high inorganic components derived from pyrolysis of WTs particularly ZnS which was formed by reaction of sulphur and ZnO. Additional inorganic elements that contributed to high ash content are Fe, Si and Ca [4]. When the organic matter in WT feedstock is decomposed and volatised during pyrolysis, most of its inorganic components remains in the resultant char. However, the quantity of the ash in the resultant char is not necessarily dependant on pyrolysis conditions rather only depends on the quantity of inorganic components in WT feedstock [58]. Darmstadt et al. [58] reported that more ash was found in the bulk rather than the surface of the char which was attributed to the formation of extra carbon

deposits that covered them on the surface. The most contributing factor on the quantity of ash content on char surface was found to be Zn which was the only element detected on the surface [58].

Table 5-2: Ultimate analysis results of UPT-char and UT-crumb

	Carbon	***Hydrogen***	***Nitrogen***	***Sulphur***	***Oxygen*** [a]	***Total***
Units	*wt.%*	*wt.%*	*wt.%*	*wt.%*	*wt.%*	*wt.%*
UPT-char	78.56	0.6335	0.21	2.366	18.23	100
UT-crumb	80.02	7,297	0,32	2.043	8.968	100

[a] *Calculated by difference*

High carbon content in UPT-char and UT-crumb is due to the carbon black in WTs used during tyre manufacturing as a filler [111]. Carbon black in the waste tyre is about 32 wt.% with 70-75 wt.% carbon content [65]. The additional carbon deposits formed on the char from organic vapours produced by pyrolysis which get adsorbed on the surface of the char might also contribute to carbon content in UPT-char [39]. The UPT-char also contains non-volatile hydrocarbons and carbonised rubber polymer [111]. Sulphur content in UT-crumb is derived from vulcanisation of rubber polymers [33] which proceeds further to UPT-char during pyrolysis as part of ash.

Conclusion

The proximate and ultimate results of UPT-char and UT-crumb are consistent with results reported in literature, to support this claim please refer to *Table 2-7* and *Table 2-8* in Chapter 2 for comparison purposes.

5.1.2 Surface morphology

This section presents the surface morphology characterisation of UPT-char and UT-crumb through scanning electron microscope (SEM) analysis and images. The quantity of the present elements can also be analysed with scanning electron microscope coupled with energy dispersive x-ray spectroscopy (EDS).

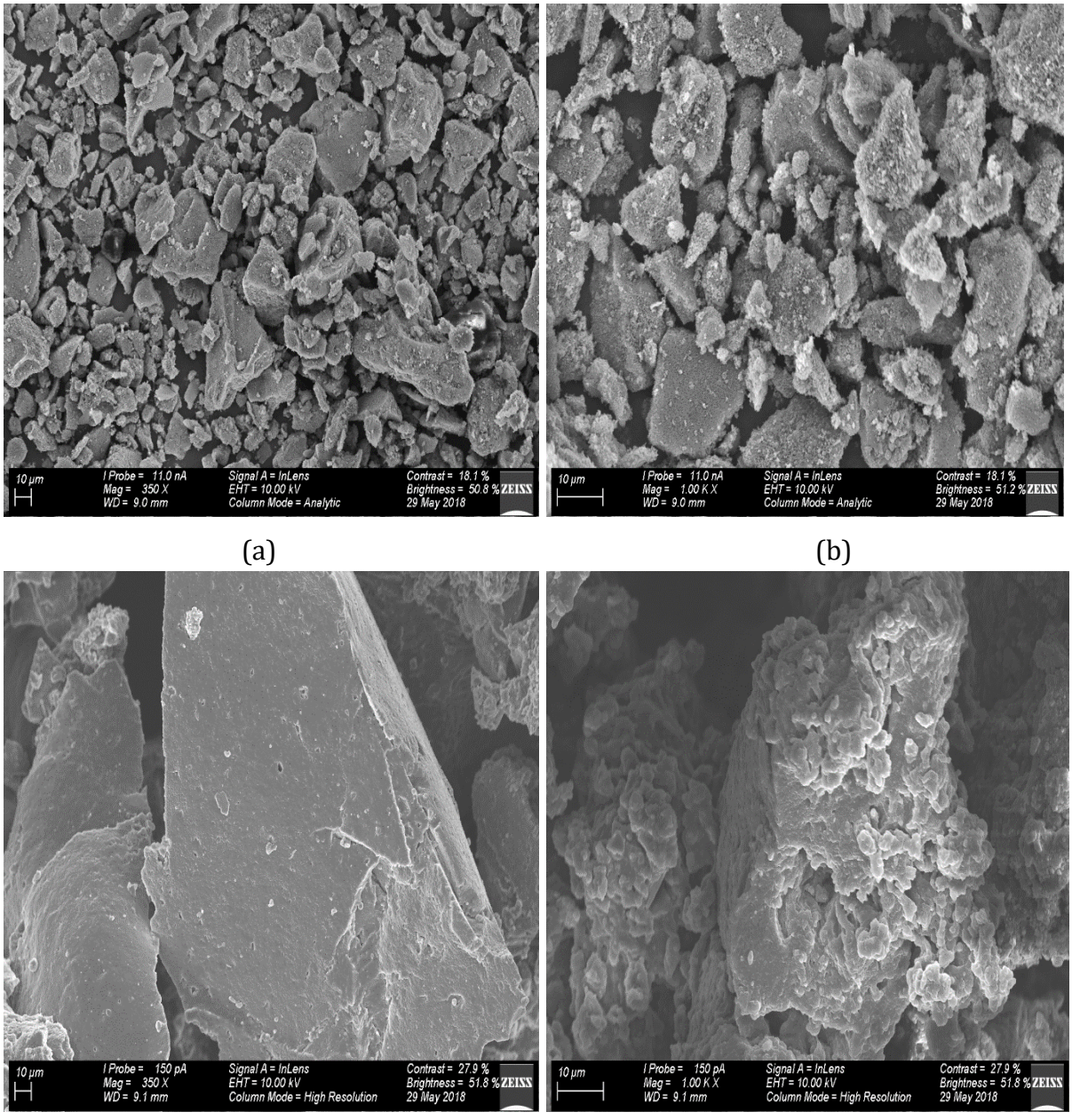

Figure 5-1: The SEM images of (a) UPT-char at 350x magnification (b) UPT-char at 1000x magnification (c) UT-crumb at 350x magnification (d) UT-crumb at 1000x magnification

The structure and morphology of carbonaceous materials is one of the key parameters in determining their possible applications. The surface of the untreated tyre crumb (c) appear to be flat and smooth [112] with almost no visible pores on it, but at higher magnification (d) the surface appears to be rough and have pores on its surface [1]. The surface of untreated pyrolytic char appears to be the same in both high (a) and low (b) magnifications and it contains particles that have rough surface with irregular shapes.

UT-crumb are naturally hydrophobic and have either very low or no polarity at all. Because of these properties, they tend to repel water and remain on the surface of an aqueous solution forming conglomerates [1].

5.2 Effect of acid-base demineralisation on properties of tyre char and crumb

5.2.1 Proximate and ultimate

This section focusses on the effect of acid-base demineralisation on the chemical composition of UPT-char and UT-crumb using proximate and ultimate analysis.

Table 5-3: Proximate analysis results of UPT-char, TPT-char, UT-crumb and TT-crumb before and after alkali-acid demineralisation.

	Volatile	***Fixed carbon***	***Moisture***	***Ash***	***Total***
Units	*wt.%*	*wt.%*	*wt.%*	*wt.%*	*wt.%*
UPT-char	7.8	75.25	0.45	16.5	100
TPT-char	9.6	87.25	1.45	1.7	100
UT-crumb	61.6	30.0	0.6	7.8	100
TT-crumb	59.7	32.2	4.2	3.9	100

Proximate analysis results demonstrated that the acid-base demineralisation influenced the properties of UPT-char and UT-crumb. *Table 5-3* show that the ash content of UPT-char was greatly reduced from 16.5 to 1.7 wt.% (90% removal) which also resulted in an increment of fixed carbon from 75.25 to 87.25 wt.%. It is believed that the inorganic components that previously covered the char's carbon surface was removed upon treatment with 1M NaOH and 1M HNO_3 solvents [47]. The 61.6 wt.% volatile content of UT-crumb is composed of about 56 wt.% of oil which is reduced during the first stage of demineralisation with 1M NaOH.

In UT-crumb acid-base demineralisation, not only inorganic component was removed but organic compounds soluble in NaOH and HNO_3 were also leached out. After the treatment, the initial weight of UT-crumb was reduced by 21.3%. Rungrodnimitchai and Kotatha [113] reported that the weight loss of UT-crumb during treatment with 1M NaOH and 1M HCl at solvent boiling point was 7.88% and 13.54% respectively, which add up to a total of 21.4%. *Equation (5.1)* was used to calculate the weight loss after the treatment.

$$Wt.loss(\%) = \left(\frac{Wt.of\ sample\ before\ treatment - Wt.of\ sample\ after\ treatment}{Wt.of\ sample\ before\ treatment}\right) \times 100 \qquad (5.1)$$

Another observation was that UT-crumb after the treatment lost its elasticity and became partially hydrophilic. The hydrophilic nature of TT-crumb may be due to oxidation of the surface by HNO_3 which introduced hydrophilic functional groups such as carbonyl (-COOH) [114]. This might have led to an increase in moisture content from 0.6 to 4.2 wt.% after demineralisation of tyre crumb. He et al. [115] mentioned that oxidation of rubber increased the oxygen content and changed its surface to be polar.

NaOH is reported to be a very capable solvent that removes oil and ash from tyre rubber particles. Mohammadi et al. [116] further explained that during the treatment of tyre rubber with NaOH, the zinc compound which was previously added as zinc stearate during the manufacturing of the rubber, reacts with NaOH to form sodium stearate. Zinc stearate on the surface of the rubber is the cause of its hydrophobic nature and make rubber resistant to oxidation. However, NaOH reacts with zinc stearate to form a water-soluble compound which is sodium stearate and it can be easily washed off with water from the rubber surface. This reaction leads to removal of zinc from rubber surface and it can be used to make rubber surface accessible for oxidation which will also make it hydrophilic.

Table 5-4: Ultimate analysis results of UPT-char, TPT-char, UT-crumb and TT-crumb before and after alkali-acid demineralisation.

	Carbon	***Hydrogen***	***Nitrogen***	***Sulphur***	***Oxygen*** [a]	***Total***
Units	*wt.%*	*wt.%*	*wt.%*	*wt.%*	*wt.%*	*wt.%*
UPT-char	78.56	0.6335	0.21	2.366	18.23	100
TPT-char	89.25	0.581	0.23	0.619	9.32	100
UT-crumb	80.02	7.297	0.32	2.043	10.32	100
TT-crumb	66.93	4.696	5.395	0.907	22.07	100

[a] *Calculated by difference*

After alkali-acid demineralisation of UPT-char and UT-crumb, the carbon content increased by ~12% for UPT-char and decreased by ~16% for UT-crumb. As mentioned before, the removal of ash content from UPT-char lead to an increase in carbon content.

The nitrogen content remained almost the same with UPT-char; however, greatly increased by 94% with UT-crumb after alkali-acid demineralisation. It is assumed that the nitrogen increment could be caused by deposition of inorganic nitrate ions (NO_3^-) from nitric acid during nitric acid treatment [114].

Sulphur content was reduced by ~73.8% in UPT-char and ~56% in UT-crumb after alkali-acid demineralisation. Nitric acid is reported to be very efficient in removing sulphur from carbonaceous materials due to its oxidising properties [47]. Consequently, the removal of sulphur is mainly attributed to nitric acid treatment. However, NaOH also proved to remove considerable amount of sulphur from UPT-char but low amount from UT-crumb according to mineralogy study under demineralisation results.

Hydrogen content was slightly reduced by ~8% in UPT-char and decreased by ~36% in UT-crumb after acid-base demineralisation.

The high oxygen content in TT-crumb could be as a result of HNO_3 treatment which introduced oxygen-containing functional groups on the crumb surface via oxidation [114].

5.2.2 Effect of demineralisation on surface morphology

The alkali-acid demineralised UPT-char and UT-crumb which are denoted TPT-char and TT-crumb respectively, are characterised based on surface morphology by SEM-EDS.

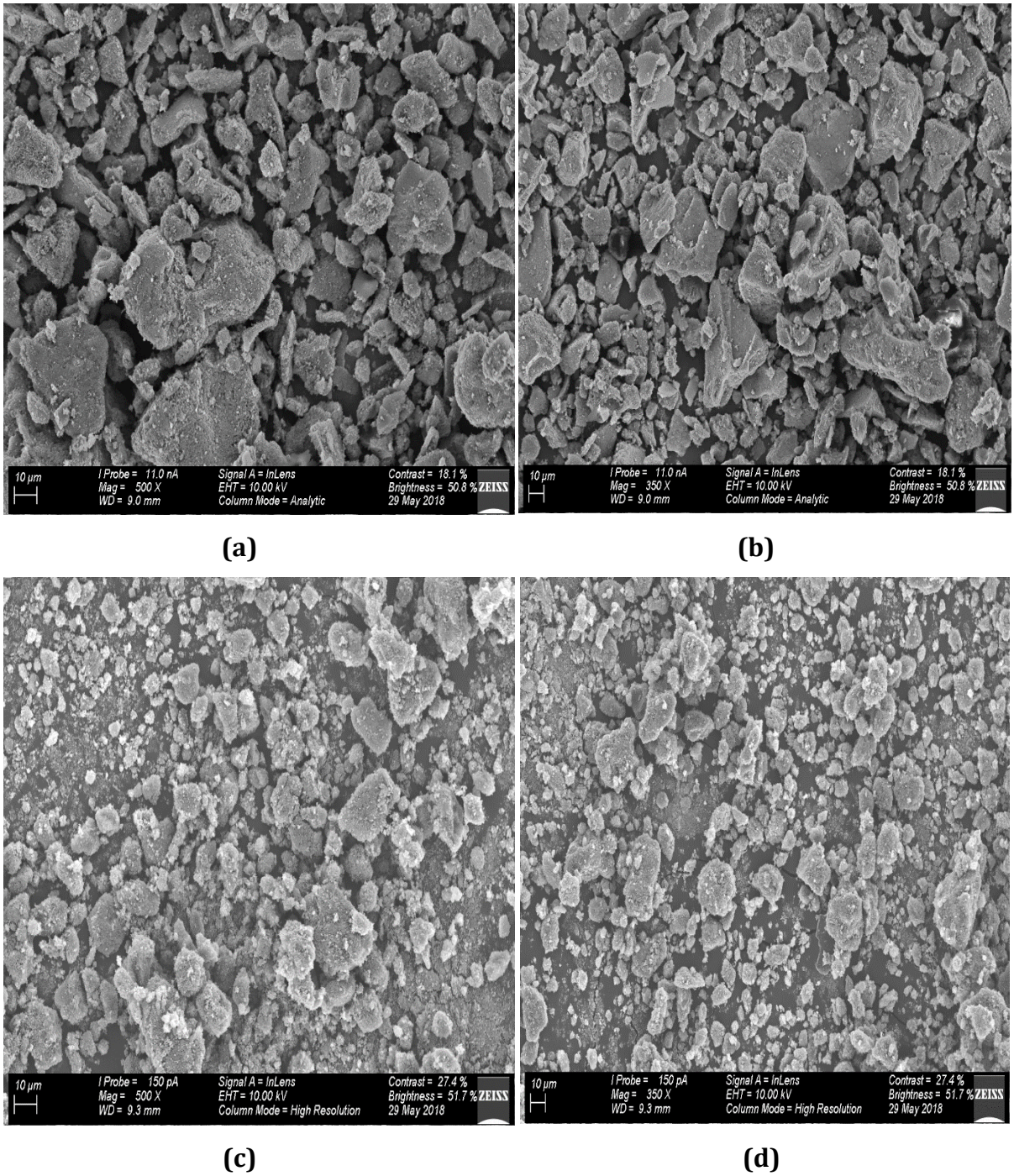

Figure 5-2: The SEM images of (a) UPT-char at 500x magnification (b) UPT-char at 350x magnification (c) TPT-char at 500x magnification (d) TPT-char at 350x magnification

Figure 5-2 shows structural morphology comparison between the untreated PT-char ((a) and (b)) and treated PT-char ((c) and (d)) in different magnification. The purpose is to evaluate the effect of acid-base demineralisation on the morphology of tyre char samples. Both (c) and (d) magnifications of TPT-char shows formation of smaller particles after acid-base demineralisation while most UPT-char particles are of bigger size. This may be attributed to the removal of ash content on the UPT-char surface which is also in agreement with proximate analysis results reported in *Table 5-3*. According to proximate analysis results, approximately 90% of ash in raw PT-char was removed by alkali-acid demineralisation.

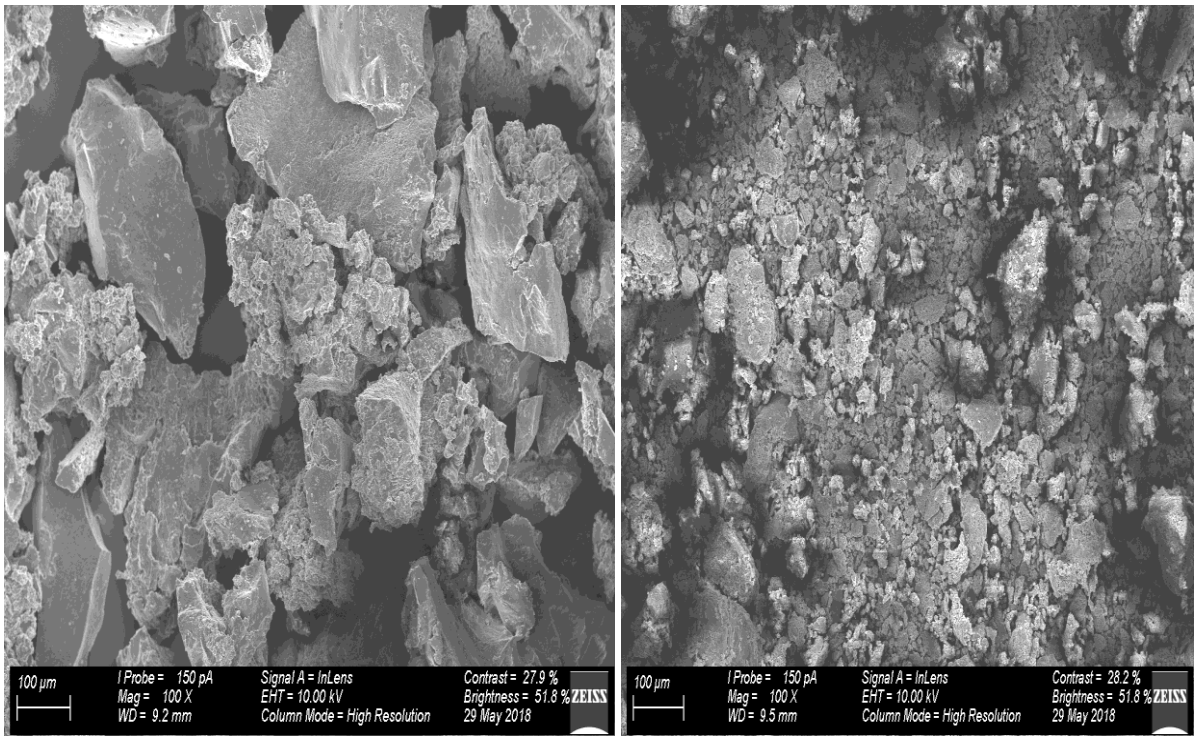

(a) **(b)**

Figure 5-3: The SEM images of (a) UT-crumb and (b) TT-crumb, at 100x magnification

The particles in acid-base treated crumb (b) appear to be very small as compared to untreated crumb in sample (a) which shows that the rubber particles were partially digested/degraded during the demineralisation. This could be attributed to the removal of high sulphur content in the crumb particle as showed by ultimate analysis results in *Table 5-4*. Sulphur to sulphur and sulphur to carbon bonds are known to hold the 3D structure of tyre rubber and cleavage of these bonds will cause a collapse of the tyre

structure. According to ultimate analysis, over 50% sulphur content in UT-crumb was removed during acid-base demineralisation which could cause a collapse of the tyre rubber structure [7]. Another possibility is that if the rubber particles are exposed to NaOH solution for a long period, it will digest the particles and cause the surface to be even more rough [116].

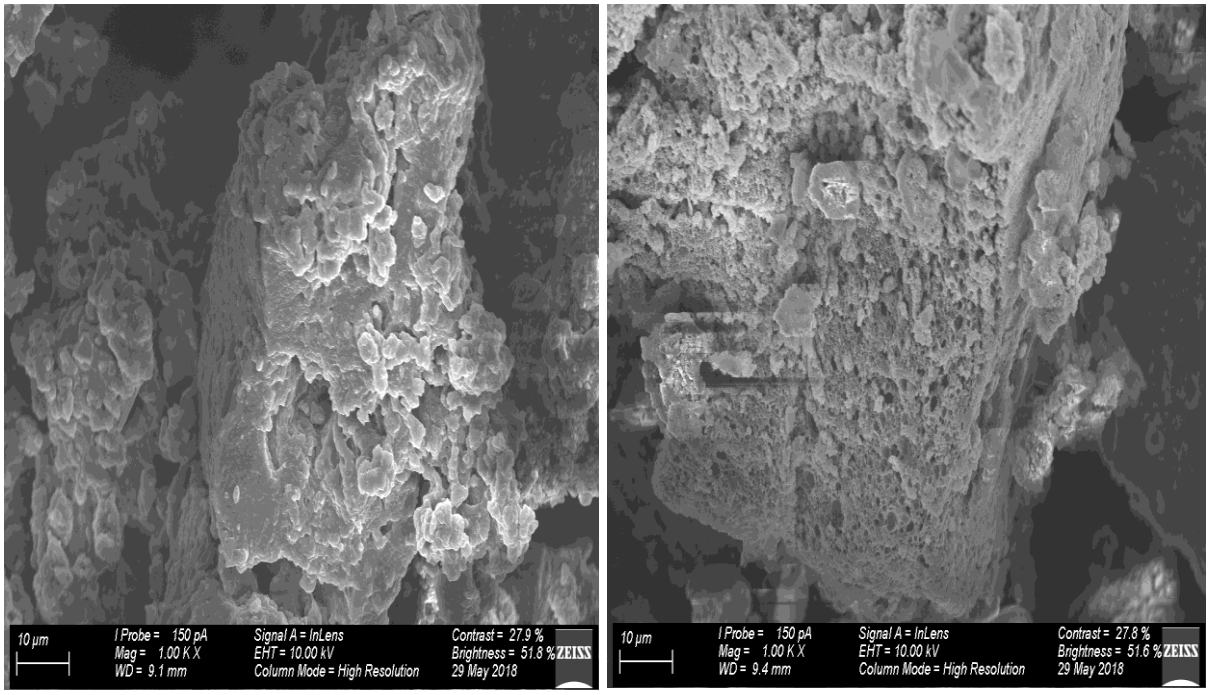

(a) **(b)**

Figure 5-4: The SEM images of (a) UT-crumb and (b) TT-crumb, at 1000x magnification

At 1000x magnification of UT-crumb and TT-crumb SEM images, the pores on the surface are visible. On the surface of UT-crumb there appear macropores and on the surface of TT-crumb there appear micropores. This shows that crumb is highly porous with irregular surface [1].

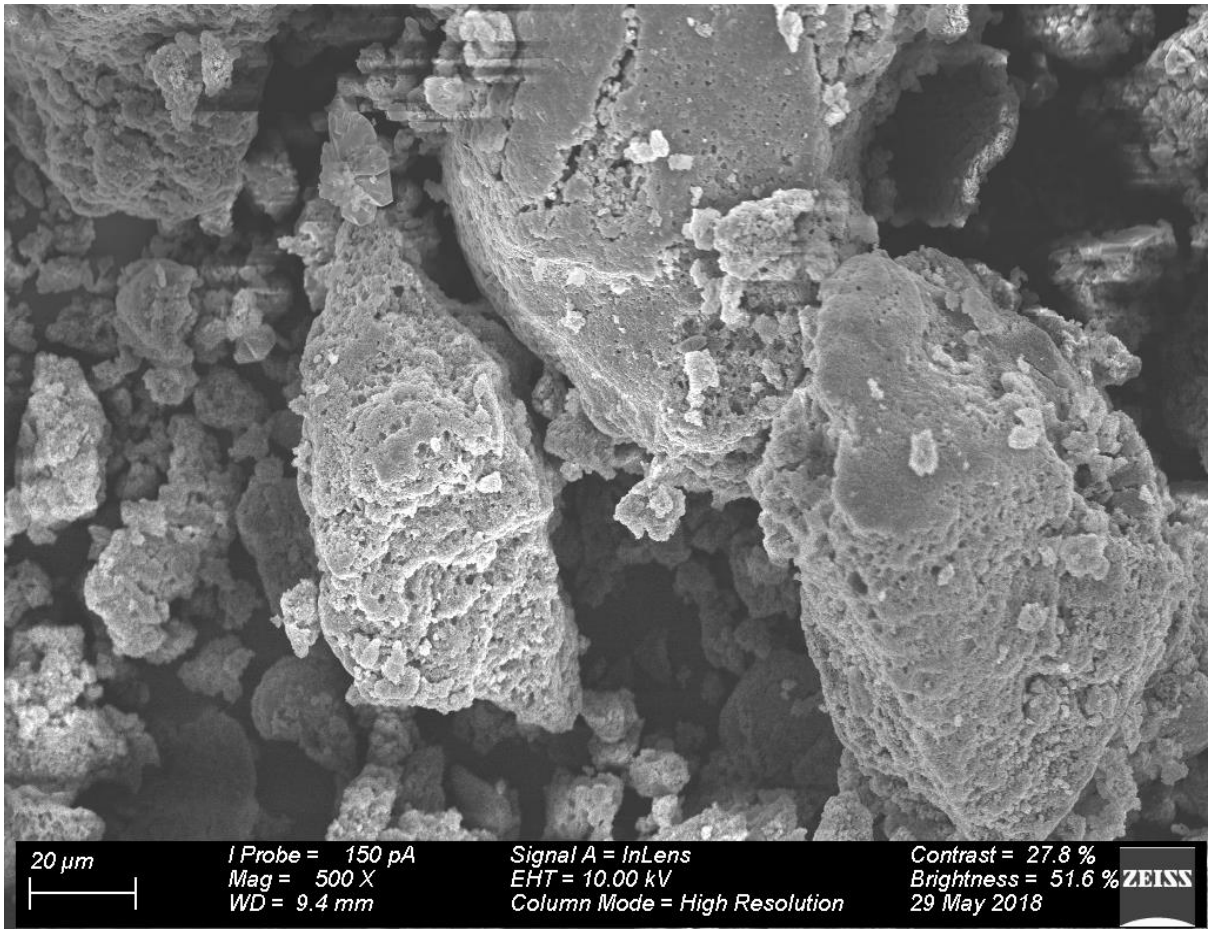

Figure 5-5: The SEM image of TT-crumb after alkali-acid demineralisation

Figure 5-5 of TT-crumb shows that there are cracks developed on the surface with what appears to be micropores formed after alkali-acid demineralisation. Moreover, compared with the original sample, the surface of the treated sample became rough with irregular particles which may cause the tyre crumb to lose its elasticity [1,113]. Mohammadi et al. [116] reported that treatment of tyre rubber with NaOH results in formation of a rough rubber surface.

5.3 SEM-EDS elemental content

Table 5-5: SEM-EDS elemental content of both treated and untreated char and crumb

	UPT-char	***TPT-char***	***UT-crumb***	***TT-crumb***
Units	*wt.%*	*wt.%*	*wt.%*	*wt.%*
C	84,7	91,14	86,29	79,06
O	9,12	8,06	9,14	18,9
Na	0,33	0	0,12	0,02
Mg	0,05	0,01	0	0
Al	0,28	0,03	0,08	0,04
Si	1,11	0,04	0,55	0,31
S	1,23	0,47	1,13	0,48
Cl	0	0	0,04	0,03
K	0,1	0	0,04	0,01
Ca	0,18	0	0,08	0
Fe	-	-	0,26	0,08
Cu	0,25	0,24	0,25	0,28
Zn	2,65	0	2,03	0,78
Total	*100*	*100*	*100*	*100*

The SEM-EDS results show that zinc metal content is abundant on the surface of both UPT-char and UT-crumb which agrees with results reported in literature [59,76,111]. The ash content is reported to contain high amount of zinc, silicon and sulphur in UPT-char [33,56,58] which were very low in TPT-char and TT-crumb. The zinc content was greatly removed during the acid-base treatment with 0 wt. % detected on the surface of TPT-char. The quantity of the detected elements appears to be very low on the surface of the treated samples which shows that high ash content was removed on surface. In conclusion, these results confirm that the acid-base demineralisation was successful in reducing ash from UPT-char and the results are in accordance with proximate analysis results.

5.4 BET surface area

Table 5-6: BET surface area of UPT-char, TPT-char, UT-crumb and TT-crumb

S_{BET} (m^2/g)			
UPT-char	***TPT-char***	***UT-crumb***	***TT-crumb***
63.96	78.89	0.322	3.49

The increment of surface area is attributed to removal of ash content on the surface of the samples and the condensed oil in UPT-char that is formed during pyrolysis. The Condensed oil usually block the pores of UPT-char and reduce its surface area. The acid-base demineralisation with 1M NaOH and HNO_3 was efficient. The surface area of both the treated and untreated samples are in accordance with results reported in literature.

5.5 FTIR analysis of PT-char

The FTIR spectrum of PT-char before and after demineralisation were collected through the analysis of the samples using KBr method.

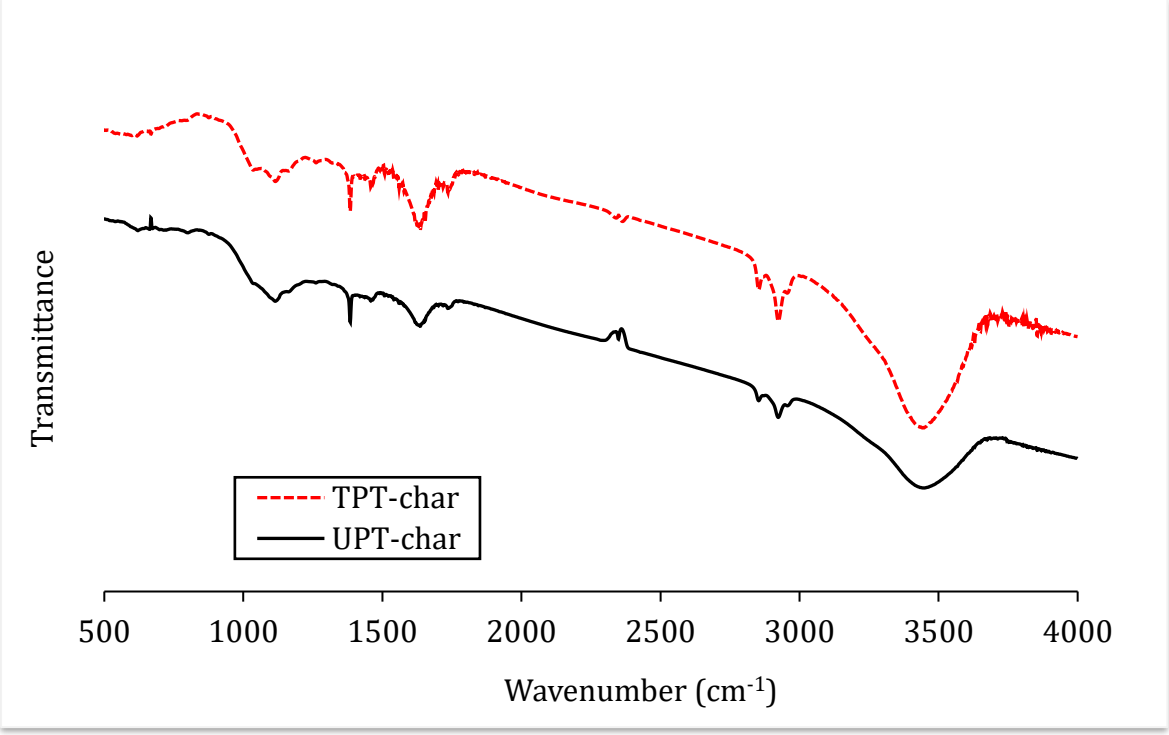

Figure 5-6: FTIR spectrum of UPT-char and TPT-char

The FTIR spectrum of PT-char before and after demineralisation shows no significant change in surface functional groups. This shows that the structure of PT-char was not destroyed or damaged by the acid-base treatment. The present functional groups in both samples are mainly oxygen-containing groups. The broad peak at around 3500 cm^{-1} can be assigned to the hydroxyl group –OH from phenolic and carboxyl groups. The increment in the intensity of a 3500 cm^{-1} peak of TPT-char is due to the increased concentration of the hydroxyl groups attached to phenolic and carboxyl groups after treatment. The increased concentration of these oxygen-containing groups is attributed to oxidation of the carbon surface of the char by nitric acid since nitric acid is an oxidizing agent [77]. The absorption at 2923 cm^{-1} can be assigned to the C–H stretching vibration of the aromatic ring. The absorption at 2852 cm^{-1} is also attributed to the –OH stretching vibration of the carboxylic functional group. The small peak at around 1735 cm^{-1} can be attributed to the C=O stretching vibration of aldehydes, carboxyl, or ketones groups [9]. The absorption at 1637 cm^{-1} can be attributed to carbonyl carboxylic groups [100]. The absorption at around 1126 cm^{-1} can be attributed to C–O vibration in carboxyl groups. The both char samples also had some nitrogen-containing functional groups such as C–N from aromatic amine which is designated by absorption band at 1384 cm^{-1} [9].

5.6 Total elemental analysis

5.6.1 Aqua regia results

The elements analysed together with their suitable wavelength are listed in *Table 5-7*. Raw data from ICP-OES is presented in Appendix 8.2.2.

Table 5-7: Elements analysed and suitable wavelength

Elements	***Symbol***	***Wavelength (nm)***
Calcium	Ca	396.847
Copper	Cu	327.396
Iron	Fe	238.204
Sodium	Na	818.326
Nickel	Ni	341.476
Sulphur	S	180.731
Silicon	Si	251.611
Zinc	Zn	206.200
Potassium	K	766.490
Aluminium	Al	308.215

The initial concentrations of the analysed elements are presented in *Table 5-8*.

Table 5-8: Concentrations of elements in aqua regia leachate solution from untreated adsorbents

Elements	***Initial concentration (ppm)***	
	Tyre Char	*Tyre Crumb*
Ca	255.05	141.15
Cu	7.95	33.3
Fe	85.95	112.25
K	153.9	88.8
Na	173.95	143.05
Ni	0.55 [a]	0.95 [a]
S	1359.95	1304.65
Si	53.7	62.6
Zn	5022.7	1984.00
Al	177.4	28.6

" [a] " *Below detection limit*

In average, aqua regia leaching worked better in tyre char than tyre crumb and this may be attributed to the particle size of the samples; however, the difference is not high except for zinc and aluminium. The small and fine particles of tyre char might have facilitated the leaching process by aqua regia because when the particles are small there is more available surface that will enhance the contact between the solvent and the sample during the leaching process [117,118]. Both tyre crumb and char are reported to contain the highest amount of zinc content in terms of weight percentage (wt.%) than any other metal [49] which could be the reason high amount of zinc was leached. According to the chemical analysis of ash in tyre rubber [2,78] and char from literature [49] the silica content is very high; however, it is one of the least leached metals by aqua regia as it can be observed from *Table 5-8*. It has been reported that aqua regia and many other acids fails to completely dissolve silica and silicate-bound metals [117,118] and hence the low concentration of silica. High amount of sulphur is leached out which usually contributes approximately 2 wt.% in both tyre crumb [2,78] and char [49]. According to ultimate

analysis results, the sulphur content was found to be 2.043 wt.% in tyre crumb and 2.366 wt.% in char. Besides the presence of silicate oxides, other metal oxides such as iron, manganese and aluminium oxides can serve as obstacles for an effective aqua regia leaching even to the elements bound to them since it cannot dissolve them completely. Factors that may affect the effectiveness of aqua regia include the aqua regia strength, organic matter content, chemical composition and the particle size of the sample. The foaming that occurred when aqua regia was added to tyre char was due to high carbonate content in the sample and this observation also occur to samples with high organic matter content. For samples containing high organic matter content (≈70%) which negatively affects aqua regia digestion, nitric acid can be used as an alternative [119]. Additionally, for total digestion of samples containing aluminosilicate content which cannot be dissolved with aqua regia, hydrofluoric acid (HF) which dissolves aluminosilicates completely can be used as an alternative [119].

5.7 Demineralisation

Introduction

Some of the advantages of the solvents from literature are; HNO_3 can act as an oxidising agent [77] and its oxidation ability is higher than some of the well-known oxidising agent such as oxygen and hydrogen peroxide [120]. NaOH is reported to be very efficient in removing zinc content which forms a major part of the ash in tyre char and crumb that might affect their surface area [116]. Apart from zinc, sodium hydroxide is likely to dissolve some elements present in tyre rubber crumb and PT-char most especially alumina and silica better than some of the well-known alkaline solvents such as KOH, NH_4^+, $Ca(OH)_2$ and Na_2CO_3 [77]. Additionally, sodium hydroxide is efficient in dissolving oil [116], therefore, it can be used to remove some of the tyre-derived oil that might have blocked the pores of tyre char during pyrolysis.

Results and discussion

The results for tyre rubber crumb and PT-char treatment with NaOH and HNO_3 at *15g/180ml* and *1g/12ml* are given in *Table 5-9* and *Table 5-10* respectively. Raw data from ICP-OES is presented in Appendix 8.3.1.

Table 5-9: Concentrations of elements after demineralisation with NaOH and HNO_3 at 15g/180ml

Elements	***Initial concentration (ppm)***			
	Tyre Char		***Tyre Crumb***	
	1M NaOH	***1M HNO_3***	***1M NaOH***	***1M HNO_3***
Ca	1.00	116.6	0.00	87.15
Cu	0.75	8.75	0.65	5.5
Fe	0.15	165.8	3.25	66.1
K	130.5	30.6	30.25	36.85
Na	-	97.3	-	333.95
Ni	0.00	1.5	0.00	0.00
S	361.85	572.25	132.2	1067.95
Si	3105.00	242.95	553.6	108.9
Zn	534.45	4757.5	82.2	315.25
Al	165.20	101.35	31.35	20.55

Table 5-10: Concentrations of elements after demineralisation with NaOH and HNO_3 at 1g/12ml

Elements	***Initial concentration (ppm)***			
	Tyre Char		***Tyre Crumb***	
	1M NaOH	***1M HNO_3***	***1M NaOH***	***1M HNO_3***
Ca	21.3	209.25	7.35	121.75
Cu	0,00	5.95	2.2	7.10
Fe	0,00	78.65	1.95	128.0
K	110.5	96.25	32.05	47.2
Na	-	147.3	-	107.45
Ni	0,00	0,00	0,00	0,00
S	660.75	837.3	262.35	938.65
Si	3335.75	202.25	2234.0	81.65
Zn	1003.35	3852.0	145.15	1021.45
Al	142.35	129.95	59.95	21.25

More elements were leached in tyre char than tyre crumb and this may be attributed to the fact that tyre rubber is not easily penetrated and digested by chemicals [77], therefore, it is difficult for the chemical solvents to reach and leach metals that are impeded in the organic matrix of the tyre rubber and for this reason tyre may be immune to chemical treatments [39]. However, with tyre char the organic matrix is burnt off during pyrolysis which leave the inorganic ash exposed on the surface of char. Some elements such as nickel and copper are already present in very low concentrations in tyre char and crumb.

The results of sodium concentration under treatment with 1M NaOH samples are excluded since the sodium from NaOH also adds to the sodium leached which will give higher values than the actual amount of sodium leached from the samples. From the results in *Table 5-9* it can be observed that in tyre char and crumb, the most leached elements are silicon and zinc during treatment with NaOH and HNO_3 respectively. The same trend is also observed in results reported in *Table 5-10*.

The inefficiency of nitric acid in leaching of silicon is mainly because majority of acids if not all cannot dissolve silicon dioxide (SiO_2) which is the main predominant form of silicon in tyre char and crumb. The only acid reported to have the capability of effectively dissolving SiO_2 is hydrofluoric acid (HF). However, NaOH reacts with SiO_2 to from a soluble compound such as sodium silicates which is also soluble in acids including HNO_3 [77]. The efficiency of silicon removal by NaOH is also reported in literature [77].

Apart from zinc and silicon, the sulphur element is also highly leached particularly with nitric acid in both tyre char and crumb. This observation is consistent with results reported in literature, nitric acid is reported to have high influence and efficiency is leaching of sulphur [47].

The acid-base demineralisation also removed organic compounds including oil from both tyre char and crumb. After the treatments, the initial weight of tyre char and crumb was reduced from 15 g to 12.57 g and 12.4 g respectively. Total mass extracted from PT-char was about 16.2 wt.% and from UT-crumb was 17.3 wt.%. The mass extracted constitutes of inorganic ash and organic matter and the ash removed from PT-char was 14.8 wt.%

according to proximate analysis results. Therefore, when the total mass extracted is subtracted from the ash removed the remaining is the organic matter which was also extracted. In PT-char the organic or oil extracted will be about 1.4 wt.% and in UT-crumb will 13.4 wt.%. In *Figure 5-7* it is clear that not only ash was extracted but also organic matter.

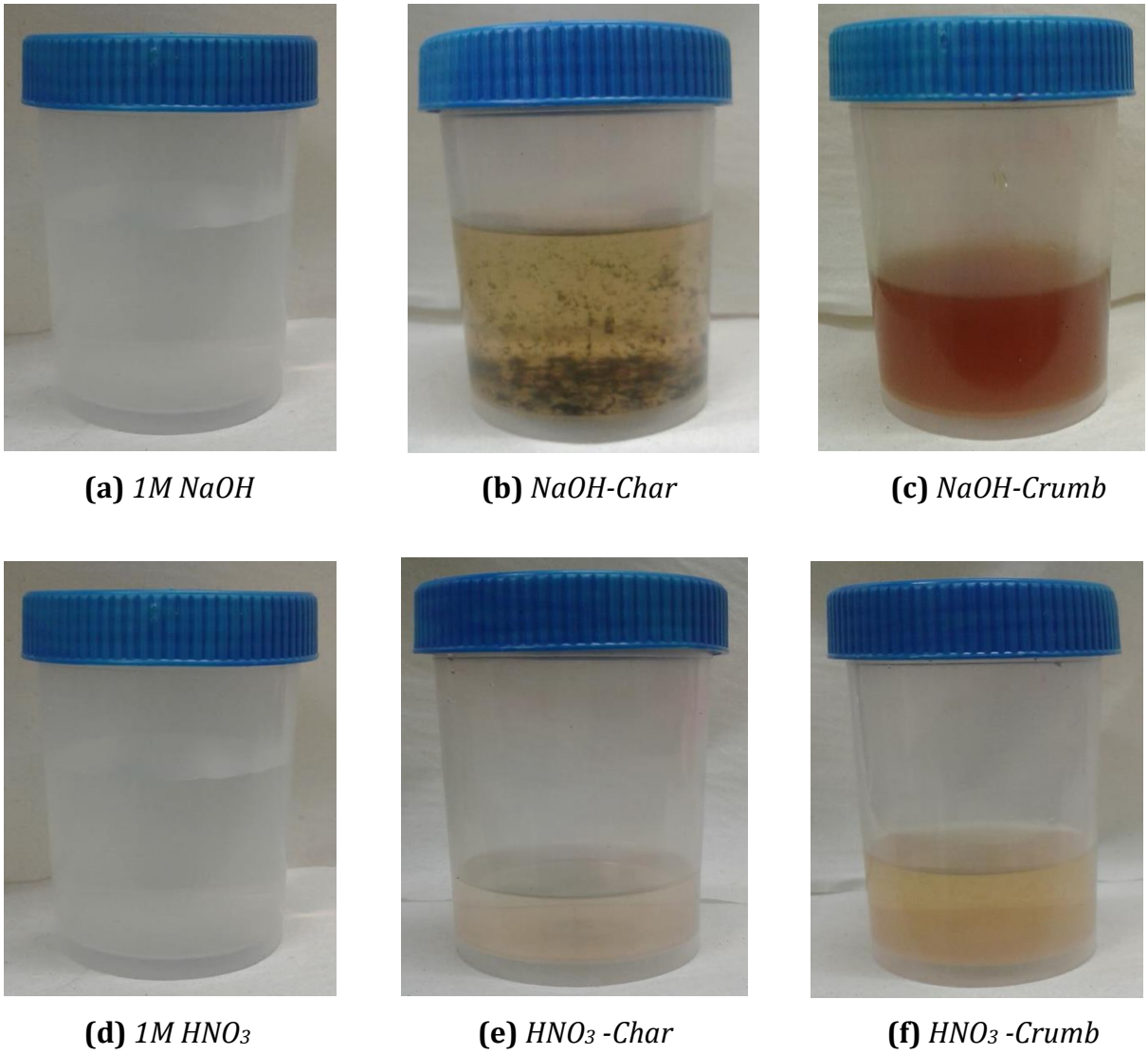

(a) *1M NaOH* **(b)** *NaOH-Char* **(c)** *NaOH-Crumb*

(d) *1M HNO_3* **(e)** *HNO_3 -Char* **(f)** *HNO_3 -Crumb*

Figure 5-7: Leachate solutions before and after alkali-acid treatment of tyre char and crumb

The acid-base treatment of UT-crumb also changed its surface chemistry from being hydrophobic (a) to partially hydrophilic (b) as demonstrated by *Figure 5-8*. These can be attributed to the formation of oxygen-containing polar functional groups to the surface of the rubber crumb [1].

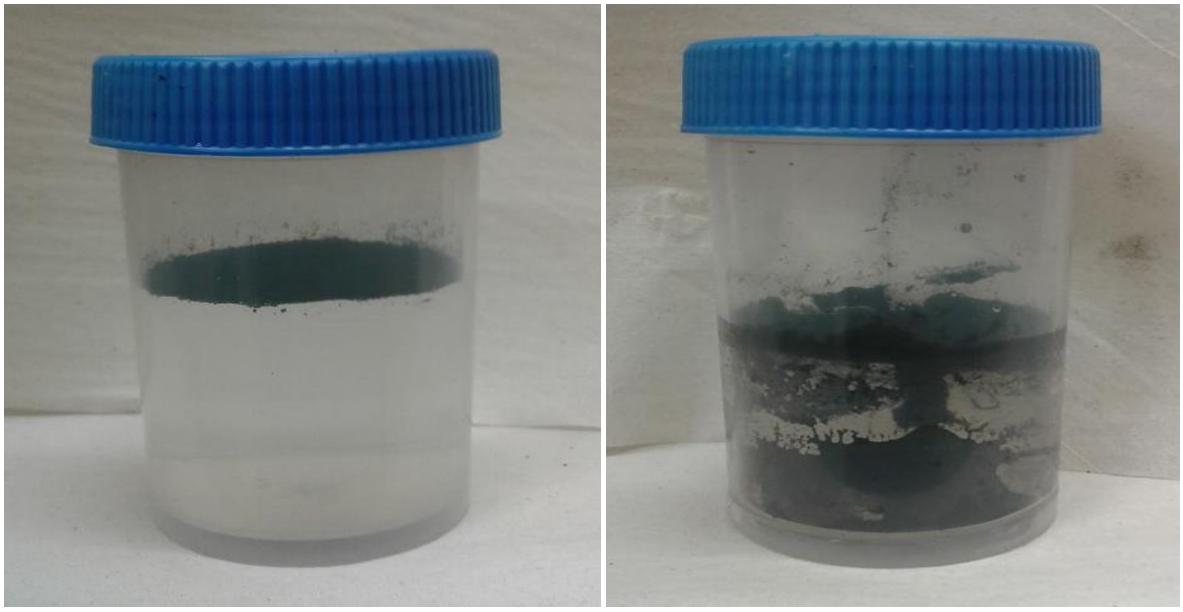

(a) *UT-crumb* **(b)** *TT-crumb*

Figure 5-8: Interaction between (a) untreated and (b) treated tyre rubber crumb with water

The texture of UT-crumb also changed after alkali-acid treatment. Physically, the untreated tyre crumb sample had small, strong, elastic chips of rubber and the treated sample was very much of a powder with fine particles. This shows that during the acid-base treatment, tyre crumb particles degraded to fine particles.

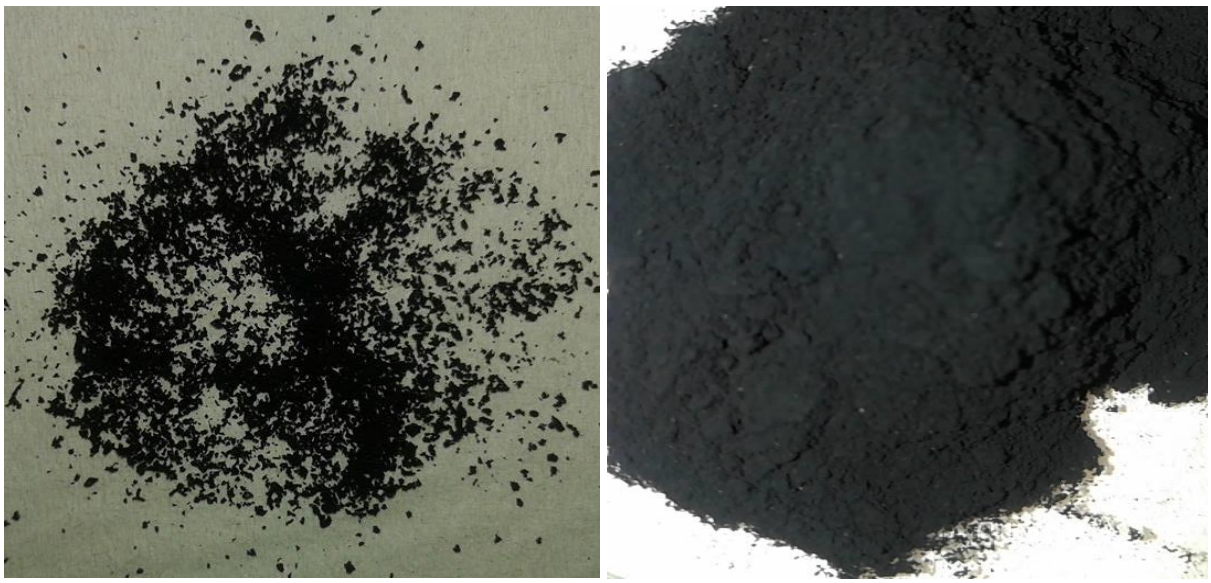

(a) *UT-crumb* **(b)** *TT-crumb*

Figure 5-9: Physical appearance of tyre crumb before (a) and after (b) alkali-acid treatment

5.8 Summary of results

The effect of alkali-acid demineralisation of UT-crumb and UPT-char was monitored and explained according to characterisations results obtained before and after the treatment. The treatment proved to be efficient in increasing the BET surface area of the adsorbents and improving the hydrophilicity of UT-crumb. An acid or alkaline is not sufficient to demineralise these adsorbents individually since some metals cannot be dissolved with acid or base alone. The treatment of the adsorbents with NaOH first is important since it tends to form hydroxides with elements that are difficult to dissolve with acid only. When the metal hydroxides are formed then it is much easier to dissolve and wash them off with an acid. The organic matrix of UT-crumb makes it difficult for the solvents to access its internal surface.

5.9 Au Adsorption conditions

5.9.1 Effect of solution pH

The pH of a solution is an important parameter as it affects metal speciation and adsorbent surface charge, consequently affecting the adsorption of adsorbates on the adsorbent. To study the effect of solution pH on the adsorption of Au(III) ions, experiments were conducted in the pH range of 1-8. Buffer solutions were used to adjust the initial pH value to the desired value and the results are presented on *Figure 5-10* below.

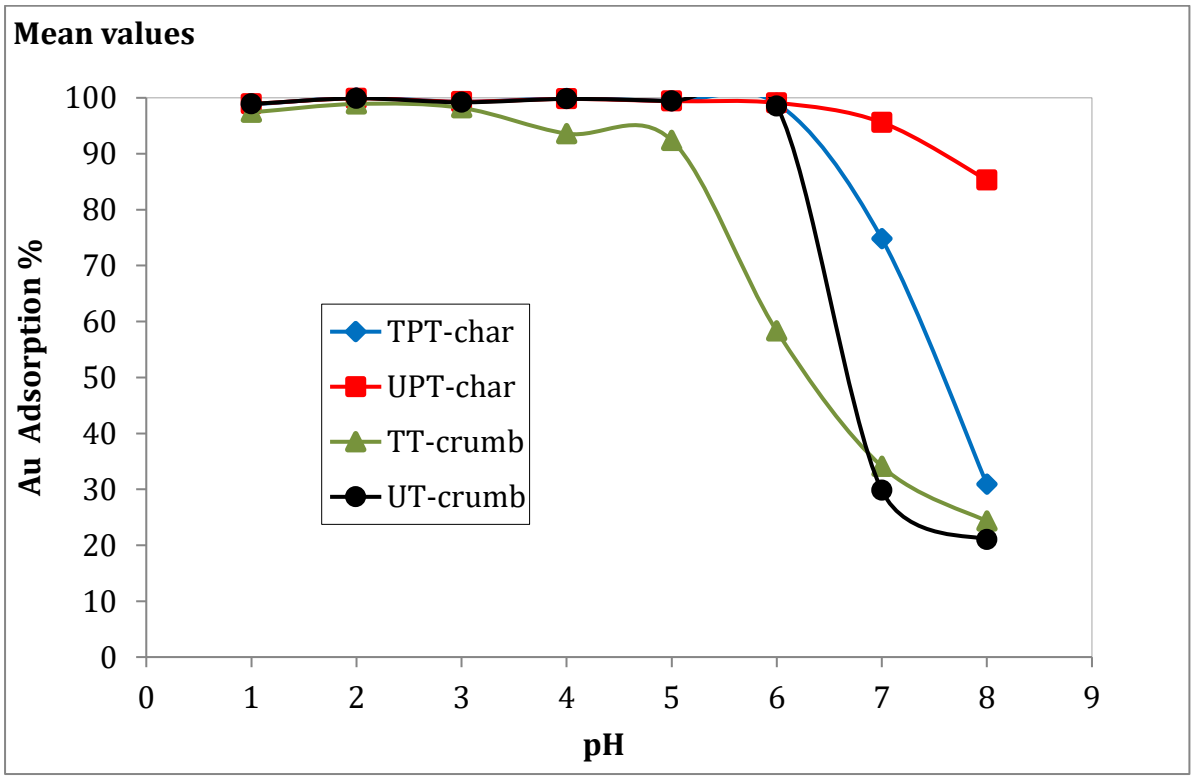

Figure 5-10: Effect of solution pH on adsorption of Au^{3+} ions (V = 0.025 L, t_{con} = 24 h, T = 25 °C, C_0 = 100 mg/L, m = 3 mg for UPT-char and 15 mg for (TPT-char, UT-crumb and TT-crumb)).

It can be observed from *Figure 5-10* that adsorption of Au(III) ions was highly dependent on solution pH and that the adsorption percentage increased with an increasing pH in acidic solution and rapidly decreased as the pH increased under basic solution (pH>7). The increase in Au(III) ions adsorption percentage in acidic solution can be attributed to the fact that at low pH values there is high concentration of H^+ ions which protonate and cover the adsorbent surface causing it to be positively charged. Since Au(III) ions are

adsorbed as anionic $AuCl_4^-$ ions; therefore, there is high electrostatic attraction between the $AuCl_4^-$ ions and the protonated adsorbent surface at low pH values. The decline in Au(III) ions adsorption percentage as the pH increases to basic solution may be due to hydrolysis of $AuCl_4^-$ ions to hydroxide-containing gold complexes (i.e., $AuCl_3(OH)^-$, $AuCl_2(OH)_2^-$, and $AuCl(OH)_3^-$) which tend to form precipitates [22]. Generally, in acidic pH and temperature below 5.8 and 150 °C, respectively, the $AuCl_4^-$ gold complex is the most stable. At pH values higher than 5.8 the $AuCl_4^-$ gold complex is hydrolysed leading to formation of chlorohydroxy complexes due to replacement of Cl^- ions by OH^- ions which may result in the formation of gold precipitates, Au(0), or Au(I) via reduction process [121]. Optimal pH range was found to be 1-6 with ≤99% Au(III) removal except for the treated tyre crumb (TT-crumb) which had optimal pH range of 1-5 with over 92% Au(III) removal. However, pH 2.0 was chosen and used as the optimum pH throughout the study to ensure maximum uptake of Au(III) ions. At this pH value the maximum Au(III) removal was 99% for TT-crumb and almost 100% for the rest of the adsorbents.

5.9.2 Effect of adsorbent concentration (g/L)

The study of the effect of adsorbent dosage on adsorption of Au(III) was conducted in an adsorbent concentration range of 0.12-10 g/L for both the untreated and treated pyrolytic tyre char and tyre crumb adsorbents. Each point was analysed at 24 and 48 hrs contact time and the adsorbent concentration was varied until equilibrium was reach. In both cases the results were plotted against adsorption capacity (Q_e). All other parameters were kept constant.

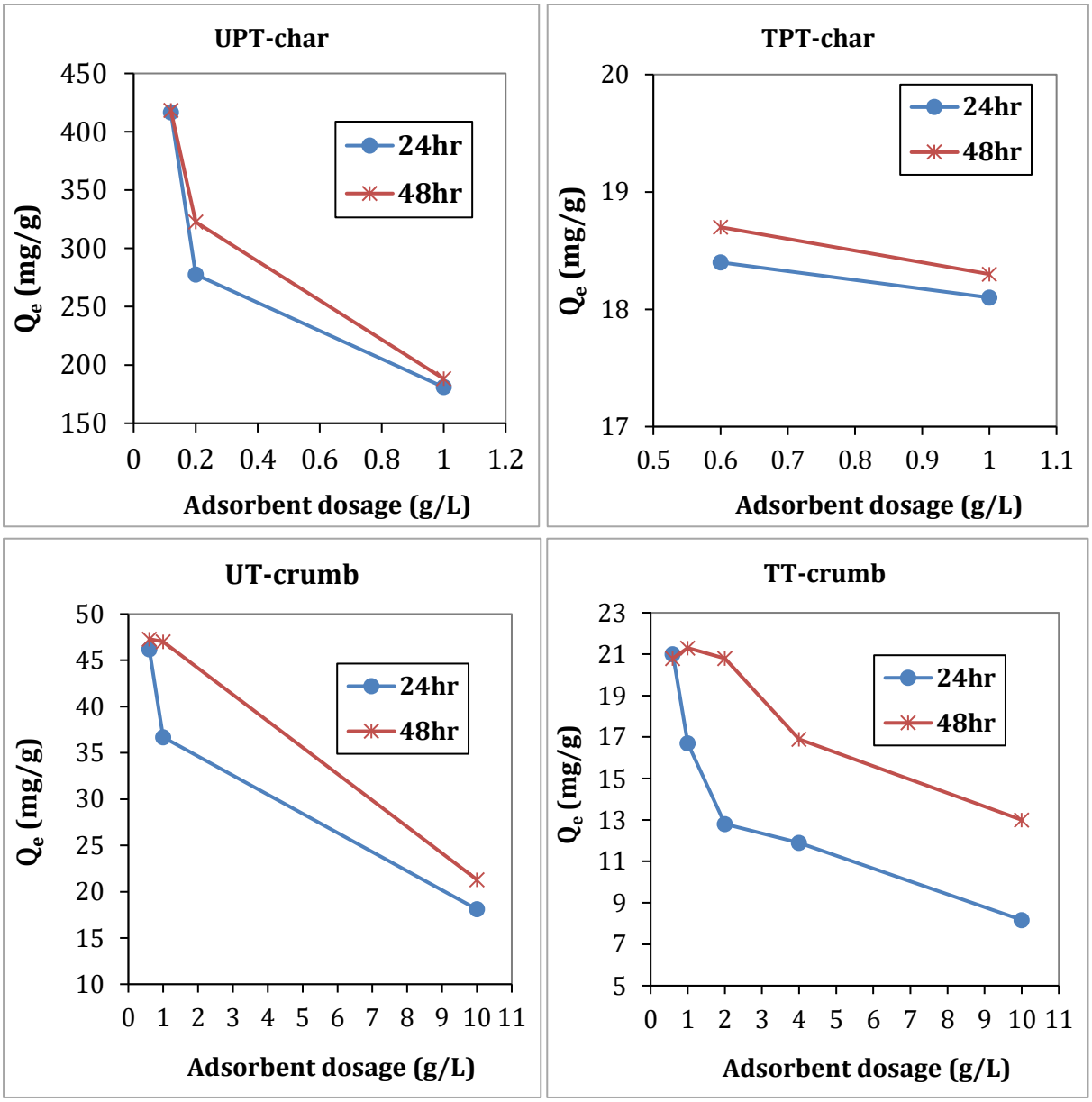

Figure 5-11: Effect of adsorbent dosage on adsorption of Au^{3+} ions (V = 0.025 L, T = 25 °C, pH = 2, C_0 = 100 mg/L for (UT-crumb and TT-crumb) and 188 mg/L for (UPT-char and TPT-char).

The initial gold concentration used was 100 mg/L and 188 mg/L for crumbs and chars respectively. The minimum adsorbent concentration at equilibrium for UPT-char was 0.12 g/L with Q_e of ~420 mg/g, for TPT-char was 0.6 g/L with adsorption capacity of ~19 mg/g, for UT-crumb was 0.6 g/L with adsorption capacity of ~47 mg/g and for TT-crumb was 0.6 g/L with adsorption capacity of ~21 mg/g. The Q_e in TPT-char remained almost the same even at higher adsorbent concentration which suggest that maximum capacity was reached quickly unlike with

UPT-char in which at higher adsorbent concentration, 1 g/L, almost all the gold in the solution was adsorbed within 24hrs. This suggest that UPT-char have high capacity and affinity for gold ions at given conditions. The summarised results are tabulate in *Table 5-11*. The adsorbent concentration for each sample in *Table 5-11* will be used for all the remaining experiments.

Table 5-11: Minimum adsorbent concentration at equilibrium

Adsorbent	***Ads. Dosage (mg)***	***Ads. Concentration (g/L)***
UPT-char	3	0.12
TPT-char	15	0.6
UT-crumb	15	0.6
TT-crumb	15	0.6

5.9.3 Effect of initial Au(III) concentration

The initial adsorbate concentration is an essential parameter for determining the rate of adsorption and the maximum adsorption capacity of an adsorbent and to obtain the adsorption isotherms. To study the effect of initial Au(III) concentration on adsorption capacity a set of experiments were conducted in an adsorbate concentration range of 0-188 mg/L for all the adsorbents. The results were plotted against adsorption percentage (A%) and capacity (Q_e) with all other parameters kept constant.

Although the results in *Figure 5-11* shows that a contact time of 24 hrs is enough to reach equilibrium at optimum adsorbent concentration for UPT-char and UT-crumb, a contact time of 48 hrs was used for these adsorbents to ensure complete adsorption. The 24hrs contact time for TPT-char and TT-crumb is more than enough for complete adsorption. Therefore, all experiment with UPT-char and UT-crumb will be conducted at 48hrs and TPT-char and TT-crumb at 24 hrs contact time.

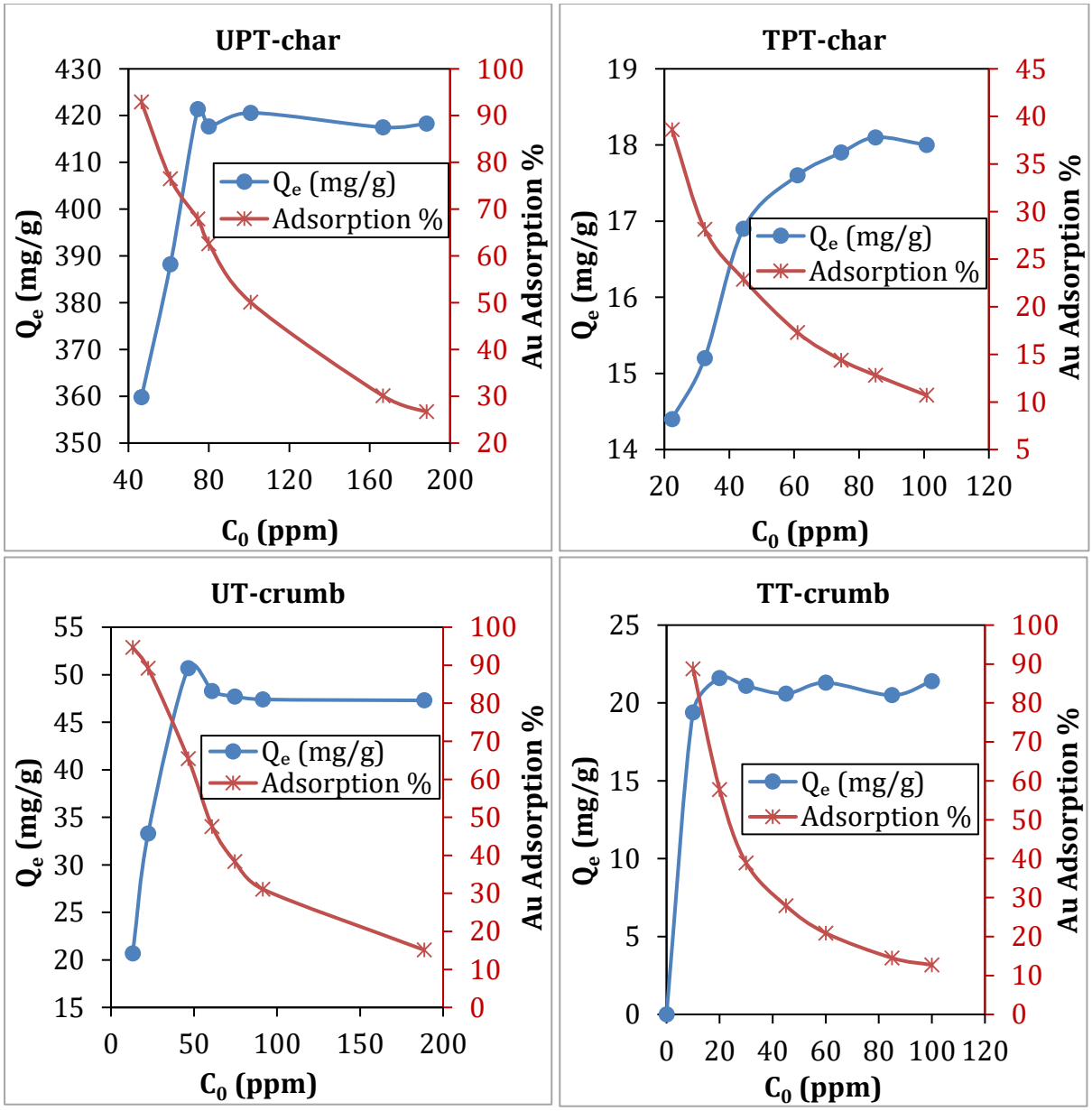

Figure 5-12: Effect of initial Au(III) concentration on adsorption capacity at (V = 0.025 L, pH = 2, T = 25 °C, t_{con} = 24 h for TPT-char and TT-crumb, t_{con} = 48 h for UPT-char and UT-crumb), m = 3 mg for UPT-char and 15 mg for (TPT-char, UT-crumb and TT-crumb).

The equilibrium curves for this data are presented in Appendix 8.9. From *Figure 5-12* an obvious trend was observed whereby an increase in adsorbate concentration led to an increase in adsorption capacity up to a maximum point. The adsorption capacity increased from 359.8 to 421.4 mg/g for UPT-char, 14.4 to 18.1 mg/g for TPT-char, 20.7 to ~48 mg/g for UT-crumb and 0 to 21.6 mg/g for TT-crumb as the initial Au(III) concentration increased. This behaviour may be attributed to the concept of concentration gradient whereby high concentration of Au(III) ions in a solution are

mobilised from the solution to the adsorbent's active binding sites on its surface. However, the adsorption percentage decreased with an increase in Au(III) concentration. This is due to the occupation of the adsorbent's active binding sites with Au(III) ions as their concentration increased leading to less surface available for further adsorption.

UPT-char adsorbent had the highest affinity and consequently the highest adsorption capacity for Au(III). The results also show that the alkali-acid demineralisation had a negative impact on adsorption of Au(III) even though the surface area of the treated adsorbents was higher than those of untreated adsorbents. It can be concluded that the adsorbent's surface area was not a key factor in adsorption of Au(III). The ultimate analysis of the adsorbents before and after alkali-acid demineralisation revealed that sulphur content in treated adsorbents was greatly decreased on the surface of the adsorbents. The sulphur content in UPT-char before alkali-acid demineralisation was 2.366 wt.% and after alkali-acid demineralisation was 0.619 wt.% which means over ~73% of sulphur content was removed from the surface of char. In UT-crumb the sulphur content before alkali-acid demineralisation was 2.043 wt.% and after alkali-acid demineralisation was 0.907 wt.% which means over ~56% of sulphur content was removed from the surface of crumb.

Many researchers emphasised on the affinity of gold towards sulphur and the ability of sulphur to selectively adsorb gold in the midst of other metal ions. Sulphur compounds are considered to have good chelating properties for metals, more especially precious metals. Gold nanoparticles are known to bind well on sulphur-containing compounds [34,122]. The bonding mechanism of sulphur as a chelating agent with metals, particularly with gold, is well explained by Pearson using hard-soft acid-base (HSAB) theory in complex formation reactions. In HSAB, soft base prefers to coordinate with soft acid and hard base with hard acid during acid-base reactions. Sulphur is considered a soft base which would prefer to coordinate with soft acids such as Au(III) hence the strong affinity [22,89]. The HSAB theory suggest that sulphur forms strong and highly stable bonds with gold in water, organic solvents and air at room temperatures. Additionally, since sulphur has a very high affinity for gold: therefore, adsorbents with high and accessible sulphur on their surface can enhance adsorption capacity and selectivity for gold ions [22,34].

Attempts have also being made to introduce sulphur content on carbonaceous adsorbents such as activated carbon specifically for adsorption of gold. Ramírez-Muñiz et al. [92] compared a conventional activated carbon with a sulphur-impregnated activated carbon on adsorption of gold. They found out that indeed the adsorption capacity of sulphur-impregnated activated carbon for gold was significantly improved and it was more than twice as high as that of conventional activated carbon. They attributed these results to the extremely high affinity of sulphur towards gold.

The adsorption of Au(III) on sulphide groups leads to reduction of gold and formation of metallic gold on the adsorbent surface [121]. In literature it is reported that ZnS is the most abundant sulphide compound on the surface of UPT-char and it forms particles which can easily be removed by demineralisation [58]. The ZnS compounds on the char surface serve as binding sites for gold and are responsible for the reduction of gold with sulphur acting as a reductant [121,123]. The mechanism in which gold is reduced from Au(III) to Au(0) by the metal sulphide compounds on the adsorbent surface occurs in two main steps. The first step is the adsorption of Au(III) on the sulphide group due to their extremely high affinity to each other. The adsorption is via ligands substitution between sulphide ligand and chloride ligand from the Au chloride complex, i.e. $AuCl_4^-$. The second step involves the reduction of Au(III) to Au(I) and Au(0) by sulphide via electron transfer from sulphur atom to the gold complex [121,123]. Once gold is reduced to metallic nanoparticles on the metal sulphide nanoparticles it becomes very reactive which act as a catalyst to further promote reduction of Au(III) leading to formation of larger Au nanoparticles [123]. Based on results obtained and literature information, the proposed mechanism adapted from [123] could be:

$$(ZnS)_n + AuCl_4^- \longrightarrow (ZnS)_n\text{–}Au^3Cl_3 + Cl^- \quad (5.2)$$

$$(ZnS)_n\text{–}AuCl_3 \longrightarrow Zn_{n-1}S_n\text{–}Au^1Cl + Zn^{2+} + 2Cl^- \quad (5.3)$$

$$Zn_{n-1}S_n\text{–}AuCl + 2Zn_nS_n \longrightarrow Zn_{n-1}S_n\text{–}Au^0 + Zn_nS_n\text{–}S_n^{2-} + nZn^{2+} + AuCl_4^- \quad (5.4)$$

Reaction *Equation (5.2)* represent the adsorption of $AuCl_4^-$ on the surface of ZnS, *Equation (5.3)* represent the reduction of Au(III) to Au(I) followed by oxidation of sulphur in ZnS to S^{2-} and lastly reaction *Equation (5.4)* represent reduction of Au(I) to Au(0) in which Au(I) undergo disproportionation to Au(0) and Au(III) leading to formation of metals and polysulphide (S_n^{2-}). The final step shows that zinc metal ions and sulphur are released into the solution after adsorption [5] and to determine their concentration ICP analysis is used. The results for analysis of zinc and sulphur concentration are presented in *Figure 5-13*.

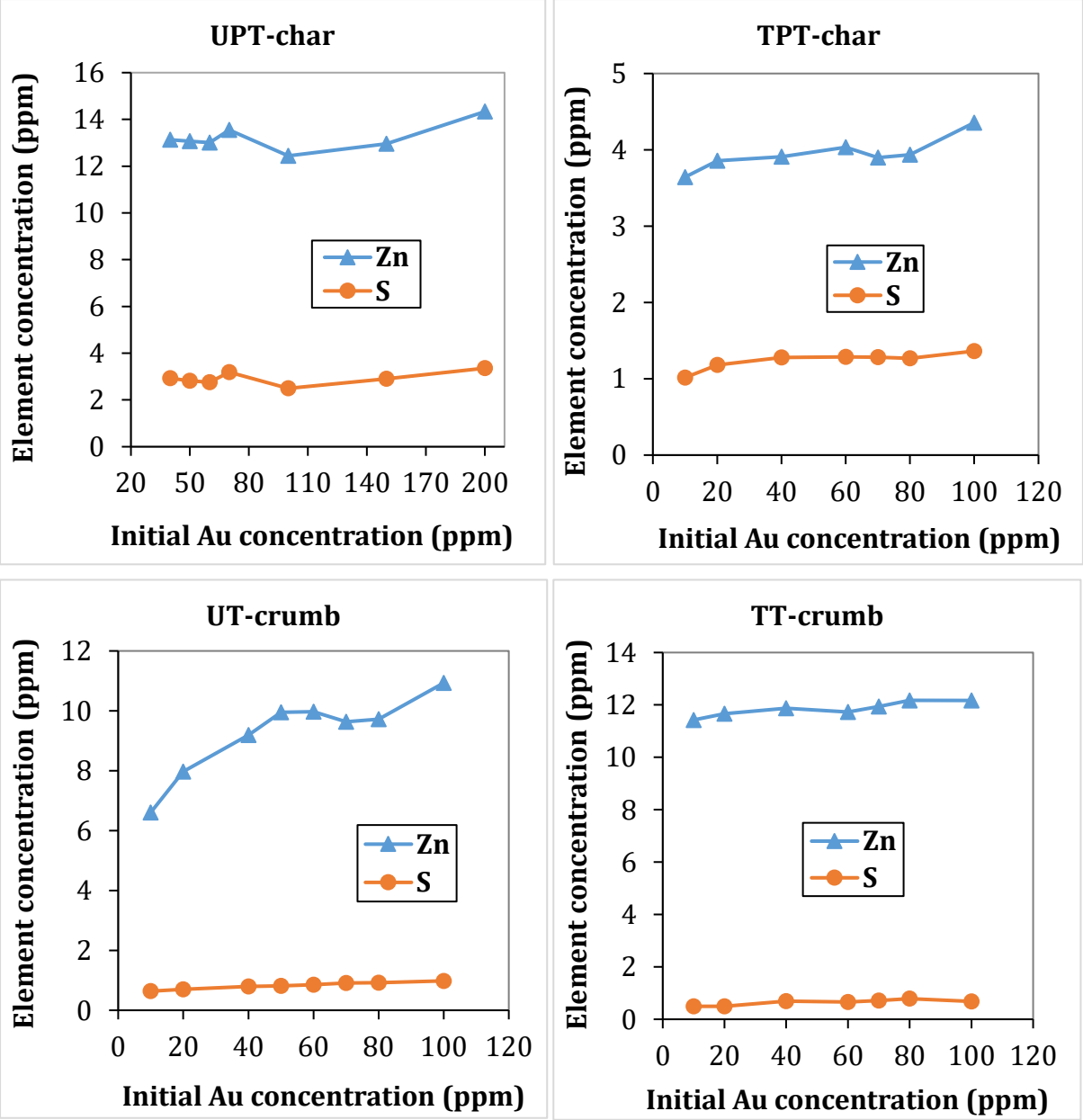

Figure 5-13: Amount of zinc and sulphur content leached during gold adsorption

It should be noted that amount of UPT-char used was five times lower than that of TPT-char which greatly affect the quantity of elements leached. However, the adsorbent dosage of UT-crumb, TT-crumb and TPT-char were equal. In each adsorbent, zinc and sulphur followed the same trend and the only difference was their concentration. The amount of zinc and sulphur leached during adsorption with UPT-char is higher than that of TPT-char despite the fact that the amount of UPT-char used was 3 mg and that of TPT-char was 15 mg. Zinc and sulphur content leached in UPT-char is almost 10x and 3x higher than in TPT-char respectively. The reason for low zinc and sulphur leached in TPT-char is because most of the zinc and sulphur content were removed from its surface during demineralisation. The trend shows that as initial gold concentration increased, the quantity of zinc and sulphur leached also increased in the same trend. Therefore, this confirms that ZnS compound was involved in the adsorption mechanism of gold as predicted by Pan et al. [123] in the abovementioned mechanism.

Therefore, a conclusion is reached that sulphur was a key binding site for gold and the high capacity of UPT-char is attributed to its high surface sulphur content. The sulphur content in UT-crumb is also high and almost equal to that of UPT-char according to ultimate analysis results, but the sulphur is imbedded within its complex organic matrix which is difficult to access [77] hence low gold adsorption capacity as compared to UPT-char. UPT-char could therefore be a potential alternative low-cost adsorbent to conventional activated carbons in recovery of gold from acidic chloride solutions due to its strong affinity for gold, high adsorption capacity and lower production costs.

The adsorption capacity of UPT-char was compared to that of adsorbents reported in literature including carbonaceous adsorbents, activated carbons and sulphur-containing adsorbents listed in *Table 5-12*.

Table 5-12: Adsorption capacity of different adsorbents for Au(III) ions

Adsorbents	***BET surface area (m^2/g)***	***Q_{max}***	***pH***	***Ref***
RS-SR-NH-SiO_2-Fe_3O_4	12.4	222.2	5	[22]
Sulphur-impregnated activated carbon	1564	126.6	10.5	[92]
Commercial activated carbon	1037	56.2	10.5	[92]
Mesoporous adsorbent	565	177.9	2	[124]
Raw data pits	285	78 ±1.1	n/a	[125]
PEI-LS	n/a	286	1	[20]
PPF resin	n/a	506	n/a	[126]
PPF resin	0.23	3025.2	2	[127]
Glycine modified crosslinked chitosan resin	n/a	169.98	2	[21]
Chitosan	n/a	30.95	4	[128]
N-Carboxymethyl Chitosan	n/a	33.90	6	
Lewatit TP 214	n/a	109.6	6.1	[129]
Activated rice husk	n/a	93.3		
Chemically modified activated carbon	n/a	33.57	1	[130]
Sawdust	4.24	3.2		
Magnetic sawdust	47.9	16.45	3	[131]
Modified composite	17.1	188.68		
GH-D-P	176.6	357.14	2.3	[132]
Oxidized multi-walled carbon nanotubes	n/a	62.3	2	[100]
Facial conjugate adsorbent	385	203.42	2	[133]
Pyrolytic tyre char	63.9	434.8	2	This study
Tyre rubber crumb	0.322	47,3	2	This study

5.9.3.1 SEM micrographs of gold loaded adsorbents

This section provides the evaluation of the surface morphology of the tyre-derived carbonaceous adsorbents after gold adsorption.

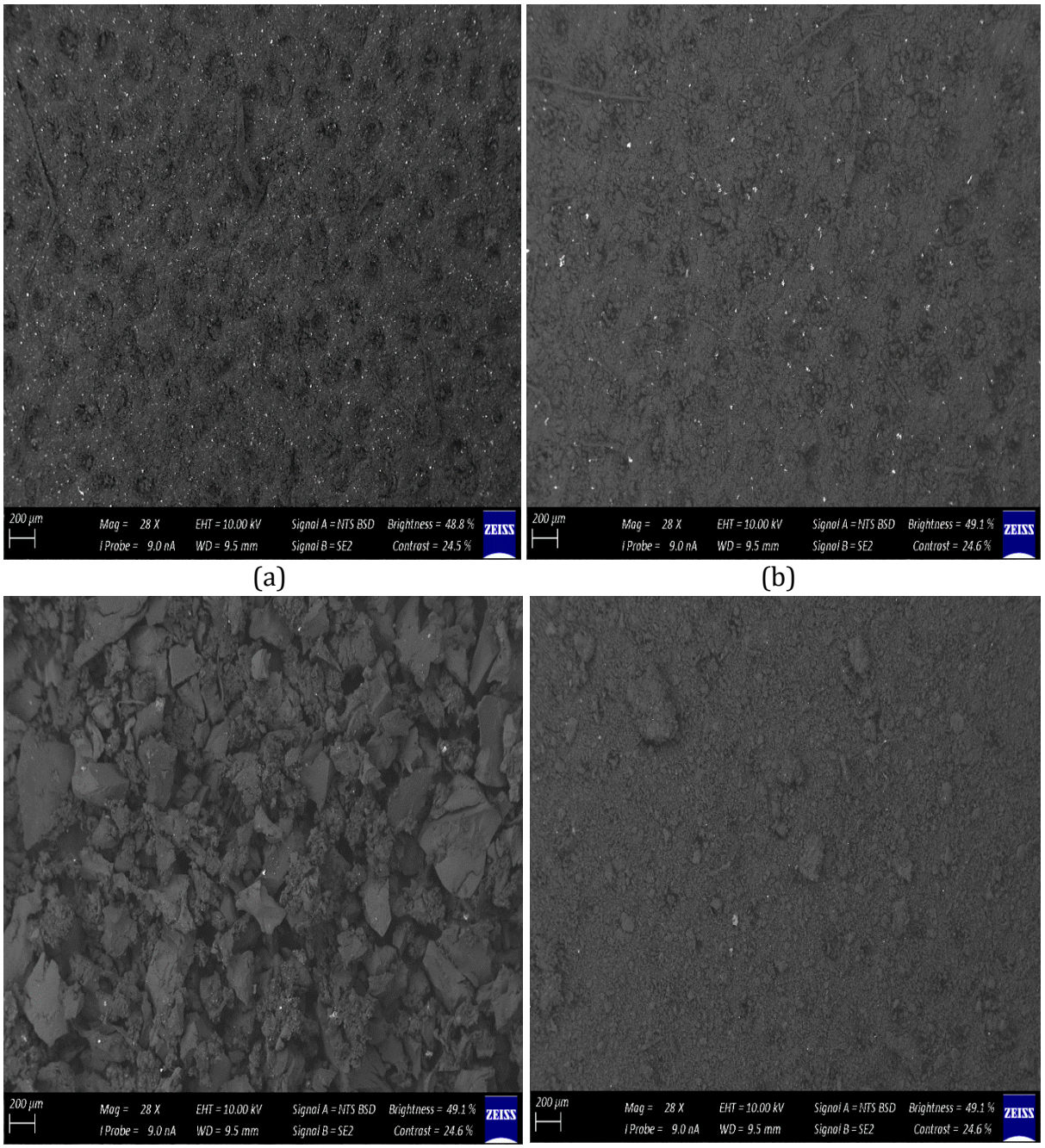

Figure 5-14: SEM images of gold loaded (a) UPT-char (b) TPT-char (c) UT-crumb and (d) TT-crumb adsorbents at 28x magnification

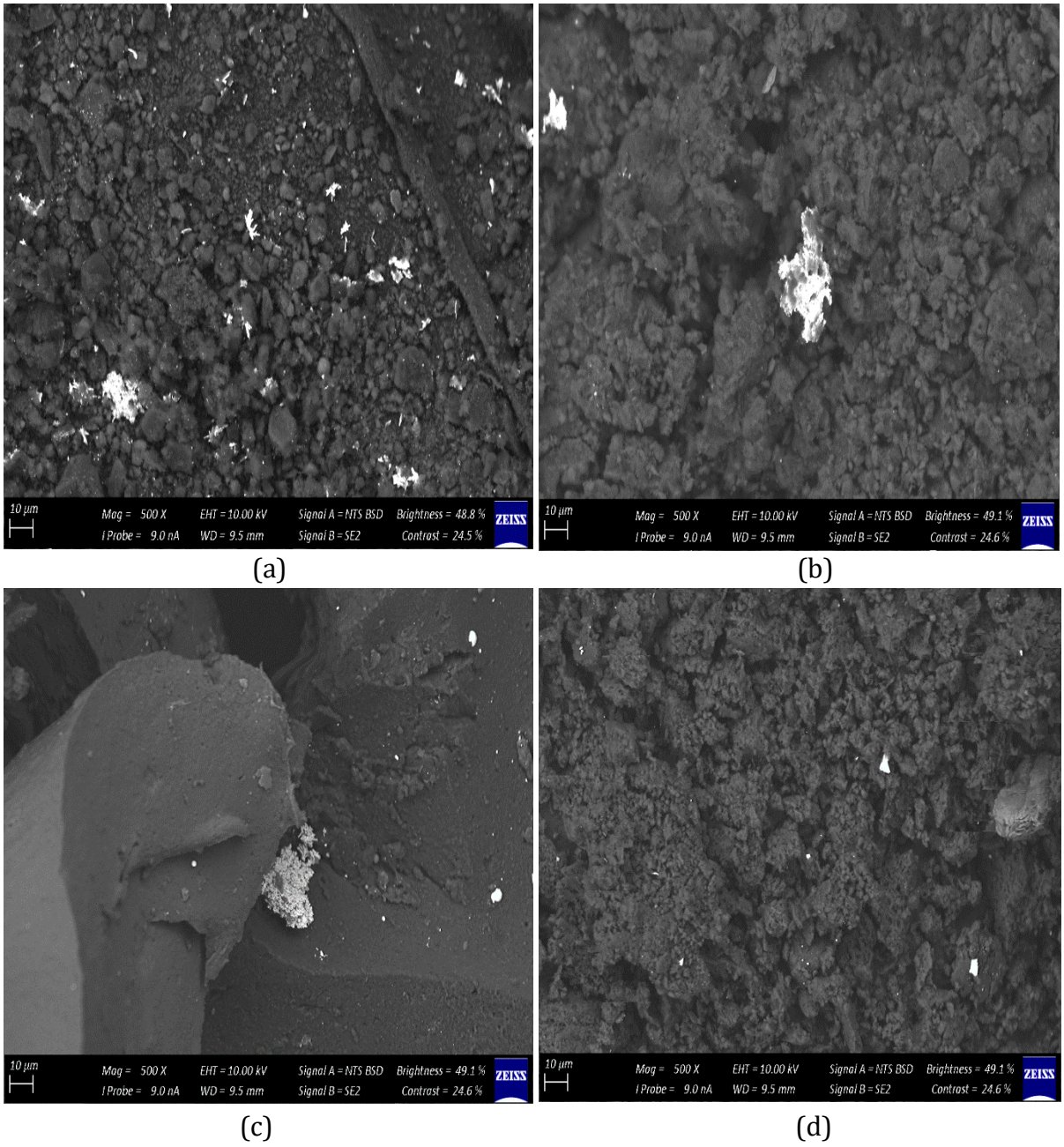

Figure 5-15: SEM images of gold loaded (a) UPT-char (b) TPT-char (c) UT-crumb and (d) TT-crumb adsorbents at 500x magnification

The adsorbents from which the SEM micrograph images were taken from, were used in adsorption of gold at initial gold concentration of 188 mg/L for 48 hrs. The bright spots on the external surface of the adsorbents in *Figure 5-14* and *Figure 5-15* are gold nanoparticles in a metallic form. This shows that when gold in a solution is adsorbed onto the surface of these adsorbents it is further reduced or precipitates to form metallic gold particles (i.e. Au(III) to Au(0) conversion). Similar observations were reported in literature for carbonaceous adsorbents. Sun and Yen [134] reported that gold chloride

complex was reduced to metallic gold on the surface of activated carbon after adsorption. They attributed this to electrical conductivity nature of activated carbon which served as an electrode for the redox reaction that occurred during the adsorption of gold chloride. They also found out that impurities such as zinc and copper ions did not have a significant impact on adsorption of gold by activated carbon. However, the presence of iron in a form of ferric ion had a great impact which facilitated the adsorption of gold due to conversion of Fe^{3+} to Fe^{2+} by activated carbon via reduction process [134]. It is worth noting that they also mentioned that reagents such as sulphur dioxide, SO_2, are usually used to recover gold chloride complex ions, $AuCl_4^-$, by reducing them from Au(III) to Au(0) precipitates. Another method they mentioned is replacement by zinc metal [134].

Aqueous chlorine is used in dissolution of gold to form gold chloride complex ions, $AuCl_4^-$. Therefore, high concentration of dissolved chlorine in the aqueous solution can slow down the rate of gold adsorption and lower the amount of gold adsorbed by the adsorbent due to redissolution of the precipitated gold particles from the adsorbent's surface back into the solution [134].

From both *Figure 5-14* and *Figure 5-15*, especially *Figure 5-14* it shows that gold particles are more concentrated on the surface of UPT-char which covered most of the surface than other adsorbents. The implication of this observation is that as more gold particles appear to be adsorbed onto UPT-char surface, therefore, UPT-char adsorb more gold on its surface and its adsorption capacity should be higher than TPT-char, UT-crumb and TT-crumb. On the surface of UT-crumb and TT-crumb, very fewer gold particles are adsorbed which means UT-crumb and TT-crumb should have less capacity for gold. These results are consistent with results reported under adsorption isotherms whereby the gold capacity increased according to the following order UPT-char > UT-crumb > TT-crumb > TPT-char. The untreated adsorbents performed better than their treated counterparts even though proximate analysis shows that ash content in treated adsorbents was reduced and the surface area was also higher in these adsorbents according to BET surface area analysis. The main reason for this is because the ash is mainly composed of ZnS which act as a key binding site for gold.

Additionally, from the evaluation of the appearance of the adsorbed gold particles it shows that in UPT-char they appear to be smaller and scattered abroad on random sites whereas in TPT-char they are a bit bigger and very big in UT-crumb. The formation of large clusters of gold particles on UT-crumb surface shows that the gold particles further aggregated. In all samples the adsorbed gold particles appear to have outgrowth of another gold nanoparticles forming agglomerates. This is due to a spontaneous growth of gold particles since once gold is reduced to metallic nanoparticles on the metal sulphide nanoparticles it becomes very reactive which act as a catalyst to further promote reduction of Au(III) leading to formation of larger Au nanoparticles [123]. Additional SEM images of gold-adsorbed adsorbents and their corresponding EDX plots are presented in Appendix 8.10.

In a case of UT-crumb, gold precipitates were not only formed on the surface, but they were also formed in the solution after adsorption as illustrated on *Figure 5-16* below.

Figure 5-16: Gold precipitates formed in the solution after adsorption with UT-crumb adsorbent.

Gold precipitates were formed in the solution when UT-crumb adsorbent was used. It means that during adsorption of gold with UT-crumb, a reducing agent was introduced into the solution to reduce gold. One possible reductant that might have been transferred

from the adsorbent into the solution is Fe^{2+} ions and Fe^{2+} chloride complex such as $FeCl_2$. Wojnicki et al. [135] reported similar results in their study titled "Kinetic studies of gold recovery from dilute aqueous solutions using Fe^{2+} chloride ions". They discovered that Fe^{2+} chloride complex and Fe^{2+} ions were able to reduce gold in a form of Au(III) chloride complex. They also studied the influence of chloride, Cl^-, ion concentration on the reduction of Au(III) chloride complex and reached a conclusion that an increase in Cl^- ion concentration facilitated in the formation of Fe^{2+} chloride complex which accelerated the reaction rate. The SEM-EDS results shows the presence of iron on UT-crumb surface higher than in UPT-char, TPT-char and TT-crumb and aqua regia results shows that high amount of iron was leached from UT-crumb than UPT-char. It has also been proven in *Figure 5-17* that during the gold adsorption with UT-crumb, iron metals were leached from the adsorbent into the solution highly concentrated with chlorine which might have led to formation of iron chloride complex and ultimately reduced Au(III) chloride complex in the solution [135]. *Figure 5-17* shows the quantity of iron leached into the solution from the adsorbent after gold adsorption. The gold particles were big enough to be separated from the solution by filtration.

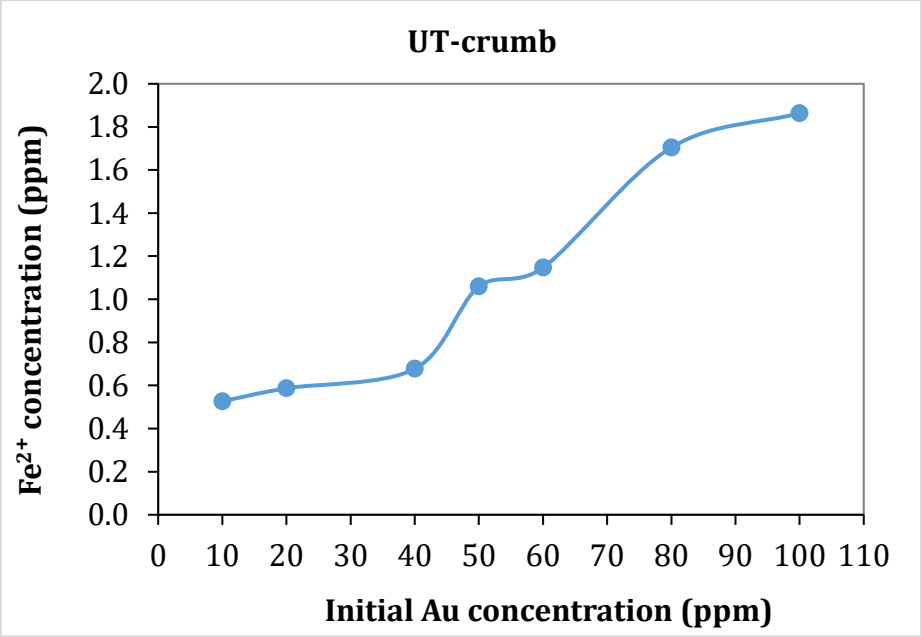

Figure 5-17: Iron metal leached during gold adsorption with UT-crumb

An increase in initial gold concentration of the solution led to an increase in iron concentration at constant adsorbent dosage. As more iron is leached into the gold solution therefore more gold precipitates might be formed.

The possible complete reaction scheme for reduction of Au(III) chloride complex to metallic gold by iron is provided by Wojnicki et al. [135]. The initial steps involve the formation of iron chloride complex which proceed to reduction reaction according to the following steps:

Iron chloride complex formation

$$Fe^{2+} + Cl^- \underset{}{\overset{k_1}{\rightleftharpoons}} FeCl^+ \quad (5.5)$$

$$FeCl^+ + Cl^- \underset{}{\overset{k_2}{\rightleftharpoons}} FeCl_2 \quad (5.6)$$

k_1 and k_2 are equilibrium constant for *Equation (5.5)* and *(5.6)*, respectively.

Reduction reactions

$$AuCl_4^- + Fe^{2+} \xrightarrow{k_{1,1}} AuCl_3^- + Fe^{3+} + Cl^- \quad (5.7)$$

$$AuCl_4^- + FeCl^+ \xrightarrow{k_{1,2}} AuCl_3^- + Fe^{3+} + Cl^- \quad (5.8)$$

$$AuCl_4^- + FeCl_2 \xrightarrow{k_{1,3}} AuCl_3^- + Fe^{3+} + Cl^- \quad (5.9)$$

$$2AuCl_3^- \xrightarrow{k_2} AuCl_2^- + AuCl_4^- \quad (5.10)$$

$$3AuCl_2^- \xrightarrow{k_3} AuCl_4^- + 2Au^0 + 2Cl^- \quad (5.11)$$

$$AuCl_2^- + Fe^{2+} + [Fe^{2+}]_{complex} \xrightarrow{k_4} Au^0 + Fe^{3+} + [Fe^{3+}]_{complex} + 2Cl^- \quad (5.12)$$

The Fe^{3+} ions in the solution after the reduction process of gold are easily hydrolysed to form complexes which might not be detected by the ICP-OES which might give lower

values of iron concentration in the resultant solutions [135]. The rate at which gold precipitates were formed in the solution was very slow since it took more than a week for the precipitates to form. This then mean that the precipitation of gold by iron in the solution did not occur simultaneously with adsorption process and therefore there was no competition between precipitation and adsorption of gold by iron.

Beside the assumption that the reduced gold in the solution is reduced by the leached iron, another possibility for this effect could also be the leached Zn and S from UT-crumb according to the mechanism suggested in *Equation (5.2) to (5.4)*.

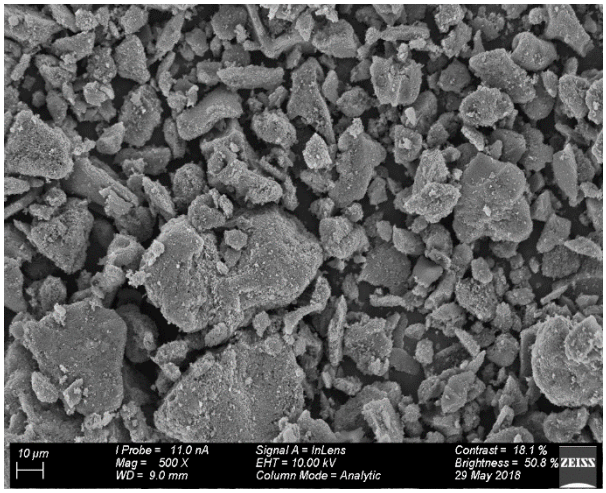

(a)

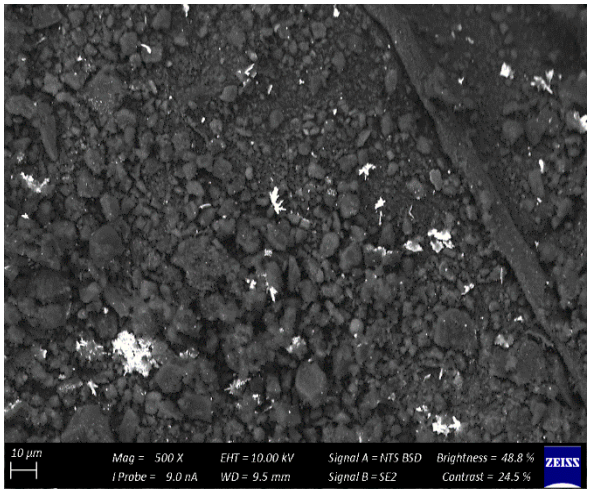

(b)

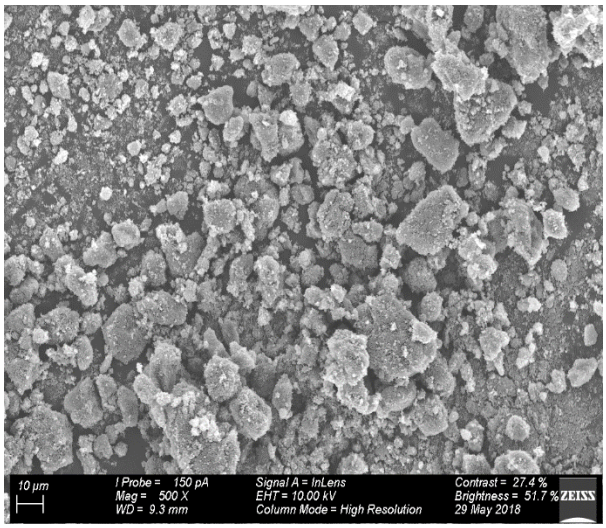

(c)

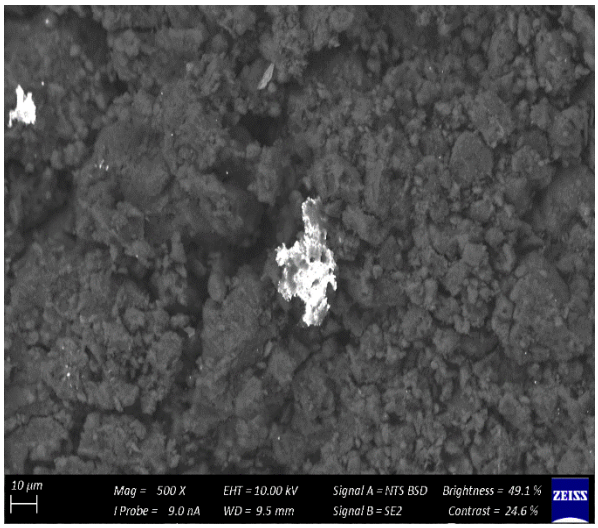

(d)

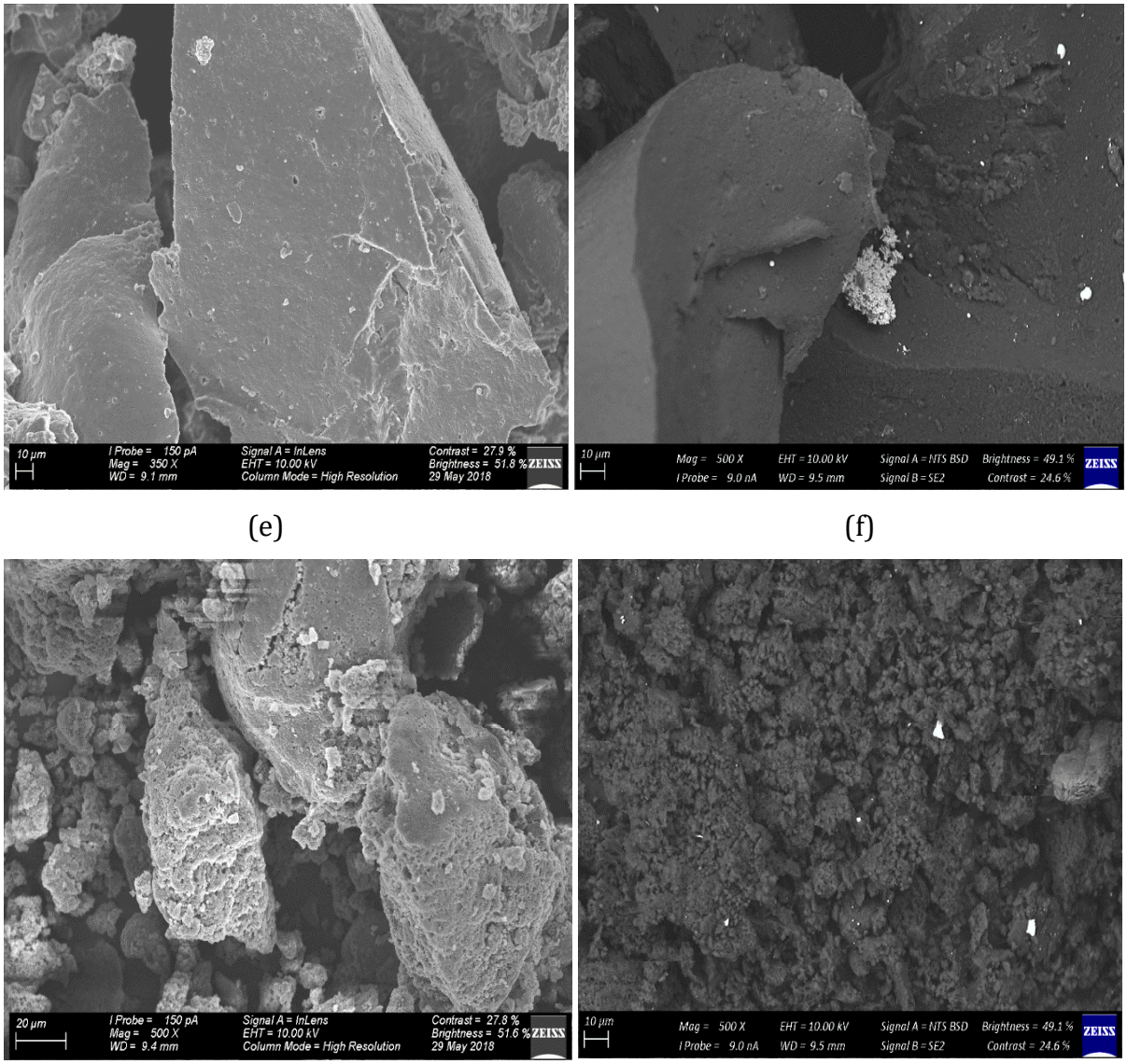

Figure 5-18: Comparison of SEM images before (a) UPT-char (c) TPT-char (e) UT-crumb (g) TT-crumb and after (b) UPT-char (d) TPT-char (f) UT-crumb (h) TT-crumb adsorption of gold at 500x magnification

The samples of untreated crumb, (e) and (f), and untreated char, (a) and (b), remain intact and show no difference in surface morphology before and after adsorption. However, the samples of treated char and treated crumb show changes in surface morphology after adsorption. Before adsorption the particles appeared to be very big especially for treated crumb, (g), and after adsorption the samples appeared to very small and aggregated to each other. This shows that the treated adsorbents were easily digested during adsorption process and this may be attributed to the acidic and corrosive nature of the adsorbate solution medium which was at pH 2. The treated adsorbents were targeted

since they had very low sulphur content according ultimate analysis results due to demineralisation. Sulphur content in tyre manufacturing is used for durability of tyre rubber by maintaining its 3D structure, providing the tyre rubber with great mechanical and chemical stability which make it immune to biodegradation [36,46]. The digestion of treated char after adsorption, (d), appear to be mild.

5.9.4 Effect of contact time

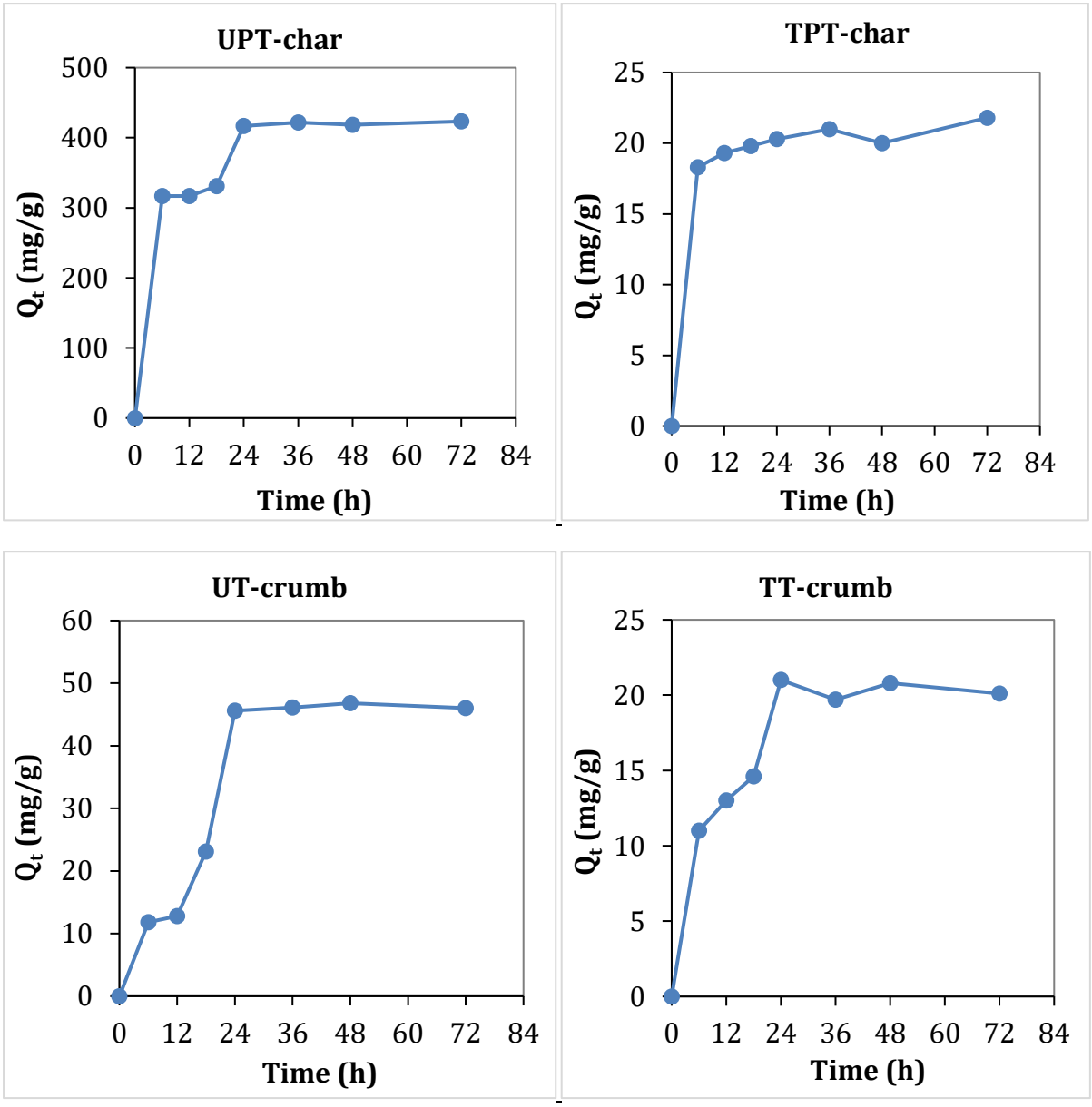

Figure 5-19: Effect of contact time on adsorption of Au^{3+} ions (T = 25 °C, V = 0.025 L, pH = 2, C_0 = 100 mg/L for (TPT-char and TT-crumb) and 188 mg/L for (UPT-char and UT-crumb), m = 3 mg for UPT-char and 15 mg for (TPT-char, UT-crumb and TT-crumb).

The initial gold concentration for UPT-char and UT-crumb was 188 ppm and for TPT-char and TT-crumb was 100 ppm in kinetics studies. UPT-char adsorbent is very sensitive when calculating the adsorption capacity, a slight difference in equilibrium gold concentration in the solution will lead to high difference in Q_t. For example, the equilibrium gold concentration at contact time 18 and 24 hrs was 148.6 and 138.3 mg/L in the solution and the calculated Q_t was 330.8 and 416.7 mg/g respectively. This cause a huge difference in adsorption capacity even at equilibrium contact time. This is caused by the fact that the adsorbent dosage of UPT-char used was very small (3 mg) and high adsorption rate caused by high adsorption affinity of UPT-char towards gold. This greatly affects the trend of the kinetic plot.

It can be observed from *Figure 5-19* that initially the uptake rate of Au(III) was faster in the first 6hrs and slowed down as the adsorption process approached the equilibrium. The presence of high volume of available binding sites on the adsorbent's surface area at t = 0-6h may be the cause for a rapid uptake rate of Au(III) ions. However, as the contact time increased the binding sites where getting occupied and the Au(III) ion concentration in the solution decreased which may have led to a decrease in the adsorption rate. The UPT-char adsorbent had the fastest uptake rate of Au(III) reaching a capacity of about 150 mg/g within the first 6 hours which may be attributed to the high affinity of UPT-char towards Au(III) ions. The high affinity is due to high accessible sulphur content on the adsorbent's surface since sulphur was reported to have the highest affinity for Au(III) at 25 °C as mentioned earlier. The Au(III) uptake rate in UT-crumb appear to be very slow reaching about 12 mg/g capacity after 6h contact time, this might be attributed to the fact that the organic matrix in this adsorbent makes it very difficult for molecules to penetrate [77].

5.10 Au(III) adsorption isotherms

The study of adsorption isotherms is an essential aspect in a sense that it provides with information regarding the interaction between the adsorbent and adsorbate. It can also be used to attain information regarding the properties, mechanism and affinity of adsorbents towards an adsorbate.

5.10.1 Langmuir and Freundlich isotherm plots

The linear form of Langmuir equation is used to plot C_e/Q_e vs C_e from *Equation (4.6)* which gives a straight-line plot with a slope that is equal to $1/Q_{max}$ and an intercept which is equal to $1/K_LQ_{max}$. These equations are usually used to calculate the maximum adsorption capacity and Langmuir equilibrium constant of an adsorbent towards a specific adsorbate.

The Freundlich parameters can also be obtained by plotting $Log Q_e$ vs $Log C_e$ from *Equation (4.9)* and the resultant linear plot is used to determine the Freundlich constants, η and K_F from the slope and the intercept, respectively.

The experimental adsorption isotherm data from *Figure 5-12* is fitted on both models based on the least square fit method. The isotherm model that fit the data well with a good correlation coefficient ($R^2 \approx 1$), is then used to describe the nature of that adsorption including the mechanism of interaction between Au(III) ions on the adsorbent surface. The *Figure 5-20* and *Figure 5-21* are the representative of Langmuir and Freundlich isotherms, respectively.

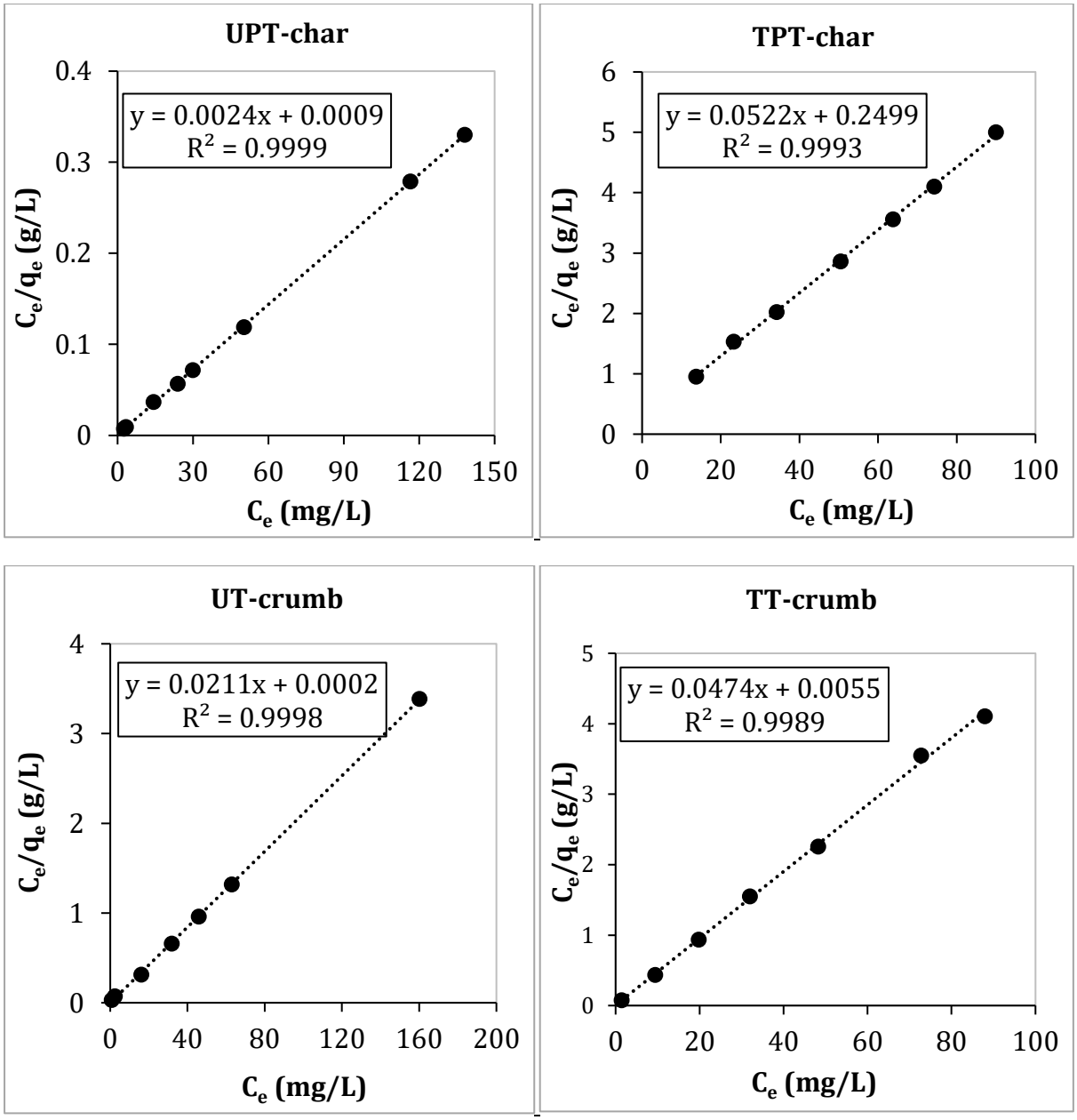

Figure 5-20: Langmuir isotherm plots of UPT-char, TPT-char, UT-crumb and TT-crumb for Au(III) at (V = 0.025 L, pH = 2, T = 25 °C, t_{con} = 24 h for TPT-char and TT-crumb, t_{con} = 48 h for UPT-char and UT-crumb), m = 3 mg for UPT-char and 15 mg for (TPT-char, UT-crumb and TT-crumb).

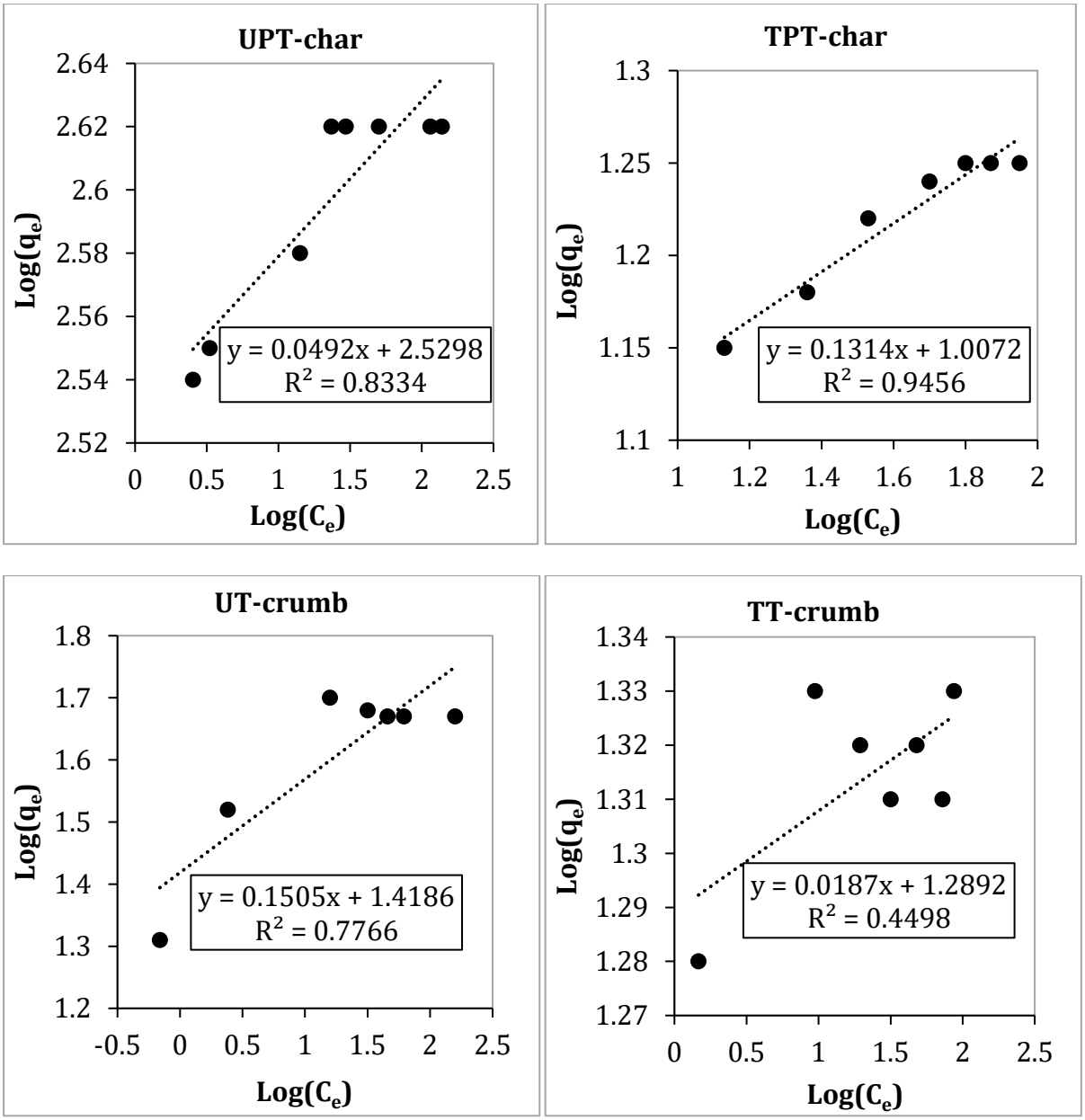

Figure 5-21: The Freundlich isotherm plots of UPT-char, TPT-char, UT-crumb and TT-crumb for Au(III) at (V = 0.025 L, pH = 2, T = 25 °C, t_{con} = 24 h for TPT-char and TT-crumb, t_{con} = 48 h for UPT-char and UT-crumb), m = 3 mg for UPT-char and 15 mg for (TPT-char, UT-crumb and TT-crumb).

The Langmuir parameters are listed in *Table 5-13* and Freundlich parameters are listed in *Table 5-14* for Au(III) adsorption with each adsorbent. Comparing the correlation coefficient values, R^2, of both models it was clear that the values of Langmuir model were closer to 1 (i.e., $R^2 \approx 1$) than those of Freundlich model. This means that the experimental data fitted well with Langmuir equation and the adsorption process can be interpreted according Langmuir adsorption isotherm. Therefore, the adsorption of Au(III) ions on

each of the above-mentioned adsorbents occurs on a homogenous surface with equal adsorption activation energy. The adsorbed Au(III) ions forms a monolayer on the surface of the adsorbent due to homogenously distributed binding sites.

The calculated maximum adsorption capacity of Au(III) from Langmuir isotherm is in excellent agreement with the maximum adsorption capacity obtained experimentally for each adsorbent as listed in *Table 5-13*. The R_L value for each adsorbent calculated using *Equation (4.8)* obeyed the following constraint whereby, $0< R_L <1$, which corresponds to a favourable adsorption process according to *Table 4-6*.

Table 5-13: Langmuir parameters for Au(III) adsorption at 25 °C

Adsorbent	$Q_{e,\,exp}$ ***(mg/g)***	$Q_{e,\,cal}$ ***(mg/g)***	K_L ***(L/mg)***	R_L	R^2
UPT-char	418.3	416.7	2.666	0.0019	0.999
TPT-char	18.1	19.2	0.208	0.0455	0.999
UT-crumb	47.3	47.4	105.5	0.0001	0.999
TT-crumb	21.4	21.1	8.617	0.0011	0.998

Table 5-14: Freundlich parameters for Au(III) adsorption at 25 °C

Adsorbent	K_F ***(mg/g)***	η	R^2
UPT-char	338.7	20.3	0.833
TPT-char	10.17	7.61	0.945
UT-crumb	26.21	6.64	0.776
TT-crumb	19.46	53.5	0.449

5.11 Adsorption kinetic models

The experimental data obtained in *Figure 5-19* was modelled using two kinetic models namely; pseudo-first and pseudo-second order kinetic models. Pseudo-first order kinetic model can be expressed by *Equation (4.11)* and pseudo-second order kinetic model can be expressed by *Equation (4.12)*

Figure 5-22 is a representative of pseudo-first order kinetic plots and *Figure 5-23* represents the kinetic plots of pseudo-second order for each adsorbent. Pseudo-first and second order kinetic parameters are listed in *Table 5-15* and *Table 5-16*, respectively.

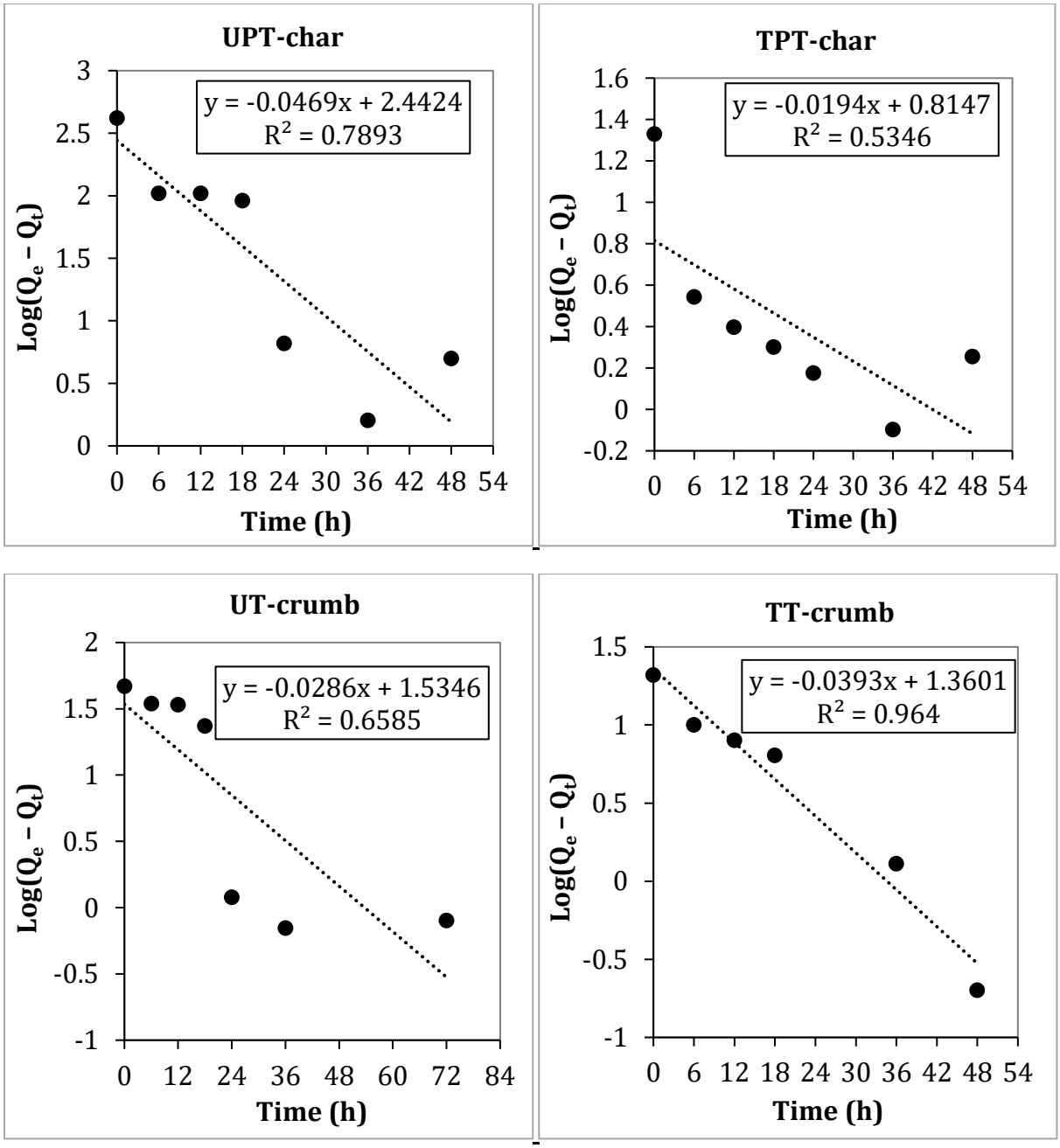

Figure 5-22: Pseudo-first order kinetic plots of UPT-char, TPT-char, UT-crumb and TT-crumb for Au(III) at pH = 2, T = 25 °C, V = 0.025 L, C_0 = 100 mg/L for (TPT-char and TT-crumb) and 188 mg/L for (UPT-char and UT-crumb), m = 3 mg for UPT-char and 15 mg for (TPT-char, UT-crumb and TT-crumb).

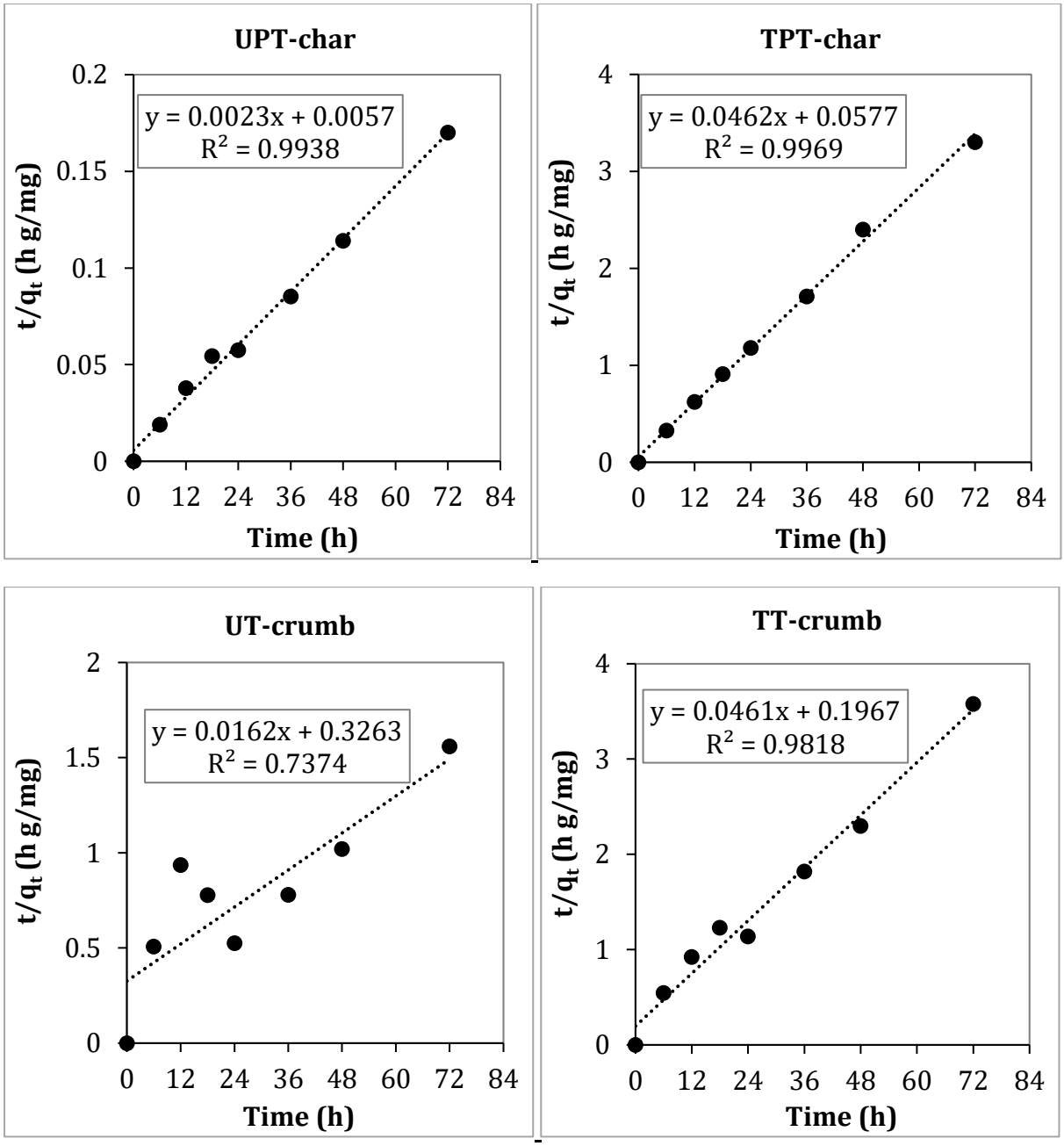

Figure 5-23: Pseudo-second order kinetic plots of UPT-char, TPT-char, UT-crumb and TT-crumb for Au(III) at pH = 2, T = 25 °C, V = 0.025 L, C_0 = 100 mg/L for (TPT-char and TT-crumb) and 188 mg/L for (UPT-char and UT-crumb), m = 3 mg for UPT-char and 15 mg for (TPT-char, UT-crumb and TT-crumb).

Table 5-15: Pseudo-first order kinetic parameters at 25 °C

Adsorbent	$Q_{e,\,exp}$ (mg/g)	Pseudo-first order model		
		$Q_{e,\,cal}$ (mg/g)	K_1 (h^{-1})	R^2
UPT-char	423.3	276.9	0.1080	0.789
TPT-char	21.8	6.526	0.0447	0.534
UT-crumb	46.0	34.24	0.0659	0.658
TT-crumb	20.1	22.91	0.0905	0.964

Table 5-16: Pseudo-second order kinetic parameters at 25 °C

Adsorbent	$Q_{e,\,exp}$ (mg/g)	Pseudo-second order model		
		$Q_{e,\,cal}$ (mg/g)	K_2 (g/mg/h)	R^2
UPT-char	423.3	434.8	0.000928	0.993
TPT-char	21.8	21.6	0.0371	0.996
UT-crumb	46.0	61.7	0.000805	0.737
TT-crumb	20.1	21.7	0.0108	0.981

The correlation coefficient values, R^2, of pseudo-second order kinetic model were closer to unity (i.e., $R^2 \approx 1$) as compared to those of pseudo-first order model. Additionally, the calculated values of the maximum adsorption capacity of Au(III) from pseudo-second order model were in good agreement with the maximum adsorption capacity obtained experimentally for each adsorbent**.** This means that the experimental data fitted well with pseudo-second order equation and therefore the adsorption kinetics can be well interpreted according to pseudo-second order model.

5.12 Summary of results

The initial Au(III) concentration of 188ppm for (UPT-char and UT-crumb) and 100.8ppm for (TPT-char and TT-crumb) adsorbents were used to study the adsorption isotherm and kinetics. The maximum adsorption capacity (Q_{max}) of Au(III) obtained from the adsorption isotherms, kinetic models and experimentally for each adsorbent was found to be almost the same at the above-mentioned Au(III) concentrations. When UPT-char

was used the Q_{max} obtained from Langmuir isotherm model was (416.7 mg/g), from pseudo-second order kinetic model was (434.8 mg/g) and experimentally were (418.3 and 423.3 mg/g). When UT-crumb was used the Q_{max} obtained from Langmuir isotherm model was (47.4 mg/g), from pseudo-second order kinetic model was (61.7 mg/g) and experimentally were (47.3 and 46 mg/g). When TPT-char was used the Q_{max} obtained from Langmuir isotherm model was (19.2 mg/g), from pseudo-second order kinetic model was (21.6 mg/g) and experimentally were (18.1 and 21.8 mg/g). When TT-crumb was used the Q_{max} obtained from Langmuir isotherm model was (21.1 mg/g), from pseudo-second order kinetic model was (21.7 mg/g) and experimentally were (21.4 and 20.1 mg/g). This shows the suitability of both models to describe the kinetic and isotherm properties of each adsorbent for adsorption of Au(III) at 25 °C.

6. CONCLUSION

6.1 Major findings

The alkali-acid demineralisation of tyre-derived adsorbents with 1M NaOH and 1M HNO_3 was successful and improved the BET surface area of the tyre-derived adsorbents from 63.96 to 78.89 m^2/g for pyrolytic tyre char and from 0.322 to 3.49 m^2/g for tyre rubber crumb. The surface area increased due to removal of ash content which consist mainly of zinc and sulphur. About 90% ash was removed from UPT-char and 50% ash removed from UT-crumb. The treatment also led to a significant decrease in sulphur content from 2.366 to 0.619 wt.% of PT-char which means that over 73% of sulphur content was removed from the surface of PT-char. The decrease in sulphur content of UT-crumb was from 2.043 to 0.907 wt.% which is over 55% removal of sulphur. The highest leaching of sulphur and zinc from both PT-char and UT-crumb was achieved in treatment with 1M nitric acid. The alkali-acid demineralisation negatively affected the adsorption capacity of both char and crumb despite the improved BET surface area. This is attributed to the removal of high sulphur content from these adsorbents.

Experimental parameters that had an effect and greatly influenced the adsorption Au(III) from acidic solutions are the solution pH, contact time and adsorbent dosage. The highest removal of gold from acidic chloride solution was achieved at pH 2 for all the adsorbents. To ensure complete gold adsorption, the most suitable contact time for the treated adsorbents was 24 h and for untreated adsorbent it was 48 h. The optimal adsorbent dosage for TPT-char, UT-crumb and TT-crumb was 0.6 g/L which is 15 mg and for UPT-crumb was 0.12 g/L which is 3 mg. The UPT-char adsorbent is very sensitive in adsorption of gold such that a small difference in adsorbent dosage lead to a very huge difference in adsorption capacity.

The mechanism for adsorption of gold involved sulphur which served as a reducing agent causing precipitation and immobilisation of gold onto the adsorbent surface as gold nanoparticle. The adsorption of Au(III) ions with UT-crumb adsorbent also led to precipitation of gold in the solution at a slow rate. The precipitation was caused by iron ions which were leached from the UT-crumb adsorbent into the solution during adsorption. The tyre-derived adsorbents namely; UPT-char, TPT-char, UT-crumb and TT-

crumb obeyed Langmuir adsorption isotherm and pseudo-second order kinetic models for adsorption of Au(III) ions at 25 °C.

Therefore, a conclusion is reached that sulphur was a key binding site for gold and the high capacity of UPT-char is attributed to its high surface sulphur content. PT-char have high adsorption capacity for gold compared to most of the carbonaceous and sulphur-containing adsorbents reported in literature. The sulphur content in UT-crumb is also high and almost equal to that of UPT-char according to ultimate analysis results, but the sulphur is imbedded within its complex organic matrix which is difficult to access hence low gold adsorption capacity as compared to UPT-char. UPT-char and UT-crumb could therefore be potential alternative low-cost adsorbents in recovery of gold from acidic chloride solutions due to strong affinity for gold, high adsorption capacity, availability and lower production costs.

6.2 Recommendations for future work

In the current pyrolysis of waste tyres, up to 78% of sulphur content from the waste tyres is retained in the resultant char. Since it was discovered that sulphur was the key binding site for gold and increased the adsorption capacity of the adsorbents; therefore, the pyrolysis of waste tyres should be studied in-depth with the aim to retain the highest possible amount of sulphur content in the resultant char.

Alkali-acid demineralisation removed over 50% of sulphur content from the adsorbents. Therefore, instead of applying alkali-acid demineralisation as a pretreatment technique for preparation of PT-char and UT-crumb adsorbents, alternative pretreatment techniques can be applied to improve the adsorption capacity of PT-char and UT-char for precious metals, especially gold. One of such pretreatment techniques includes sulfonation of PT-char and UT-crumb with sulphuric acid (H_2SO_4) or hydrogen sulphide (H_2S) to introduce sulphur content in these adsorbents which is a good chelating agent for precious metals and can significantly improve their adsorption capacity.

Sulphur is not only a good chelating and reducing agent but also very selective towards gold and form highly stable bonds with gold in water, organic solvents and air at room temperatures. Therefore, a study of selective adsorption of gold in a solution containing

a mixture of other metal ions is recommended. Gold in the solution is adsorbed as an anionic chloride complex, $AuCl_4^-$, at very low pH values and base metals are adsorbed as cationic ions, M^{n+}, at higher pH values, usually pH 6. Thus, in a case where the solution is containing a mixture of metal ions which are base metals, the solution pH should be taken into consideration.

It is recommended that when conducting gold adsorption experiments with UT-crumb adsorbents, the gold concentration remaining in the filtrate solution after adsorption should be analysed immediately because with time the iron leached from UT-crumb reacts with gold and forms precipitates. When the precipitates are formed they cannot be detected by the AAS or ICP which results in incorrect readings and this will affect the calculated adsorption capacity.

More experiments are required for application of PT-char and UT-crumb in the adsorption of gold from real-life environmental wastewater and e-waste leachates. The study of the application of PT-char in the adsorption and optimisation of the adsorption parameters of other precious metals other than gold is highly recommended since they also have affinity towards sulphur. Additionally, more work can be focused on the optimisation of desorption tests on gold-adsorbed adsorbents.

7. REFERENCES

[1] C. Xiaowei, H. Sheng, G. Xiaoyang, D. Wenhui, Crumb waste tire rubber surface modification by plasma polymerization of ethanol and its application on oil-well cement, Applied Surface Science. 409 (2017) 325–342.

[2] G. Lopez, J. Alvarez, M. Amutio, N.M. Mkhize, B. Danon, P. van der Gryp, J.F. Görgens, J. Bilbao, M. Olazar, Waste truck-tyre processing by flash pyrolysis in a conical spouted bed reactor, Energy Conversion and Management. 142 (2017) 523–532.

[3] E.B. Machin, D.T. Pedroso, J.A. de Carvalho Jr., Energetic valorization of waste tires, Renewable and Sustainable Energy Reviews. 68 (2017) 306–315.

[4] E.L.K. Mui, W.H. Cheung, G. McKay, Tyre char preparation from waste tyre rubber for dye removal from effluents, Journal of Hazardous Materials. 175 (2010) 151–158.

[5] H.Y. Ismaila, A. Abbasb, F. Azizia, J. Zeaite, Pyrolysis of waste tires: A modelling and parameter estimation study using Aspen Plus, Waste Management. 60 (2017) 482–493.

[6] T.A. Saleha, A.A. Al-Saadi, V.K. Gupta, Carbonaceous adsorbent prepared from waste tires: Experimental and computational evaluations of organic dye methyl orange, Journal of Molecular Liquids. 191 (2014) 85–91.

[7] S. Ramarad, M. Khalid, C.T. Ratnam, A.L. Chuah, W. Rashmi, Waste tire rubber in polymer blends: A review on the evolution, properties and future, Progress in Materials Science. 72 (2015) 100–140.

[8] E. Aylon, A. Fernandez-Colino, R. Murillo, M.V. Navarro, T. Garcia, A.M. Mastral, Valorisation of waste tyre by pyrolysis in a moving bed reactor, Waste Management. 30 (2010) 1220–1224.

[9] S. Seng-eiad, S. Jitkarnka, Untreated and HNO_3-treated pyrolysis char as catalysts for pyrolysis of waste tire: In-depth analysis of tire-derived products and char characterization, Journal of Analytical and Applied Pyrolysis. 122 (2016) 151–159.

[10] G.-G. Choi, S.-H. Jung, S.-J. Oh, J.-S. Kim, Total utilization of waste tire rubber through pyrolysis to obtain oils and CO_2 activation of pyrolysis char, Fuel Processing Technology. 123 (2014) 57–64.

[11] A. Kumar, M. Holuszko, D.C.R. Espinosa, E-waste: An overview on generation, collection, legislation and recycling practices, Resources, Conservation and Recycling. 122 (2017) 32–42.

[12] X. Zeng, H. Duan, F. Wang, J. Li, Examining environmental management of e-waste: China's experience and lessons, Renewable and Sustainable Energy Reviews. 72 (2017) 1076–1082.

[13] A.K. Awasthi, J. Li, Management of electrical and electronic waste: A comparative evaluation of China and India, Renewable and Sustainable Energy Reviews. 76 (2017) 434–447.

[14] A. Julander, L. Lundgren, L. Skare, M. Grander, B. Palm, M. Vahter, C. Liden, Formal recycling of e-waste leads to increased exposure to toxic metals: an occupational exposure study from Sweden, Environ International. 73 (2014) 243–251.

[15] Q. Wu, J.Y.S. Leung, X. Geng, S. Chen, X. Huang, H. Li, Z. Huang, L. Zhu, J. Chen, Y. Lu, Heavy metal contamination of soil and water in the vicinity of an abandoned e-waste recycling site: implications for dissemination of heavy metals, Science of the Total Environment. 506–507 (2015) 217–225.

[16] A. Tuncuk, V. Stazi, A. Akcil, E.Y. Yazici, H. Deveci, Aqueous metal recovery techniques from e-scrap: Hydrometallurgy in recycling, Minerals Engineering. 25 (2012) 28–37.

[17] E.M. Iannicelli-Zubiani, C. Cristiani, G. Dotelli, P.G. Stampino, Recovery of valuable metals from electronic scraps by clays and organo-clays: Study on bi-ionic model solutions, Waste Management. 60 (2017) 582–590.

[18] Q. Yi, R. Fan, F. Xie, H. Min, Q. Zhang, Z. Luo, Selective recovery of Au(III) and Pd(II) from waste PCBs using ethylenediamine modified persimmon tannin adsorbent, Procedia Environmental Sciences. 31 (2016) 185–194.

[19] Y. Lu, Z. Xu, Precious metals recovery from waste printed circuit boards: A review for current status and perspective, Resources, Conservation and Recycling. 113 (2016) 28–39.

[20] B.C. Choudhary, D. Paul, A.U. Borse, D.J. Garole, Surface functionalized biomass for adsorption and recovery of gold from electronic scrap and refinery wastewater, Separation and Purification Technology. 195 (2018) 260–270.

[21] A. Ramesh, H. Hasegawa, W. Sugimoto, T. Maki, K. Ueda, Adsorption of gold(III), platinum(IV) and palladium(II) onto glycine modified crosslinked chitosan resin, Bioresource Technology. 99 (2008) 3801–3809.

[22] N.F.A. Razak, M. Shamsuddin, S.L. Lee, Adsorption kinetics and thermodynamics studies of gold(III) ions using thioctic acid functionalized silica coated magnetite nanoparticles, Chemical Engineering Research and Design. 130 (2018) 18–28.

[23] M. Wojnicki, M. Luty-Blocho, R.P. Socha, K. Mech, Z. Pedzich, K. Fitzner, E. Rudnik, Kinetic studies of sorption and reduction of gold(III) chloride complex ions on activated carbon Norit ROX 0.8, Journal of Industrial and Engineering Chemistry. 29 (2015) 289–297.

[24] M.A. Zazycki, E.H. Tanabe, D.A. Bertuol, G.L. Dotto, Adsorption of valuable metals from leachates of mobile phone wastes using biopolymers and activated carbon, Journal of Environmental Management. 188 (2017) 18–25.

[25] C. Souza, D. Majuste, M.S.S. Dantas, V.S.T. Ciminelli, Selective adsorption of gold over copper cyanocomplexes on activated carbon, Hydrometallurgy. 147–148 (2014) 188–195.

[26] C. Troca-Torrado, M. Alexandre-Franco, C. Fernandez-Gonzalez, M. Alfaro-Dominguez, V. Gomez-Serrano, Development of adsorbents from used tire rubber their use in the adsorption of organic and inorganic solutes in aqueous solution, Fuel Processing Technology. 92 (2011) 206–212.

[27] M. Alexandre-Franco, C. Fernandez-Gonzalez, M. Alfaro-Dominguez, J.M. Palacios Latasa, V. Gomez-Serrano, Devulcanisation and demineralisation of used tire rubber by thermal chemical methods: A study by X-ray diffraction, Energy Fuels. 24 (2010) 3401–3409.

[28] W.R. Knocke, L.H. Hemphill, Mercury(II) sorption by waste rubber, Water Research. 15 (1981) 275–282.

[29] A. Imyim, T. Sirithaweesit, V. Ruangpornvisuti, Arsenite and arsenate removal from wastewater using cationic polymer-modified waste tyre rubber, Journal of Environmental Management. 166 (2016) 574–578.

[30] F. Calisir, F.R. Roman, L. Alamo, O. Perales, M.A. Arocha, S. Akman, Removal of Cu(II) from aqueous solutions by recycled tire rubber, Desalination. 249 (2009) 515–518.

[31] L.A. Alamo-Nolea, O. Perales-Perez, F.R. Roman-Velazquez, Sorption study of toluene and xylene in aqueous solutions by recycled tires crumb rubber, Journal of Hazardous Materials. 185 (2011) 107–111.

[32] A. Chaala, H. Darmstadt, C. Roy, Acid-base method for the demineralization of pyrolytic carbon black, Fuel Processing Technology. 46 (1996) 1–15.

[33] G. Lopez, M. Olazar, M. Artetxe, M. Amutio, G. Elordi, J. Bilbao, Steam activation of pyrolytic tyre char at different temperatures, Journal of Analytical and Applied Pyrolysis. 85 (2009) 539–543.

[34] M.L. Arrascue, H.M. Garcia, O. Horna, E. Guibal, Gold sorption on chitosan derivatives, Hydrometallurgy. 71 (2003) 191–200.

[35] L.S. Rodríguez, J.M.B. Muñoz, A. Zambon, J.P. Faure, Determination of the biomass content of end-of-life tyres, Biomass Volume Estimation and Valorization for Energy. (2017) 444–462.

[36] D. Czajczyńska, R. Krzyżyńska, H. Jouhara, N. Spencer, Use of pyrolytic gas from waste tire as a fuel: A review, Energy. 134 (2017) 1121–1131.

[37] A. Nieto-Marquez, A. Pinedo-Flores, G. Picasso, E. Atanes, R.S. Kou, Selective adsorption of Pb^{2+}, Cr^{3+} and Cd^{2+} mixtures on activated carbons prepared from waste tires, Journal of Environmental Chemical Engineering. 5 (2017) 1060–1067.

[38] I. Hita, M. Arabiourrutia, M. Olazar, J. Bilbao, J.M. Arandes, P. Castaño, Opportunities and barriers for producing high quality fuels from the pyrolysis of scrap tires, Renewable and Sustainable Energy Reviews. 56 (2016) 745–759.

[39] J.D. Martinez, N. Puy, R. Murillo, T. Garcia, M.V. Navarro, A.M. Mastral, Waste tyre pyrolysis – A review, Renewable and Sustainable Energy Reviews. 23 (2013) 179–213.

[40] T.A. Saleh, V.K. Gupta, Processing methods, characteristics and adsorption behaviour of tire derived carbons: A review, Advances in Colloid and Interface Science. 211 (2014) 93–101.

[41] B. Manochehr, O. Mahdiyeh, Z.M. Hassan, Simultaneous removal of nickel (II) and cadmium (II) from aqueous solutions by waste tire rubber ash as a low-cost adsorbent, Advances in Environmental Biology. 8 (2014) 29–39.

[42] A.B. Reddy, G.S.M. Reddy, J. Jayaramudu, K. Sudhakar, B. Manjula, S.S. Ray, E.R. Sadiku, 5-Polyethylene Terephthalate-Based Blends: Natural Rubber and Synthetic Rubber, Poly(Ethylene Terephthalate) Based Blends, Composites and Nanocomposites. (2015) 75–98.

[43] A.B. Samsuri, A.A. Abdullahi, Degradation of Natural Rubber and Synthetic Elastomers, Reference Module in Materials Science and Materials Engineering. 3 (2010) 2407–2438.

[44] A.M. Ajam, S.H. AL-nesrawy, M.H. AL-Maamori, Effect of reclaim rubber loading on the mechanical properties of SBR composites, International Journal of Chemical Science. 14 (2016) 2439–2449.

[45] S. Liu, J. Yu, K. Bikane, T. Chen, C. Ma, B. Wang, L. Sun, Rubber pyrolysis: Kinetic modeling and vulcanization effects, Energy. 155 (2018) 215–225.

[46] A.Y. Coran, Chapter 7 – Vulcanization, The Science and Technology of Rubber (Fourth Edition). (2013) 337–381.

[47] G. Li, B. Shen, F. Lu, The mechanism of sulfur component in pyrolyzed char from waste tire on the elemental mercury removal, Chemical Engineering Journal. 273 (2015) 446–454.

[48] B. Acevedo, C. Barriocanal, Texture and surface chemistry of activated carbons obtained from tyre wastes, Fuel Processing Technology. 134 (2015) 275–283.

[49] P.T. Williams, Pyrolysis of waste tyres: A review, Waste Management. 33 (2013) 1714–1728.

[50] J. Alvarez, G. Lopez, M. Amutio, N.M. Mkhize, B. Danon, P. van der Gryp, J.F. Görgens, J. Bilbao, M. Olazar, Evaluation of the properties of tyre pyrolysis oils obtained in a conical spouted bed reactor, Energy. 128 (2017) 463–474.

[51] S.Q. Li, Q. Yao, S.E. Wen, Y. Chi, J.H. Ya, Properties of pyrolytic chars and activated carbons derived from pilot-scale pyrolysis of used tires, Air and Waste Management Association. 55 (2005) 1315–1326.

[52] J. Shah, M. Rasul, F. Mabood, M. Shahid, Conversion of waste tyre into carbon black and their utilization as adsorbent, Journal of the Chinese Chemical Society. 53 (2006) 1085–1089.

[53] M. Juma, Z. Korenova, J. Markos, J. Annus, L. Jelemensky, Pyrolysis and combustion of scrap tyre, Petroleum and Coal. 48 (2006) 15–26.

[54] N. Nkosi, E. Muzenda, A review and discussion of waste tyre pyrolysis and derived products, Proceedings of the World Congress on Engineering. 2 (2014) 2–4.

[55] I. Meza, A. Guevara, E. de la Torre, Conversion of waste tires into activated carbon through pyrolysis and physical activation with CO_2, Enviromine. (2013) 4–6.

[56] N. Antoniou, G. Stavropoulos, A. Zabaniotou, Activation of end of life tyres pyrolytic char for enhancing viability of pyrolysis – Critical review, analysis and recommendations for a hybrid dual system, Renewable and Sustainable Energy Reviews. 39 (2014) 1053–1073.

[57] J.F. González, J.M. Encinar, J.L. Canito, J.J. Rodríguez, Pyrolysis of automobile tyre waste. Influence of operating variables and kinetics study, Journal of Analytical and Applied Pyrolysis. 58–59 (2001) 667–683.

[58] H. Darmstadt, C. Roy, S. Kaliagljine, Characterization of pyrolytic carbon blacks from commercial tire pyrolysis, Carbon. 33 (1995) 1449–1455.

[59] A.M. Cunliffe, P.T. Williams, Properties of chars and activated carbons derived from the pyrolysis of used tyres, Environmental Technology. 19 (1998) 1177–1190.

[60] J.A. Conesa, I. Martin-Gullon, R. Font, J. Jauhiainen, Complete study of the pyrolysis and gasification of scrap tires in a pilot plant reactor, Environmental Science and Technology. 38 (2004) 3189–3194.

[61] M. Kyari, A. Cunliffe, P.T. Williams, Characterization of oils, gases, and char in relation to the pyrolysis of different brands of scrap automotive tires, Energy Fuel. 19 (2005) 1165– 1173.

[62] S. Ucar, S. Karagoz, A. R. Ozkan, J. Yanik, Evaluation of two different scrap tires as hydrocarbon source by pyrolysis, Fuel. 84 (2005) 1884–1892.

[63] O.S. Chan, W.H. Cheung, G. McKay, Preparation and characterisation of demineralised tyre derived activated carbon, Carbon. 49 (2011) 4674–4687.

[64] P.T. Williams, R.P. Bottrill, A.M. Cunliffe, Combustion of tyre pyrolysis oil, Process Safety and Environmental Protection. 76 (1998) 291–301.

[65] X. Zhang, T. Wang, L. Ma, and J. Chang, Vacuum pyrolysis of waste tires with basic additives, Waste Management. 28 (2008) 2301–2310.

[66] J.A. Conesa, R. Font, A. Marcilla, Gas from the pyrolysis of scrap tires in a fluidised bed reactor, Energy and Fuels. 10 (1996) 134–140.

[67] G. Lopez, M. Olazar, R. Aguado, J. Bilbao, Continuous pyrolysis of waste tyres in a conical spouted bed reactor, Fuel. 89 (2010) 1946–1952.

[68] M. Olazar, R. Aguado, M. Arabiourrutia, G. Lopez, A. Barona, J. Bilbao, Catalyst effect on the composition of tire pyrolysis products, Energy and Fuels. 22 (2008) 2909–2916

[69] E. Aylon, A. Fernandez-Colino, M.V. Navarro, R. Murillo, T. Garcia, A.M. Mastral, Waste tire pyrolysis: comparison between fixed bed reactor and moving bed reactor, Industrial and Engineering Chemistry Research. 47 (2008) 4029–4033.

[70] G. López, M. Olazar, M. Amutio, R. Aguado, J. A. Bilbao, Influence of tire formulation on the products of continuous pyrolysis in a conical spouted bed reactor, Energy Fuels. 23 (2009) 5423–5431.

[71] A. Quek, R. Balasubramanian, Preparation and characterization of low energy post-pyrolysis oxygenated tire char, Chemical Engineering Journal. 170 (2011) 194–201.

[72] A.M. Fernandez, C. Barriocanal, R. Alvarez, Pyrolysis of a waste from the grinding of scrap tyres, Journal of Hazardous Materials. 203–204 (2012) 236–243.

[73] M. Hofman, R. Pietrzak, Adsorbents obtained from waste tires for NO_2 removal under dry conditions at room temperature, Chemical Engineering Journal. 170 (2011) 202–208.

[74] F.A. López, T.A. Centeno, F.J. Alguacil, B. Lobato, Distillation of granulated scrap tires in a pilot plant, Journal of Hazardous Materials. 190 (2011) 285–292.

[75] C.M. Long, M.A. Nascarella, P.A. Valberg, Carbon black vs. black carbon and other airborne materials containing elemental carbon: physical and chemical distinctions, Environmental Pollution. 181 (2013) 271–286.

[76] H. Hu, Y. Fang, H. Liu, R. Yu, G. Luo, W. Liu, A. Li, H. Yao, The fate of sulfur during rapid pyrolysis of scrap tires, Chemosphere. 97 (2014) 102–107.

[77] I. Iraola-Arregui, P. van der Gryp, J.F. Görgens, A review on the demineralisation of pre- and post-pyrolysis biomass and tyre wastes, Waste Management. 79 (2018) 667–688.

[78] S. Maroufi, M. Mayyas, V. Sahajwalla, Nano-carbons from waste tyre rubber: An insight into structure and morphology, Waste Management. 69 (2017) 110–116.

[79] F.A. López, T.A. Centeno, O. Rodríguez, F.J. Alguacil, Preparation and characterization of activated carbon from the char produced in the thermolysis of granulated scrap tyres, Journal of the Air and Waste Management Association. 63 (2013) 534–544.

[80] A.S. Al-Rahbi, P.T. Williams, Hydrogen-rich syngas production and tar removal from biomass gasification using sacrificial tyre pyrolysis char, Applied Energy. 190 (2017) 501–509.

[81] M. Khandelwal, T.N. Singh, Prediction of macerals contents of Indian coals from proximate and ultimate analyses using artificial neural networks, Fuel. 89 (2010) 1101–1109.

[82] Y.D. Singh, P. Mahanta, U. Bora, Comprehensive characterization of lignocellulosic biomass through proximate, ultimate and compositional analysis for bioenergy production, Renewable Energy Volume. 103 (2017) 490–500.

[83] K.T. Klasson, Biochar characterization and a method for estimating biochar quality from proximate analysis results, Biomass and Bioenergy. 96 (2017) 50–58.

[84] S. Ouyang, D. Xiong, Y. Li, L. Zou, J. Chen, Pyrolysis of scrap tyres pretreated by waste coal tar, Carbon Resources Conversion. In Press (2018).

[85] M. Bernardo, S. Mendes, N. Lapa, M. Gonçalves, B. Mendes. F. Pinto, H. Lopes, Leaching behaviour and ecotoxicity evaluation of chars from the pyrolysis of forestry biomass and polymeric materials, Ecotoxicology and Environmental Safety. 107 (2014) 9–15.

[86] S. Galvagno, S. Casu, T. Casabianca, A. Calabrese, G. Cornacchia, Pyrolysis process for the treatment of scrap tyres: preliminary experimental results, Waste Management. 22 (2002) 917–923.

[87] S.Q. Li, Q. Yao, Y. Chi, J.H. Yan, K.F. Cen, Pilot-scale pyrolysis of scrap tires in a continuous rotary kiln reactor, Industrial and Engineering Chemistry Research. 43 (2004) 5133–5145.

[88] E.L.K. Mui, D.C.K. Ko, G. McKay, Production of active carbons from waste tyres–a review, Carbon. 42 (2004) 2789–2805.

[89] W. Kicinski , M. Szala, M. Bystrzejewski, Sulfur-doped porous carbons: Synthesis and applications-Review, Carbon. 68 (2014) 1–32.

[90] S.D. Gisi, G. Lofrano, M. Grassi, M. Notarnicola, Characteristics and adsorption capacities of low-cost sorbents for wastewater treatment: A review, Sustainable Materials and Technologies. 9 (2016) 10–40.

[91] E. Worch, Adsorption technology in water treatment - fundamentals, Processes, and Modeling, Berlin/Boston: De Gruyter (2012). ISBN 978-3-11-024023-8.

[92] K. Ramírez-Muñiz, S. Song, S. Berber-Mendoza, S. Tong, Adsorption of the complex ion $Au(CN)_2^-$ onto sulfur-impregnated activated carbon in aqueous solutions, Journal of Colloid and Interface Science. 349 (2010) 602–606.

[93] P. Cyganowski, K. Garbera, A. Lesniewicz, J. Wolska, P. Pohl, D. Jermakowicz-Bartkowiak, The recovery of gold from the aqua regia leachate of electronic parts using a core–shell type anion exchange resin, Journal of Saudi Chemical Society. 21 (2017) 741–750.

[94] R. Sousa, A. Futuro, A. Fiuza, M.C. Vila, M.L. Dinis, Bromine leaching as an alternative method for gold dissolution, Minerals Engineering. 118 (2018) 16–23.

[95] J. Cui, L. Zhang, Metallurgical recovery of metals from electronic waste: A review, Journal of Hazardous Materials. 158 (2008) 228–256.

[96] F. Xiu, Y. Qi, F. Zhang, Leaching of Au, Ag, and Pd from waste printed circuit boards of mobile phone by iodide lixiviant after supercritical water pre-treatment, Waste Management. 41 (2015) 134–141.

[97] A. Rabieh, J.J. Eksteen, B. Albijanic, The effect of grinding chemistry on cyanide leaching of gold in the presence of pyrrhotite, Hydrometallurgy. 173 (2017) 115–124.

[98] E.A. Oraby, J.J. Eksteen, B.C. Tanda, Gold and copper leaching from gold-copper ores and concentrates using a synergistic lixiviant mixture of glycine and cyanide, Hydrometallurgy. 169 (2017) 339-345.

[99] R. Chand, T. Watari, K. Inoue, H. Kawakita, H.N. Luitel, D. Parajuli, T. Torikai, M. Yada, Selective adsorption of precious metals from hydrochloric acid solutions using porous carbon prepared from barley straw and rice husk, Minerals Engineering. 22 (2009) 1277–1282

[100] H.A. Shaheen, H.M. Marwani, E.M. Soliman, Selective adsorption of gold ions from complex system using oxidized multi-walled carbon nanotubes, Journal of Molecular Liquids. 212 (2015) 480–486.

[101] X. Gao, Y. Zhang, Y. Zhao, Biosorption and reduction of Au (III) to gold nanoparticles by thiourea modified alginate, Carbohydrate Polymers. 159 (2017) 108–115.

[102] J. Yang, F. Kubota, Y. Baba, N. Kamiya, M. Goto, Application of cellulose acetate to the selective adsorption and recovery of Au(III), Carbohydrate Polymers. 111 (2014) 768–774.

[103] B. Feng, C. Yao, S. Chen, R. Luo, S. Liu, S. Tong, Highly efficient and selective recovery of Au(III) from a complex system by molybdenum disulfide nanoflakes, Chem. Eng. J. 350 (2018) 692–702.

[104] M. Fırlak, E.K. Yetimoğlu, M.V. Kahraman, Adsorption of Au(III) ions from aqueous solutions by thiol-ene photoclick hydrogels and its application to electronic waste and geothermal water, J. Water Process Eng. 3 (2014) 105–116.

[105] W. Wei, D.H.K. Reddy, J.K. Bediako, Y. Yun, Aliquat-336-impregnated alginate capsule as a green sorbent for selective recovery of gold from metal mixtures, Chemical Engineering Journal. 289 (2016) 413–422.

[106] D. Feng, H. Tan, J.S.J. van Deventer, Ultrasonic elution of gold from activated carbon, Minerals Engineering. 16 (2003) 257–264.

[107] H. Elomaa, S. Seisko, T. Junnila, T. Sirvio, B.P. Wilson, J. Aromaa, M. Lundstrom, The effect of the redox potential of aqua regia and temperature on the Au, Cu, and Fe dissolution from WPCBs, Recycling. 2 (2017) 14.

[108] T. Milicevic, D. Relic, S. Skrivanj, Z. Tesic, A Popovic, Assessment of major and trace element bioavailability in vineyard soil applying different single extraction procedures and pseudo-total digestion, Chemosphere. 171 (2017) 284–293.

[109] T. Radu, D. Diamond, Comparison of soil pollution concentrations determined using AAS and portable XRF techniques, Journal of Hazardous Materials. 171 (2009) 1168–1171.

[110] M. Chen, L.Q. Ma, Comparison of three aqua regia digestion methods for twenty Florida soils, Soil Science Society of America Journal. 65 (2001) 491–499.

[111] M. Bernardo, N. Lapa, M. Gonçalves, B. Mendes, F. Pinto, Study of the organic extraction and acidic leaching of chars obtained in the pyrolysis of plastics, tire rubber and forestry biomass wastes, Procedia Engineering. 42 (2012) 1739–1746.

[112] M.C. Zanetti, S. Fiore, B. Ruffino, E. Santagata, D. Dalmazzo, M. Lanotte, Characterization of crumb rubber from end-of-life tyres for paving applications, Waste Management. 45 (2015) 161–170.

[113] S. Rungrodnimitchai, D. Kotatha, Chemically modified ground tire rubber as fluoride ions adsorbents, Chemical Engineering Journal. 282 (2015) 161–169.

[114] J.P. Chen, S. Wu, Acid/Base-Treated Activated Carbons: Characterization of Functional Groups and Metal Adsorptive Properties, Langmuir. 20 (2004) 2233–2242.

[115] L. He, Y. Ma, Q. Liu, Y. Mu, Surface modification of crumb rubber and its influence on the mechanical properties of rubber-cement concrete, Construction and Building Materials. 120 (2016) 403–407.

[116] I. Mohammadi, H. Khabbaz, K. Vessalas, Enhancing mechanical performance of rubberised concrete pavements with sodium hydroxide treatment, Materials and Structures. 49 (2016) 813–827.

[117] S.P. McGrath, C.H. Cunliffe, A simplified method for the extraction of the metals Fe, Zn, Cu, Ni, Cd, Pb, Cr, Co and Mn from soils and sewage sludges, Journal of the Science of Food and Agriculture. 36 (1985) 794–798.

[118] A. Santoro, A. Held, T.P.J. Linsinger, A. Perez, M. Ricci, Comparison of total and aqua regia extractability of heavy metals in sewage sludge: The case study of a certified reference material, TrAC Trends in Analytical Chemistry. 89 (2017) 34–40.

[119] J. Sastre, A. Sahuquillo, M. Vidal, G. Rauret, Determination of Cd, Cu, Pb and Zn in environmental samples: microwave-assisted total digestion versus aqua regia and nitric acid extraction, Analytica Chimica Acta. 462 (2002) 59–72.

[120] H. Xu, B. Shen, P. Yuan, F. Lu, L. Tian, X. Zhang, The adsorption mechanism of elemental mercury by HNO3-modified bamboo char, Fuel Processing Technology. 154 (2016) 139–146.

[121] S. Mohammadnejad, J.L. Provis, J.S.J. van Deventer, Reduction of gold(III) chloride to gold(0) on silicate surfaces, Journal of Colloid and Interface Science. 389 (2013) 252–259.

[122] D. Kaur, S. Kaur, S. Srivastava, Sulphur adsorption on gold monolayer, American Institute of Physics. 1832 (2017) 050151.

[123] H. Pan, S. Huang, X. Li, P. Li, W. Zhu, Spontaneous growth of Au nanoparticles onto CdS, ZnS or PbS thin films for electrochemical immunosensors, International Journal of Electrochemical Science. 11 (2016) 3364–3375.

[124] R. Awual, A. Khaleque, M. Ferdows, A.M.S. Chowdhury, Rapid recognition and recovery of gold(III) with functional ligand immobilized novel mesoporous adsorbent, Microchemical Journal. 110 (2013) 591–598.

[125] H.M. Al-Saidi, The fast recovery of gold(III) ions from aqueous solutions using raw date pits: Kinetic, thermodynamic and equilibrium studies, Journal of Saudi Chemical Society. 20 (2016) 615–624.

[126] R. Fan, F. Xie, X. Guan, Q. Zhang, Z. Luo, Selective adsorption and recovery of Au(III) from three kinds of acidic systems by persimmon residual based bio-sorbent: A method for gold recycling from e-wastes, Bioresource Technology. 163 (2014) 167–171.

[127] F. Xie, Z. Fan, Q. Zhang, Z. Luo, Selective adsorption of Au^{3+} from aqueous solutions using persimmon powder-formaldehyde resin, Journal of Applied Polymer Science. 130 (2013) 3937–3946.

[128] W.S.W. Ngah, K. H. Liang, Adsorption of Gold(III) Ions onto Chitosan and N-Carboxymethyl Chitosan: Equilibrium Studies, Industrial and Engineering Chemistry Research. 38 (1999) 1411–1414.

[129] S. Aktas, M.H. Morcali, Gold uptake from dilute chloride solutions by a Lewatit TP 214 and activated rice husk, International Journal of Mineral Processing. 101 (2011) 63–70.

[130] H.M. Albishri, H.M. Marwani, Chemically modified activated carbon with tris(hydroxymethyl)aminomethane for selective adsorption and determination of gold in water samples, Arabian Journal of Chemistry. 9 (2016) 252–258.

[131] M. Bayat, M.H. Beyki, F. Shemirani, One-step and biogenic synthesis of magnetic Fe_3O_4–Fir sawdust composite: Application for selective preconcentration and determination of gold ions, Journal of Industrial and Engineering Chemistry. 21 (2015) 912–919.

[132] W. Liu, P. Yin, X. Liu, X. Dong, J. Zhang, Q. Xu, Thermodynamics, kinetics, and isotherms studies for gold(III) adsorption using silica functionalized by diethylenetriaminemethylenephosphonic acid, Chemical Engineering Research and Design. 91 (2013) 2748–2758.

[133 R. Awuala, M. Ismael, Efficient gold(III) detection, separation and recovery from urban mining waste using a facial conjugate adsorbent, Sensors and Actuators B. 196 (2014) 457–466.

[134] T.M. Sun, W.T. Yen, Kinetics of gold chloride adsorption onto activated carbon, Minerals Engineering. 6 (1993) 17–29.

[135] M. Wojnicki, K. Fitzner, M. Luty-Blocho, Kinetic studies of gold recovery from dilute aqueous solutions using Fe^{2+} chloride ions, Transactions of Nonferrous Metals Society of China, 25 (2015) 2027−2036.

8. APPENDIX

8.1 Particle size distribution

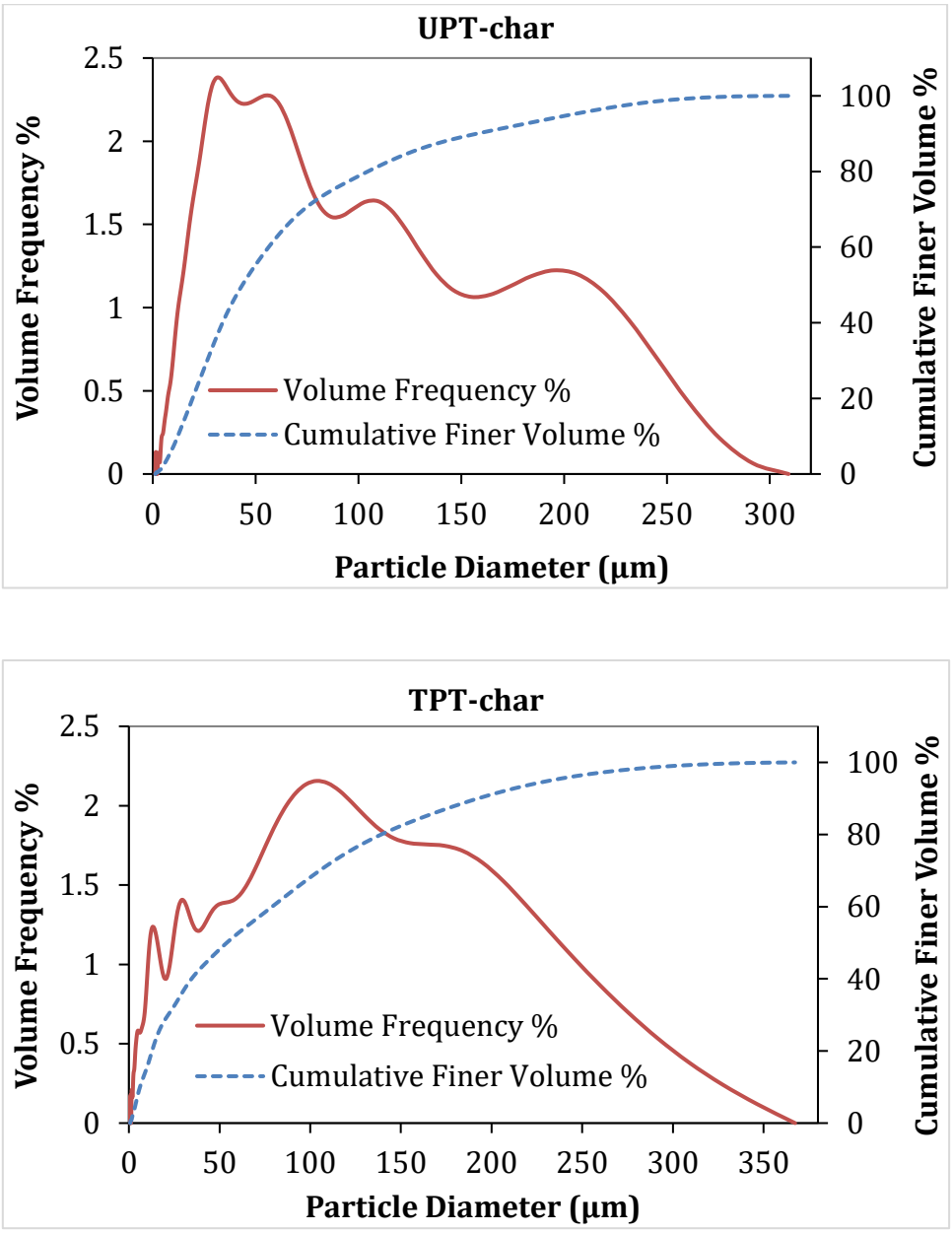

Figure 8-1: Particle size distribution of the untreated (UPT-char) and treated (TPT-char) pyrolytic tyre char adsorbent

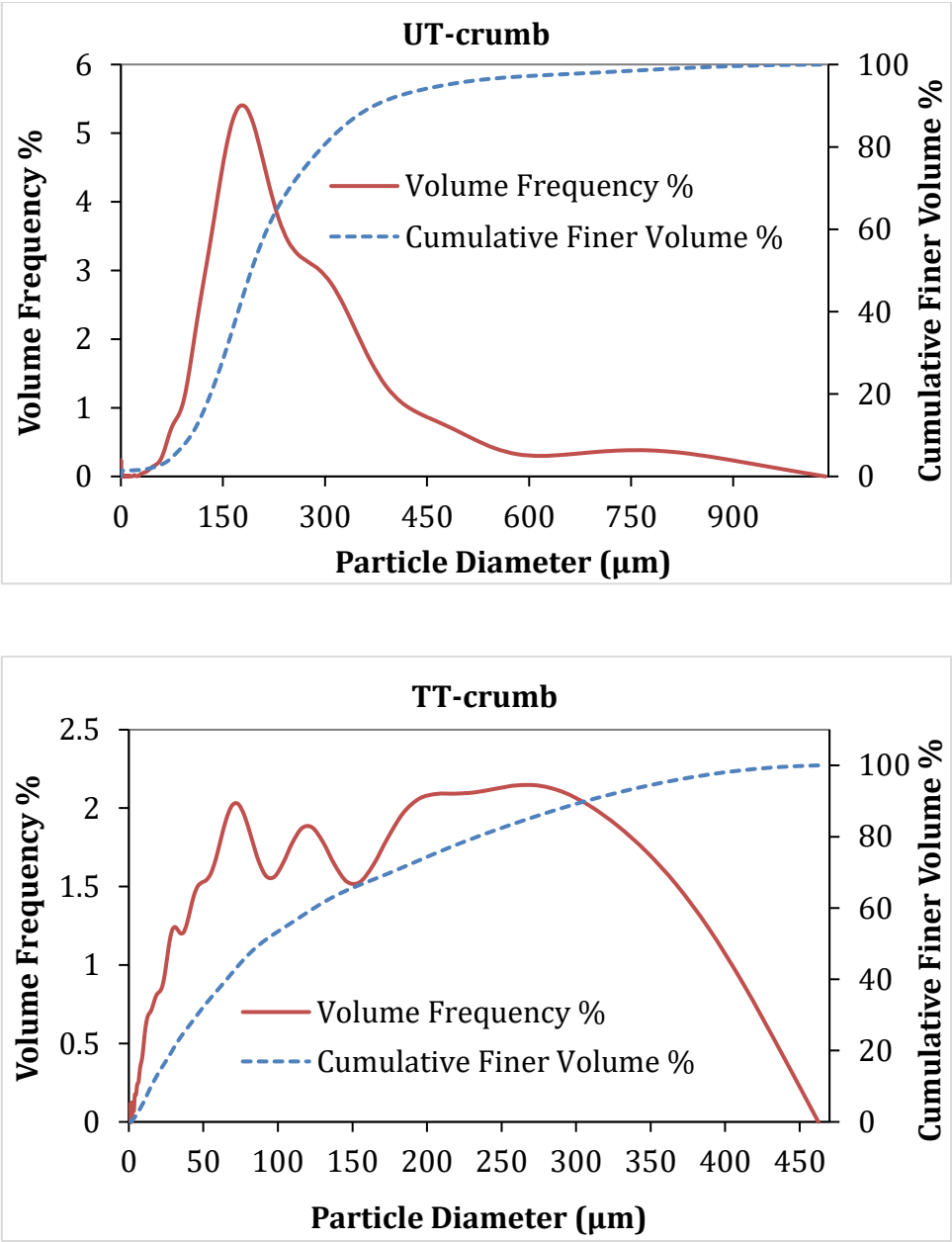

Figure 8-2: Particle size distribution of the untreated (UT-crumb) and treated (TT-crumb) 40 mesh tyre crumb adsorbent

8.2 Aqua regia

8.2.1 Calculations

This section provides the calculations and equations used in preparation of aqua regia.

Equations:

$$n = cv \tag{8.1}$$

$$n = \frac{m}{M_r} \tag{8.2}$$

$$\rho = \frac{m}{v} \tag{8.3}$$

Where $n\ (mol)$ is the number of moles, $c\left(\frac{mol}{L}\right)$ is the molar concentration, $m\ (g)$ is the mass, $v\ (L)$ is solution volume, $M_r\left(\frac{g}{mol}\right)$ is the molar mass and $\rho\left(\frac{g}{mL}\right)$ is the density of the acid. Therefore, the equation to calculate the molar concentration of each acid is derived from the above equations and is presented as;

$$c = \left(\frac{\rho}{M_r}\right) * Assay \tag{8.4}$$

$$c_{HCl} = \frac{\left(1{,}16\frac{g}{mL}\right) * \left(1000\frac{mL}{L}\right)}{\left(36.46\frac{g}{mol}\right)} * 32\%$$

$$c_{HCl} = \mathbf{10.18\ M}$$

$$c_{HNO_3} = \frac{\left(1{,}34\frac{g}{mL}\right) * \left(1000\frac{mL}{L}\right)}{\left(63.01\frac{g}{mol}\right)} * 55\%$$

$$c_{HNO_3} = \mathbf{11.69\ M}$$

To calculate the volume ratio of nitric acid and hydrochloric acid in molar ratio of 1:3 for the preparation of aqua regia solution with a final volume of 30mL (0.03L), the following stoichiometry and simultaneous equations were used.

$$v_{NHO_3} + v_{HCl} = 0.03L \tag{8.5}$$

$$\frac{11.69\, v_{NHO_3}}{10.18\, v_{HCl}} = \frac{1}{3} \tag{8.6}$$

$$v_{HCl} = 3.445\, v_{HNO_3} \tag{8.7}$$

Substitute *Equation (8.7)* into *Equation (8.5)*

$$v_{HNO_3} + 3.445\, v_{HNO_3} = 0.03L \tag{8.8}$$

Therefore, $v_{HNO_3} = 6.75\text{mL}$ and $v_{HCl} = 23.25\text{mL}$

8.2.2 Raw data from ICP-OES analysis

Table 8-1: Raw data of concentrations of elements in aqua regia leachate solution

Elements	***Initial concentration (ppm)***	
	Tyre Char	*Tyre Crumb*
Ca	5,101	2,823
Cu	0,159	0,666
Fe	1,719	2,245
K	3,078	1,776
Na	3,479	2,861
Ni	0,011	0,019
S	27,199	26,093
Si	1,074	1,252
Zn	100,454	39,680
Al	3,548	0,572

8.3 Alkali-acid demineralisation

8.3.1 Raw data from ICP-OES analysis

Table 8-2: Raw data of concentrations of elements after demineralisation with NaOH and HNO_3 1g/12ml

Elements	*Initial concentration (ppm)*			
	Tyre Char		*Tyre Crumb*	
	1M NaOH	*1M HNO_3*	*1M NaOH*	*1M HNO_3*
Ca	0,426	4,185	0,147	2,435
Cu	0,00[a]	0,119	0,044[a]	0,142
Fe	0,00[a]	1,573	0,039[a]	2,560
K	2,210	1,925	0,641	0,944
Na	[b]	2,946	[b]	2,149
Ni	0,00[a]	0,00[a]	0,00[a]	0,00[a]
S	13,215	16,746	5,247	18,773
Si	66,715	4,045	44,680	1,633
Zn	20,067	77,040	2,903	20,429
Al	2,847	2,599	1,199	0,425

"a" *Below detection limit*
"b" *Above detection limit*

Table 8-3: Raw data of concentrations of elements after demineralisation with NaOH and HNO_3 15g/180ml

Elements	*Initial concentration (ppm)*			
	Tyre Char		*Tyre Crumb*	
	1M NaOH	*1M HNO_3*	*1M NaOH*	*1M HNO_3*
Ca	0,020[a]	2,332	0,00[a]	1,743
Cu	0,015[a]	0,175	0,013[a]	0,110
Fe	0,003[a]	3,316	0,065	1,322
K	2,610	0,612	0,605	0,737
Na	[b]	1,946	[b]	6,679
Ni	0,00[a]	0,030[a]	0,00[a]	0,00[a]
S	7,237	11,445	2,644	21,359
Si	62,100	4,859	11,072	2,178
Zn	10,689	95,150	1,644	6,305
Al	3,304	2,027	0,627	0,411

"[a]" *Below detection limit*
"[b]" *Above detection limit*

8.4 ICP-OES sample preparation

8.4.1 Calculations

The concentration of each element was in parts per million (ppm) which is equivalent to milligrams per litre (mg/L). The elements concentration values obtained from ICP-OES analysis are in diluted form and here are calculated back to their initial concentration before dilution according to the following calculations:

$$c_i v_i = c_f v_f \tag{8.9}$$

c_i = *initial concentration before dilution*

v_i = *initial volume before dilution*

c_f = *final concentration after dilution*

v_f = *final volume after dilution*

According to the dilution factor used in sample preparation for ICP-OES analysis, the final volume is 50 times the initial volume;

$$v_f = 50 * v_i \tag{8.10}$$

Therefore;

$$c_i = \frac{c_f * (50 * v_i)}{v_i} \tag{8.11}$$

$$c_i = c_f * 50 \tag{8.12}$$

8.5 Buffer preparations

This section provides the calculations used in preparation of buffer solutions for adjustment of solution pH from pH 1 to pH 8. *Equation (8.4)* was used to calculate the stock initial concentration of all the acids used. And to calculate the required amount in volume of the acids to prepare a stock solution at the desired concentration, *Equation (8.9)* was used. Lastly, *Equation (8.13)* was used to determine the required mass, in grams of the solid chemicals, to prepare a stock solution at the desired final concentration.

For pH (1.0 and 2.0), HCl/KCl buffer solution

Firstly, prepare 0.2M HCl in 1L and 0.2M KCl in 1L with distilled water (both separately).

- Prepare 0.2M HCl in 1L distilled water

$$c_i = \left(\frac{\rho}{M_r}\right) * Assay$$

$$= \left(\frac{1160\ g/L}{36.46\ g/mol}\right) * 32\%$$

$$c_i = \mathbf{10.18\ M}$$

$$c_i v_i = c_f v_f$$

$$v_i = \left(\frac{0.2\ \text{M} * 1000\ \text{mL}}{10.18\ \text{M}}\right)$$

$$v_i = \mathbf{19.65\ mL}$$

- Prepare 0.2M KCl in 1L distilled water

$$m = M_r cv * Assay \tag{8.13}$$

$$= \left(\left(74.55\,\frac{\text{g}}{\text{mol}}\right) * \left(0.2\,\frac{\text{mol}}{\text{L}}\right) * (1\text{L})\right) * 99.75\%$$

$$m = \mathbf{14.87\ g}$$

Secondly, mix the solutions together as follows:
Approximate amount in volumes of the prepared acids and alkaline stock solutions and distilled water were mixed under agitation and using pH meter at the same time until the required value is reached

pH1:
250 mL KCl + 670 mL HCl + 7 mL water

pH2:
250 mL KCl + 65 mL HCl + 685 mL water

For pH (3.0–6.0), acetate buffer (CH_3COONa/CH_3COOH)
First, prepare 0.1M CH_3COOH in 2L and 0.1M CH_3COONa in 2L with distilled water (both separately).

- Prepare 0.1M CH_3COOH in 2L distilled water

$$c_i = \left(\frac{\rho}{M_r}\right) * Assay$$

$$= \left(\frac{1050\ g/L}{60.05\ g/mol}\right) * 97\%$$

$$c_i = \mathbf{16.96\ M}$$

$$c_i v_i = c_f v_f$$

$$v_i = \left(\frac{0.1\ \text{M} * 2000\ \text{mL}}{16.96\ \text{M}}\right)$$

$$v_i = \mathbf{11.79\ mL}$$

- Prepare 0.1M CH_3COONa in 2L distilled water

$$m = M_r cv * Assay$$

$$= \left(\left(82.03\ \frac{\text{g}}{\text{mol}}\right) * \left(0.1\ \frac{\text{mol}}{\text{L}}\right) * (2\text{L})\right) * 99\%$$

$$m = \mathbf{16.41\ g}$$

Secondly, mix the solutions together as follows:
Approximate amount in volumes of the prepared acids and alkaline stock solutions and distilled water were mixed under agitation and using pH meter at the same time until the required value is reached. Since a weak acid is used, therefore, there is no need to add water to adjust pH.

pH3:
982.3 mL CH_3COOH + 17.7 mL CH_3COONa

pH4:
847 mL CH_3COOH + 153 mL CH_3COONa

pH5:
357mL CH_3COOH + 643mL CH_3COONa

pH6:
52.2 mL CH_3COOH + 947.8mL CH_3COONa

For pH (7.0–8.0), phosphate buffer (K_2HPO_4/HCl)

First, prepare 0.1M K_2HPO_4 in 2L and 0.1M HCl in 1L with distilled water (both separately).

- Prepare 0.1M K_2HPO_4 in 2L distilled water

$$m = M_r cv * Assay$$

$$= \left(\left(174.18 \frac{\text{g}}{\text{mol}}\right) * \left(0.1 \frac{\text{mol}}{\text{L}}\right) * (2\text{L})\right) * 99.5\%$$

$$m = \mathbf{34.66\ g}$$

- Prepare 0.1M HCl in 1L distilled water

$$c_i v_i = c_f v_f$$

$$v_i = \left(\frac{0.1\ \text{M} * 1000\ \text{mL}}{10.18\ \text{M}}\right)$$

$$v_i = \mathbf{9.82\ mL}$$

Secondly, mix the solutions together as follows:
Approximate amount in volumes of the prepared acids and alkaline stock solutions and distilled water were mixed under agitation and using pH meter at the same time until the required value is reached. Since a weak acid is used, therefore, there is no need to add water to adjust pH.

pH7:
756.0 mL K_2HPO_4 + 244 mL HCl

pH8:
955.1 mL K_2HPO_4 + 44.9 mL HCl

8.6 Calibration curves

The calibration curves were obtained in three sets of gold concentration range which are low range (0-10ppm), medium range (0-100ppm) and high range (0-200ppm). Analysis of gold concentration within low range is done with the flame burner head at 180° and 45° for gold concentration within medium and high range due to high concentration. To obtain a correct calibration curve the standard solutions must be re-run each time the instrument is used for the first time and for accurate analysis the flame burner should always be cleaned before being used. The analytes should also be free from undissolved solids to avoid blockage of the nebuliser which affects the results repeatability and reproducibility.

Low range (0-10ppm)

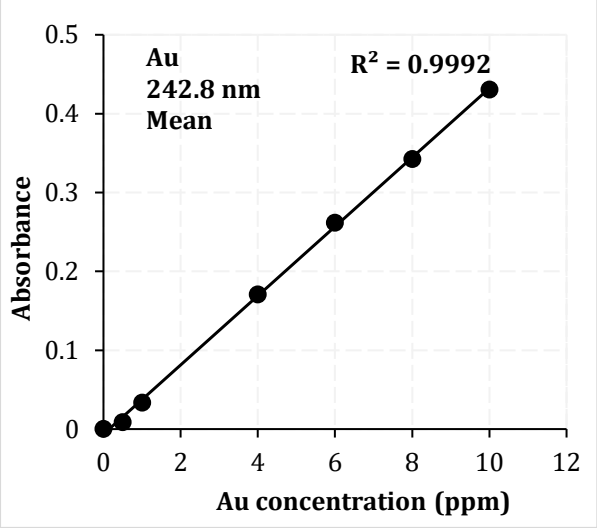

Medium range (0-100ppm)

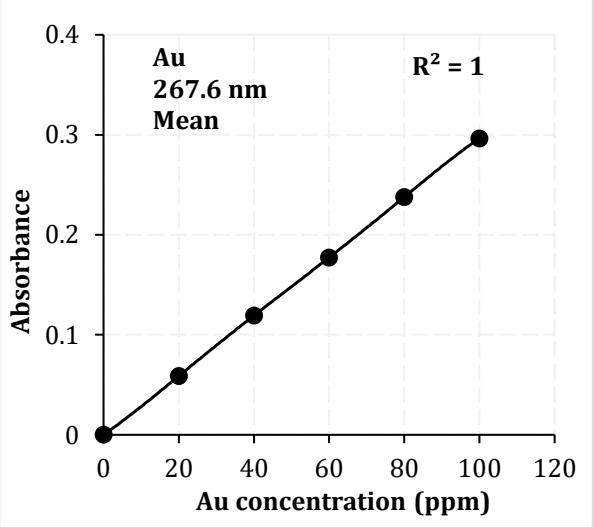

High range (0-200ppm)

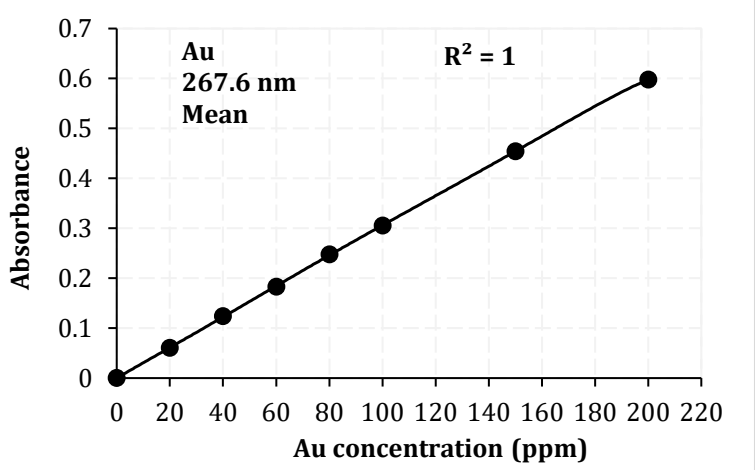

Figure 8-3: FAAS calibration curves used for gold concentration analysis

8.7 Adsorption raw data

Table 8-4: Raw data for effect of pH

pH	***Adsorption %***			
	UPT-char	***TPT-char***	***UT-crumb***	***TT-crumb***
1	99.1	99.9	100.0	96.4
	99.0	97.7	97.8	99.2
	98.6	98.9	98.9	96.7
2	100.0	99.9	100.0	98.6
	100.0	99.8	99.8	99.3
	99.7	100.0	100.0	98.7
3	100.0	99.1	99.8	98.2
	99.8	96.8	98.0	97.8
	98.2	100.0	99.7	98.5
4	99.7	99.9	100.0	89.5
	100.0	99.7	99.5	98.0
	99.9	100.0	99.8	93.2
5	98.8	99.9	99.0	90.4
	99.6	100.0	99.8	95.2
	99.9	98.2	99.3	91.7
6	98.3	97.0	99.3	58.5
	99.7	100.0	97.2	60.1
	99.2	99.7	98.9	56.2
7	89.2	69.7	27.9	32.3
	98.3	76.8	30.8	34.2
	99.4	78.0	30.6	35.9
8	84.4	33.6	21.2	24.9
	84.0	30.2	19.9	23.5
	88.2	28.8	20.7	24.6

Table 8-5: Raw data effect of adsorbent dosage at 24 h

Dosage (mg)	***Q_e (mg/g)***			
	24 hr			
	UPT-char	***TPT-char***	***UT-crumb***	***TT-crumb***
3	420.2 411.7 418.1	-	-	-
5	280.2 276.6 275.7	-	-	-
15	-	18.8 17.3 19.2	44.2 48.2 46.3	21.1 19.0 22.1
25	178.2 183.0 181.1	18.3 18.5 17.4	37.3 36.8 35.9	16.7 15.4 18.1
50	-	-	-	13.7 11.4 13.3
100	-	-	-	13.3 10.7 11.8
250	-	-	17.9 18.6 17.9	7.29 9.10 8.11

Table 8-6: Raw data effect of adsorbent dosage at 48 h

Dosage (mg)	***Q_e (mg/g)***			
	48 hr			
	UPT-char	***TPT-char***	***UT-crumb***	***TT-crumb***
3	418.3 416.5 420.0	-	-	-
5	315.8 327.4 324.2	-	-	-
15	-	19.1 18.3 18.8	46.8 47.2 47.9	19.5 22.2 20.6
25	190.2 186.2 188.3	18.1 18.3 18.6	46.7 46.2 48.1	21.4 19.7 22.7
50	-	-	-	20.7 21.4 20.8
100	-	-	-	17.1 16.4 17.3
250	-	-	21.9 20.0 22.1	13.9 12.1 13.0

Table 8-7: Raw data effect of contact time

Time (h)	***Q_t (mg/g)***			
	UPT-char	***TPT-char***	***UT-crumb***	***TT-crumb***
6	314.8	18.1	9.89	11.2
	317.2	18.7	13.6	10.8
	318.0	18.2	11.8	11.0
12	316.1	19.2	10.8	12.9
	317.3	18.7	13.2	13.0
	316.8	20.1	14.5	13.1
18	328.8	19.8	21.8	14.3
	332.2	20.1	23.4	14.9
	331.3	19.6	24.2	14.5
24	419.3	20.0	46.9	21.2
	418.9	20.8	45.1	20.7
	411.8	20.2	44.7	21.2
36	421.6	21.1	45.3	18.8
	422.5	21.8	46.2	21.2
	420.9	19.9	46.7	19.2
48	419.0	20.2	47.8	22.6
	417.6	20.0	46.5	20.2
	418.2	19.7	46.2	19.7
72	424.4	21.3	46.7	21.2
	421.2	21.8	45.2	19.4
	424.2	22.3	46.1	19.7

Table 8-8: Raw data Effect of initial Au(III) concentration

C_0 (ppm)	Q_e (mg/g)			
	UPT-char	TPT-char	UT-crumb	TT-crumb
10	-	-	19.8 20.9 21.3	18.6 20.1 19.4
20	-	13.8 14.3 15.0	35.4 32.8 31.7	21.3 20.8 22.6
30	-	15.4 14.9 15.2	-	22.3 19.8 21.1
45	354.2 358.7 366.4	16.9 17.4 16.4	53.8 49.3 48.9	20.5 21.0 20.5
60	384.2 392.7 387.8	18.2 17.6 16.9	48.3 48.0 48.6	22.2 20.1 21.5
75	423.3 418.9 422.1	17.6 18.1 17.9	50.2 46.7 46.3	-
80	416.7 417.3 419.1	19.2 17.3 17.9	-	20.3 19.9 21.2
100	421.5 420.6 419.8	18.2 17.9 18.0	-	20.7 22.1 21.5
188	417.7 419.7 417.4	-	46.9 47.2 47.8	-

8.8 Calculations for adsorption data

This calculation is used as an example for all the adsorbents.

Adsorbent: UT-crumb, C_0 = 10.1 ppm, C_e = 0.0221 ppm, m_{ads} = 15 mg, V = 25 mL

8.8.1 Adsorption percentage (*%A*)

$$\%A = \left(\frac{C_0 - C_e}{C_0}\right) * 100\%$$

$$\%A = \left(\frac{10.1 - 0.0221}{10.1}\right) * 100\%$$

$$\%A = 0.998 * 100\%$$

$$\%A = \mathbf{99.8}\%$$

8.8.2 Equilibrium adsorption capacity

$$Q_e = \left(\frac{C_0 - C_e}{m}\right) * V$$

$$Q_e = \left(\frac{10.1 - 0.0221}{0.015\ g}\right) * 0.025\ L$$

$$Q_e = \left(\frac{10.1 - 0.0221}{0.015\ g}\right) * 0.025\ L$$

$$Q_e = \left(671.86\ \frac{mg}{g/L}\right) * 0.025\ L$$

$$Q_e = \mathbf{16.8}\ \frac{mg}{g}$$

8.8.3 Adsorption capacity at time *t*

$$Q_t = \left(\frac{C_0 - C_t}{m}\right) * V$$

$$Q_t = \left(\frac{10.1-0.0221}{0.015\ g}\right) * 0.025\ L$$

$$Q_t = \left(\frac{10.1-0.0221}{0.015\ g}\right) * 0.025\ L$$

$$Q_t = \left(671.86\ \frac{mg}{g/L}\right) * 0.025\ L$$

$$Q_t = \mathbf{16.8}\ \frac{mg}{g}$$

8.9 Equilibrium curves

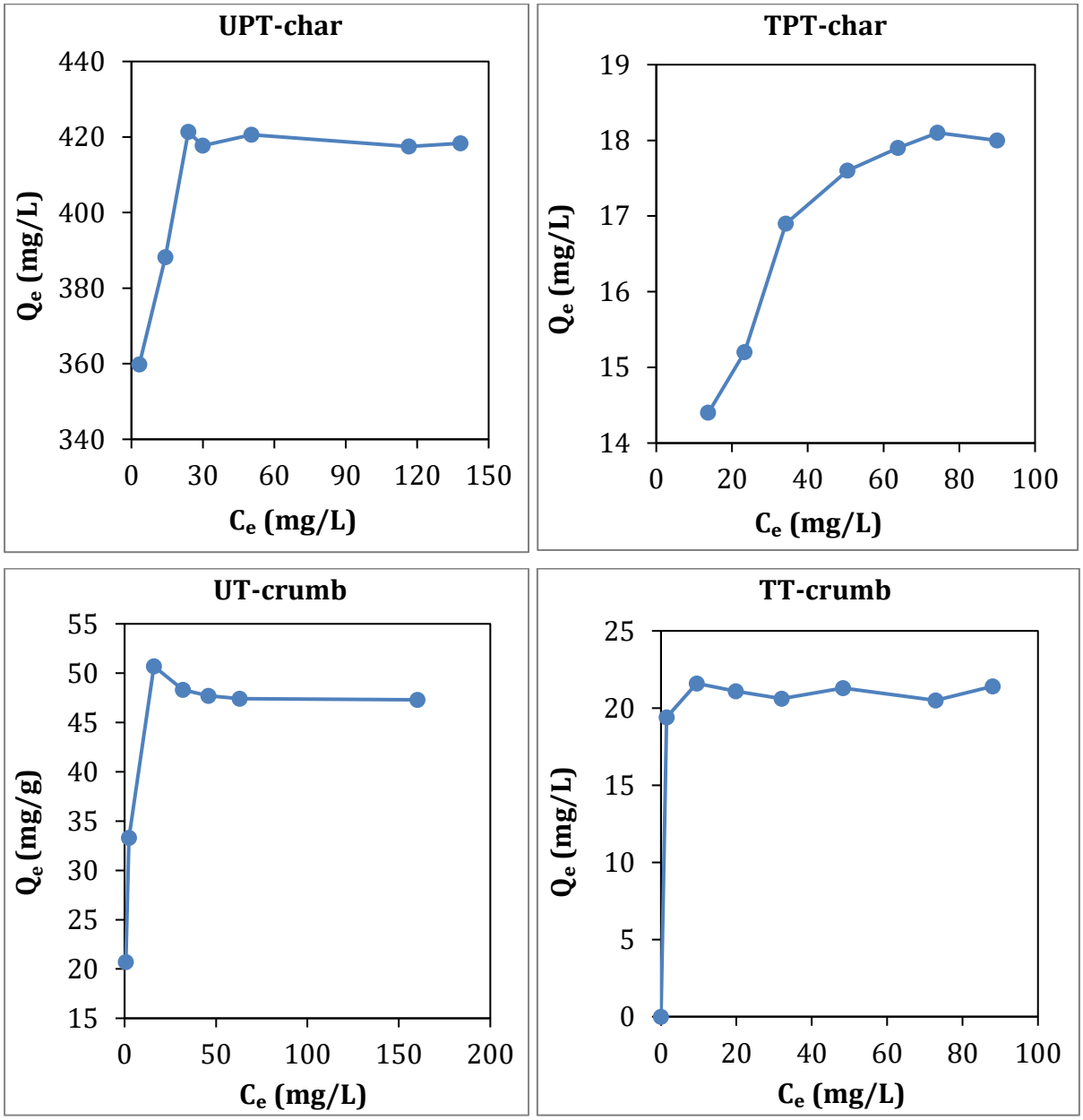

Figure 8-4: Effect of initial Au(III) concentration on adsorption capacity at (V = 0.025 L, pH = 2, T = 25 °C, t_{con} = 24 h for TPT-char and TT-crumb, t_{con} = 48 h for UPT-char and UT-crumb), m = 3 mg for UPT-char and 15 mg for (TPT-char, UT-crumb and TT-crumb).

8.10 SEM images and EDS spectrums

This section shows the additional SEM images and EDS spectrums of the gold-adsorbed adsorbents. The bright spots on the surface of the adsorbents were identified as gold by EDS method.

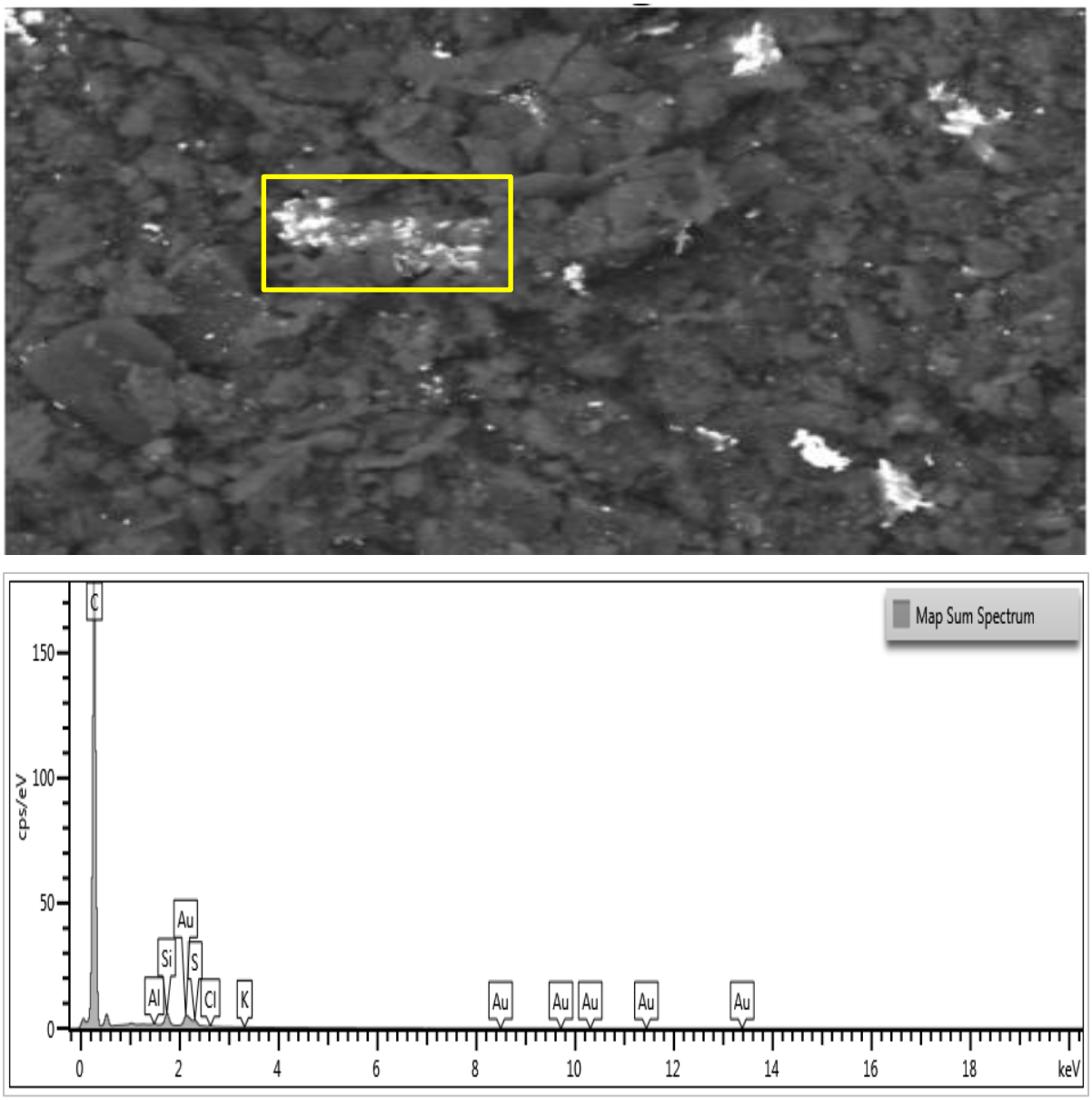

Figure 8-5: SEM image and EDS spectrum for identification of gold on the surface of gold-adsorbed UPT-char

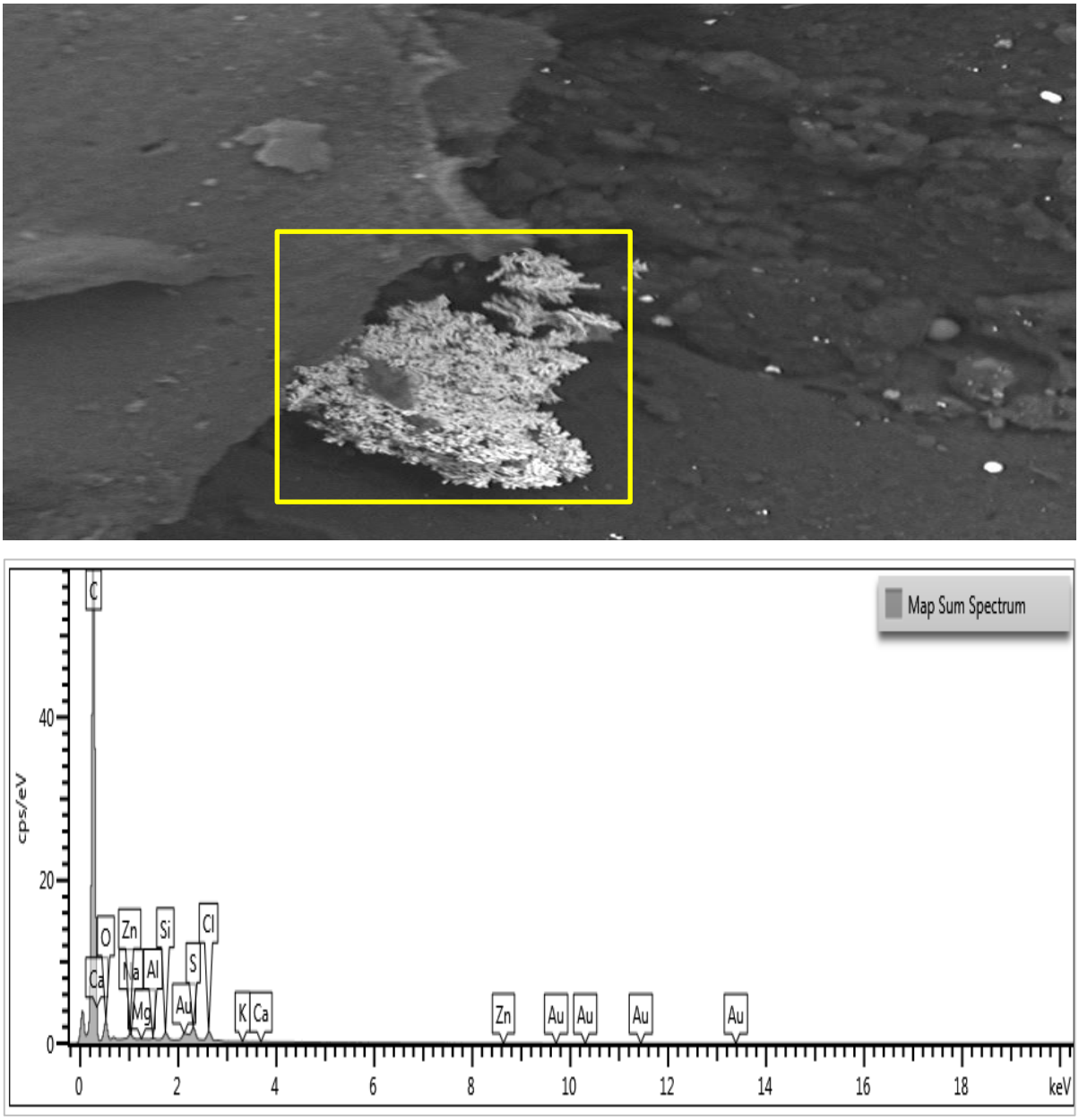

Figure 8-6: SEM image and EDS spectrum for identification of gold on the surface of gold-adsorbed UT-crumb

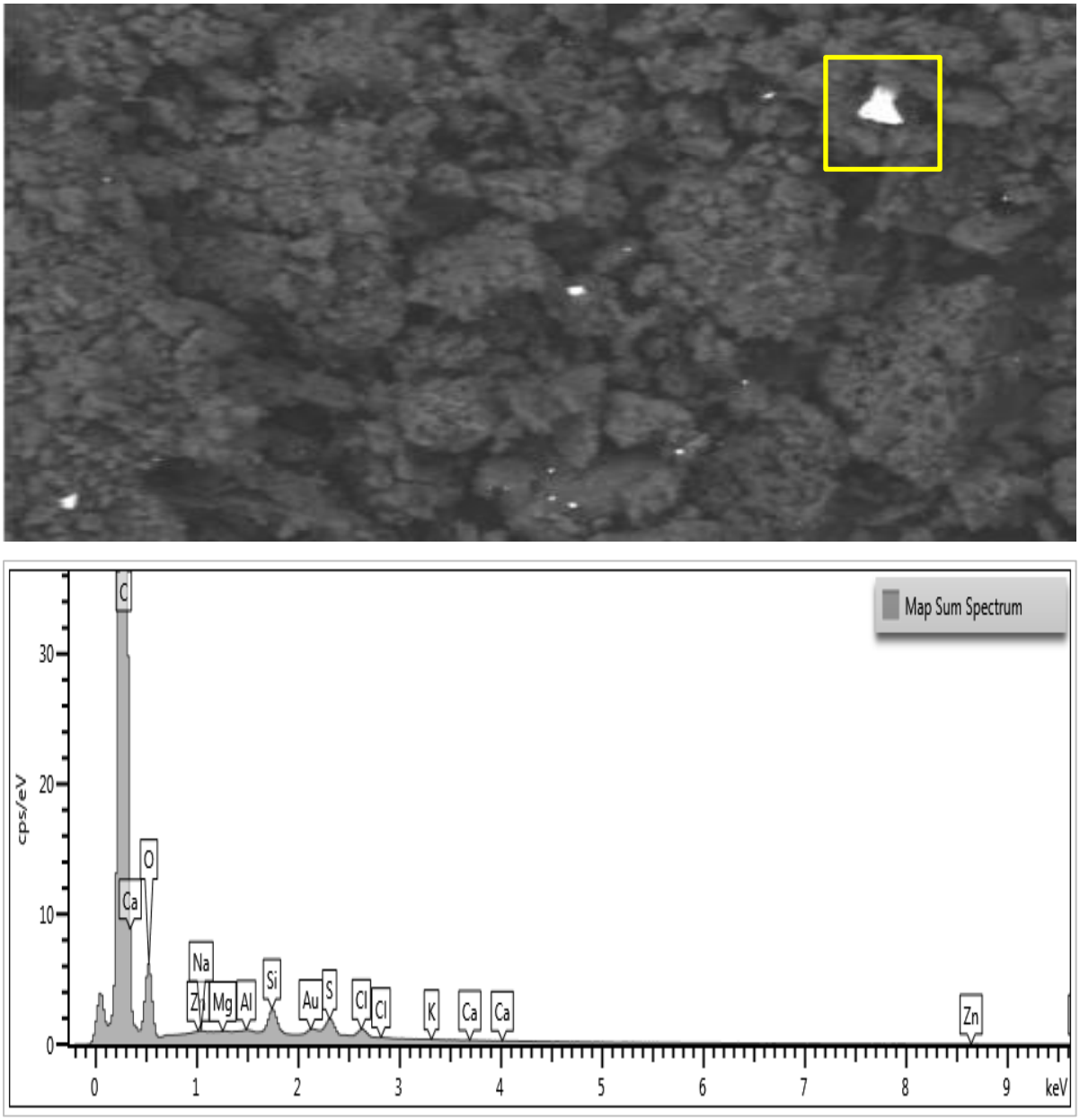

Figure 8-7: SEM image and EDS spectrum for identification of gold on the surface of gold-adsorbed TT-crumb

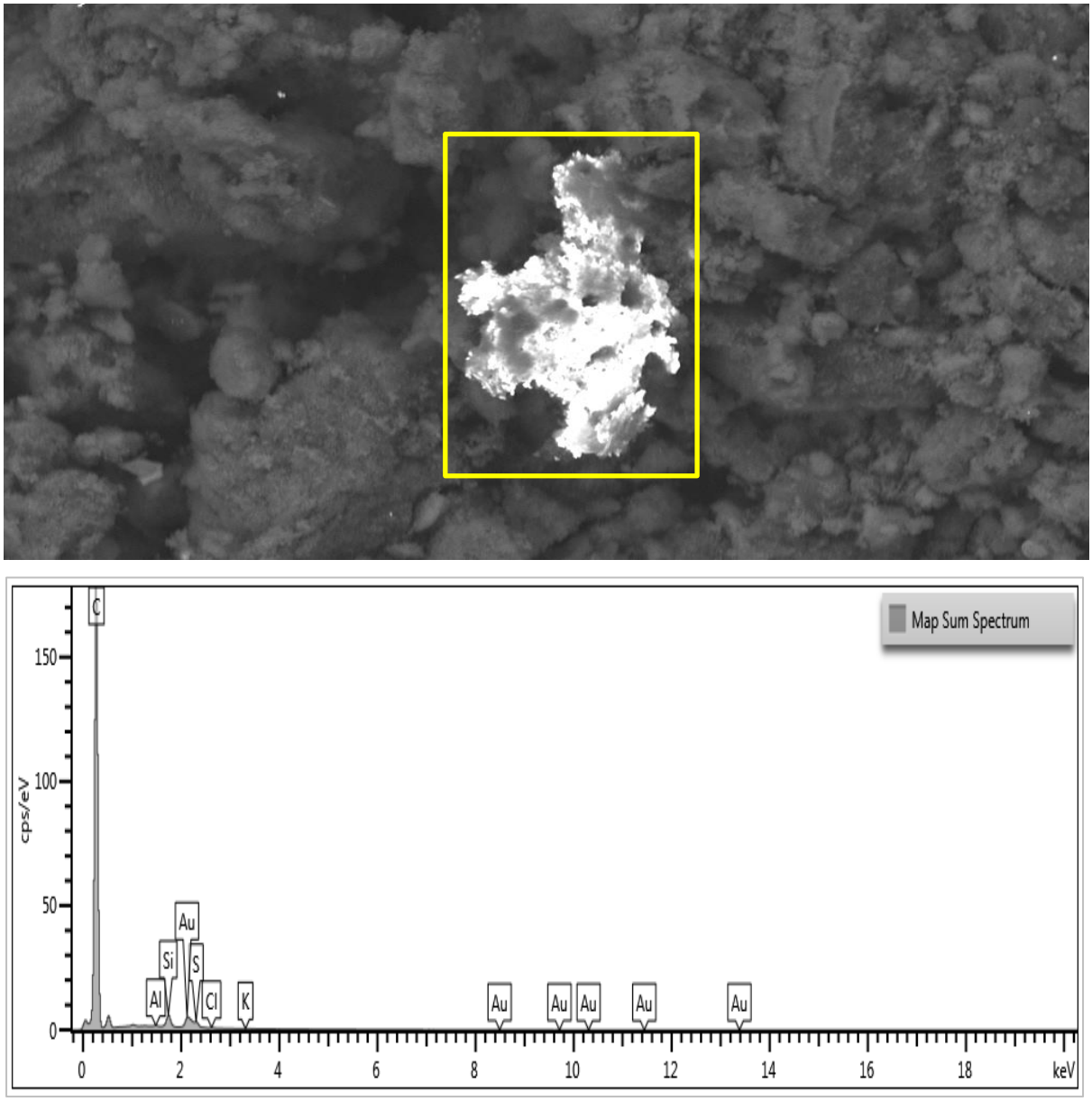

Figure 8-8: SEM image and EDS spectrum for identification of gold on the surface of gold-adsorbed TPT-char

8.11 Standard deviation and standard error

This calculation is used as an example for all the adsorbents.

Adsorbent: TT-crumb;

t_{con} = 72 h.

Mean value ($\bar{X}$):

$$\bar{X} = \frac{1}{n}\sum_{i=1}^{n} X_i$$

$$\bar{X} = \frac{1}{3} * (21.2 + 19.4 + 19.7)\ \%$$

$$\bar{X} = 20.1\ \%$$

Variance (S^2):

$$S^2 = \frac{1}{n-1}\sum_{i=1}^{n}(X_i - \bar{X})^2$$

$$S^2 = \frac{1}{3-1} * [(21.2 - 20.1)^2 + (19.4-20.1)^2 + (19.7-20.1)^2]\ \%$$

$$S^2 = 0.93\ \%$$

Standard deviation (SD):

$$SD = \pm\sqrt{S^2}$$

$$SD = \sqrt{0.93}\ \%$$

$$SD = 0.964\ \%$$

Standard error (SE):

$$SE = \frac{SD}{\sqrt{n}}$$

$$SE = \frac{0.964\ \%}{\sqrt{3}}$$

$$SE = 0.557\ \%$$